Neural noise and suppression in visual processing

Greta Vilidaite

Doctor of Philosophy

University of York

Psychology

December 2017

Abstract

Signal transduction in sensory systems is affected by two major neural mechanisms: neural noise and suppression. Both of these factors present limits on the perceptual abilities of the observer. For example, in contrast discrimination both elevate thresholds. Suppression and neural noise have been implicated in normal sensory development, ageing and several neurological disorders. Of particular interest are autism spectrum conditions (ASCs), in which both neural noise and suppressive mechanisms seem to be atypical.

This thesis addresses several issues surrounding the measurement and neural implications of neural noise and suppression. Firstly, it investigates where in the brain neural noise affects sensory processing. Using machine learning algorithms to analyse electro- and magneto-encephalography data, it was found that the main source of neural noise is early sensory cortex. Secondly, it compares psychophysical paradigms used to dissociate the effects of noise and suppression, and suggests refined methods, in particular, using double-pass consistency. Thirdly, it investigates the neural effects of modulating neural noise and suppression selectively using transcranial magnetic stimulation (TMS). It reveals that two existing TMS protocols are suitable for this: single pulses suppress neural signals, whereas triple-pulse TMS increases neural noise.

Lastly, the thesis investigates neural noise and gain control (a suppressive mechanism) in ASC. The findings show a relationship between sensory noise and autistic traits in the neurotypical population. Furthermore, electrophysiology data from ASC children and adults as well as a genetic *Drosophila* model of autism revealed a deficit in the transient dynamics of ASC visual systems, which changes over the course of development. Striking similarities between the fruit fly (*Nhe3*) model and humans suggests that the genetic model is suitable for further research on ASC sensory symptoms. Taken together, this thesis expands the understanding of neural noise and suppression as well as the situations in which these mechanisms are implicated.

List of Contents

List of Tables

List of Figures

Acknowledgements

First and foremost, I would like to thank my supervisor, Daniel Baker, for noticing my potential when I was an undergraduate and giving me the opportunity to pursue science. I am grateful for the countless hours of answering my never-ending questions on signal detection, and for coaching me through many hiccups during the PhD, and in life. You have been one of the most influential figures in my life.

I also thank Alex Wade, my secondary supervisor, who has been exceptionally important in widening my horizons in academia and whole-heartedly supporting my every endeavour. Without you my thesis would have been much duller (i.e. contained more psychophysics).

Special thanks go to the members of my thesis committee that have been incredibly supportive and encouraging of my ever-lengthening list of projects: Emma Hayiou-Thomas and Gary Green. I would also like to thank Anthony Norcia for welcoming me to his laboratory and his home and for mentoring me throughout this past year. I am grateful to Chris Elliott, Ryan West and Stavroula Petridi for teaching me fruit fly electrophysiology and for many valuable discussions. I apologise for the many failed Western blots and my terrible pipetting skills.

I would like to thank all of the wonderful people at the Psychology Department that became my new family at York. Thank you for lending me your eyes and brain for countless hours of button presses in a darkened room as well as general support and late nights out. Please remember me when you are all famous scientists.

I am grateful to my best friend and best woman Tamsin for keeping my sanity levels up, for making me laugh no matter the situation, and for helping me feel better about my caffeine addiction in comparison. You deserve all the chocolate in the world.

I thank my mum, who has made my scientific journey possible through endless support, love and belief in me. I dedicate this thesis to her, even if she cannot read it. Mama, dedikuoju šitą darbą Tau. Ačiū už Tavo meilę ir palaikymą.

Finally and most importantly, I would like to thank the person who has changed my life forever, my dearest partner Frank Thomas. Thank you for inspiring, motivating and taking care of me, and picking me up back up every time I fall. You are the world's top belayer, both in life and in climbing.

"Because it's there." –

George Mallory, when asked why he wanted to climb Mt Everest

Author's declaration

I declare that this thesis is a presentation of original work that is my own, carried out under the supervision of Dr Daniel Baker. This work has not previously been presented for an award at this, or any other, University. All sources are acknowledged as References. Some of the data in Chapters 2, 3, 5 and 6 has been collected in collaboration with BSc and MSc students, whom I co-supervised. The children's data in Chapter 6 was collected by Dr Francesca Pei, who is a co-author on the corresponding publication. Some of the data analysis was performed together with Dr Daniel Baker, in particular the MEG analysis in Chapter 2.

The study visit to Stanford University, resulting in empirical work presented in Chapter 6, was funded by the Experimental Psychology Society.

The empirical work presented in this thesis has been published or is currently under review in the form of the following articles:

Vilidaite, G., Marsh, E. & Baker, D. H. (submitted). Internal noise in contrast discrimination propagates forwards from early visual cortex. *Neuroimage.*

Vilidaite, G., & Baker, D. H. (2016). Individual differences in internal noise are consistent across two measurement techniques. *Vision Research*, in press

Vilidaite, G., & Baker, D. H. (under review). The effects and non-effects of TMS on contrast perception. *Journal of Cognitive Neuroscience*.

Vilidaite, G., Yu, M. & Baker, D. H. (2017). Internal noise estimates correlate with autistic traits. *Autism Research, 10*, 1384-1391.

Vilidaite, G., Norcia, A. M., West, R. J. H. Elliott, C. J. H., Pei, F., Wade, A. R. & Baker, D. H. (under review). Autism sensory dysfunction in an evolutionarily conserved system. *PNAS.*

Data used in this thesis has been presented in the following conference presentations:

Vilidaite, G. & Baker, D.H. Differential effects of four types of TMS on signal processing. *Poster at VSS 2017, St Pete Beach, Florida, USA*.

Vilidaite, G. & Baker, D.H. Predicting perception from the electroencephalogram. *Poster at European Conference on Visual Perception (ECVP) 2016, Barcelona, Spain*.

Vilidaite, G., Yu, M. & Baker, D.H. Highly correlated internal noise across three perceptual and cognitive modalities. *Poster at VSS 2016, St Pete Beach, Florida, USA*.

Vilidaite, G., Elliott, C.J.H., Wade, A.R., & Baker, D.H. Abnormal contrast responses in a fruit-fly model of autism. *Poster at International Meeting for Autism Research (IMFAR) 2016, Baltimore, Maryland, USA*.

Baker, D.H. & Vilidaite, G. Abnormalities in the steady-state contrast response of adults with high-functioning autism. *Poster at IMFAR 2016, Baltimore, Maryland, USA*.

Vilidaite, G. & Baker, D.H. What is the best way to measure internal noise in the visual system? *Poster at the Applied Vision Association (AVA) annual general meeting, 2015, Nottingham, UK*.

Primary Supervisor's Statement

I am listed as a co-author on the 5 empirical papers which make up the main body of this thesis:

Vilidaite, G., Marsh, E. & Baker, D. H. (submitted). Internal noise in contrast discrimination propagates forwards from early visual cortex. *Neuroimage.*

Vilidaite, G., & Baker, D. H. (2016). Individual differences in internal noise are consistent across two measurement techniques. *Vision Research*, in press

Vilidaite, G., & Baker, D. H. (under review). The effects and non-effects of TMS on contrast perception. *Journal of Cognitive Neuroscience*.

Vilidaite, G., Yu, M. & Baker, D. H. (2017). Internal noise estimates correlate with autistic traits. *Autism Research, 10*, 1384-1391.

Vilidaite, G., Norcia, A. M., West, R. J. H. Elliott, C. J. H., Pei, F., Wade, A. R. & Baker, D. H. (under review). Autism sensory dysfunction in an evolutionarily conserved system. *PNAS.*

In each of the reported studies, the work is primarily that of Greta Vilidaite. For each paper, Greta collected and analysed the majority of the data. The most notable exception to this is that some of the data reported in the 5th study listed above (that involving human children with ASD) was collected by one of the other co-authors on the paper (Francesca Pei), but was then analysed by Greta. Greta wrote the first draft of each paper and did the majority of editing.

Dr Daniel H. Baker

5/12/2017

Secondary supervisor's statement

I am listed on one of the papers that form Greta Vilidaite's thesis that is currently in review:

Vilidaite, G., Norcia, A. M., West, R. J. H. Elliott, C. J. H., Pei, F., Wade, A. R. & Baker, D. H. (under review). Autism sensory dysfunction in an evolutionarily conserved system. *PNAS*.

In this study, the work is primarily that of Ms Greta Vilidaite. Greta designed and executed the experiments, analyzed the data and wrote the first (and many subsequent) drafts of the manuscript.

Professor Alex R. Wade

5/12/2017

Chapter 1

Introduction

1.1 Sensory signal transduction

The nature of sensory processing is paradoxical: although the brain strives to produce a stable model of the world surrounding us, neural signals encoding this model are inherently stochastic. In vision, an entirely faithful representation of the amount of light at each location of the visual field is not behaviourally useful. Rather, neural sensitivity is regulated by a process called gain control, in order for sensory percepts to remain constant in transient environmental conditions (Carandini & Heeger, 2012; Tsai, Wade, & Norcia, 2012) For example, if we see a white cat in the night we have no problem determining its colour, although in reality white cats in the night look gray rather than white. This is because our visual systems are able to adjust our percepts according to the surrounding visual input (in this case, the darkness of the night). At the same time, the representations of sensory input are also affected by the stochastic property of signal transduction – internal (neural) noise. Looking at the same picture of a cat repeatedly produces slight variations in neural firing rate on each occasion.

In the visual system, suppressive mechanisms and neural noise can be readily observed in the response to contrast (the difference between light and dark regions in an image) in low level thalamic and cortical visual areas. Internal noise and suppression shape the way neural populations in the visual system encode the contrast of an object or a scene. Early theoretical accounts of visual perception postulated a step function describing the relationship between stimulus intensity and neural activation. Such a response pattern would have a clear threshold, at the point of minimum intensity (e.g. brightness of a light) that can elicit a neural response. However, due to neural noise, when measured over many stimulus presentations, this neurometric function (Palmer, Cheng, & Seidemann, 2005) follows a sigmoid shape: at low stimulus levels, the neural response accelerates as a function of intensity, at medium levels it increases monotonically, and at high levels it saturates. This same sigmoid function can be observed in the psychometric function of psychophysical observers, which plots the percentage trials on which a stimulus was perceived as a function of stimulus intensity (Burgess & Colborne, 1988). In contrast transduction, both noise and suppression can shift the contrast response function horizontally, changing the sensitivity of the visual system.

As both suppression and internal noise manifest as a deterioration of performance on discrimination tasks, dissociating the effects of each presents a problem. Recent evidence suggests that previous attempts at estimating internal noise psychophysically may have been contaminated by the effects of gain control (Baker & Meese, 2012; Baker & Vilidaite, 2014). Furthermore, previous behavioural methods for studying noise and suppression involved long psychophysical testing sessions, which are not appropriate for some research questions. For example, faster and easily implementable paradigms for measuring sensory neural noise and suppression are desirable for developmental research, research on neural stimulation paradigms and research into clinical conditions, such as schizophrenia, epilepsy, and autism spectrum conditions (ASCs).

In regards to the latter, sensory symptoms in ASC have generated substantial interest in the last decade. Hyper- and hypo-sensitivity to sensory stimulation (e.g. bright lights) in autism has been explained by both suppressive abnormalities (Dickinson, Bruyns-Haylett, Smith, Myles, & Milne, 2016) and increased

(Simmons et al., 2009) as well as decreased (Davis & Plaisted-Grant, 2014) levels of internal noise. Improved methodology for measuring neural noise and suppression could provide insight into the sensory abnormalities of ASC.

Another such research question concerns the mechanisms underlying transcranial magnetic stimulation (TMS). TMS is used to establish links between brain areas and behaviour by decreasing task performance (Mckeefry, Gouws, Burton, & Morland, 2009). Impaired performance (such as higher thresholds in a discrimination paradigm) can be attributed to changes in suppression, neural noise or a combination of both. Understanding how TMS affects neural signaling would improve interpretation of existing TMS research as well as inform future stimulation protocol and methodological choices.

The current thesis aims to address the issues of measuring and separating gain control (suppression) and neural noise in early visual areas. It also investigates the effects of neural noise and suppression by linking perceptual decision making and neural responses and by changing levels of neural noise and suppression with TMS. Furthermore, it addresses a clinical question in which the separation between noise and suppression is crucial: sensory processing in ASC. The remainder of *Chapter 1* will discuss the background literature and rationale of these research questions.

1.2 Neural suppression

1.2.1 What is neural suppression?

The combination of excitatory and inhibitory inputs in early visual cortex is often modeled as a divisive gain control normalisation (Carandini & Heeger, 1994; Heeger, 1992; Legge & Foley, 1980). This normalisation is thought to underlie several notable suppressive effects, such as saturation, as well as within- and cross-channel masking. Although the terms 'suppression' and 'gain control' are often used interchangeably in the literature (Carandini & Heeger, 1994; Carandini, Heeger, & Senn, 2002) and throughout this thesis, the distinction is worth noting. Suppression is a broad term describing the decrease of stimulus-driven neural

signals. Gain control, on the other hand, is an inherent property of sensory systems which regulates neural population activity in order to achieve optimal sensitivity to sensory stimuli across a wide range of conditions. Gain control may suppress or amplify stimulus-related signals according to their spatial and/or temporal context. However, as gain control is the main suppressive mechanism under normal viewing conditions, both suppression and gain control are often used to refer to the same neural property.

Suppression is evident across different sensory modalities and can be observed in visual (Carandini et al., 2002), auditory (Keine & Ru, 2016), olfactory (Olsen, Bhandawat, & Wilson, 2011) and somatosensory (Bernier, Burle, & Vidal, 2009) processing. Furthermore, variations of it can be found at many different stages of sensory systems. For example, in the visual system gain control has been observed in retinal ganglion cells (Shapley & Victor, 1981), lateral geniculate nucleus (LGN; Freeman, Durand, Kiper, & Carandini, 2002), V1 (Heeger, 2009), V5 (Majaj, Carandini, & Movshon, 2007) and higher ventral areas (Kouh & Poggio, 2008). Finally, normalisation is a cross-species phenomenon found in primates (Smith, Bair, & Movshon, 2006), other mammals (Osaki, Naito, Sadakane, Okamoto, & Sato, 2011), other vertebrates (e.g. zebrafish; Zhu, Frank, & Friedrich, 2013) and even insects (e.g. *Drosophila*; Olsen, Bhandawat, & Wilson, 2011).

1.2.2 Neural basis of suppression

The understanding of the neurophysiological mechanisms by which suppression affects sensory processing has changed considerably in the last few decades. Early accounts of suppression in the early visual cortex suggested that V1 neurons, tuned to different orientations and spatial frequencies mutually inhibit each other thus inhibiting the detecting channel (stimulus-related signals; Heeger, 1992). This process was thought to be driven by $GABA_A$ inhibitory connections between the neurons (Morrone, Burr, & Maffei, 1982). However, Katzner, Busse & Carandini (2011) found no influence of $GABA_A$ inhibitor, gabazine, on contrast gain control. This suggests that gain control may not be primarily produced by GABA-ergic inhibitory connections, at least in cat V1, and instead may be

inherited from subcortical structures such as the LGN (Li, Thompson, Duong, Peterson, & Freeman, 2006). However, it is not clear how generalizable this result is to other sensory systems, levels within systems, or other organisms. For example, in the olfactory system of *Drosophila* suppression was found to be GABA-ergic (Olsen et al., 2011).

Another explanation of suppression states that suppression in V1 is the product of thalamocortical depression, happening several synapses before the primary visual cortex (Carandini et al., 2002; Priebe & Ferster, 2006). Furthermore, although suppression has long been assumed to be inhibitory, a growing body of evidence suggests that it relies on excitatory connections as well (Katzner et al., 2011). Recently, clinical investigations into gain control impairments use the term excitation/inhibition (E/I) imbalance to reflect this (Gao & Penzes, 2015; Nguyen, McKendrick, & Vingrys, 2015; Said, Egan, Minshew, Behrmann, & Heeger, 2013).

Suppression shapes the neural response function by normalizing neural responses to stimuli in order to maximize neural sensitivity over a range of stimuli and viewing conditions. This has several implications. First, suppression sharpens the tuning curves of sensory cells (Keine & Ru, 2016). Adjusting response functions in order to use the neuron's dynamic response range increases sensitivity to stimuli in variable environments. For example, gain control in retinal ganglion cells discards information about the overall level of light in the visual field (Shapley & Victor, 1981). Second, gain control normalizes responses to high level stimuli (such as high contrast) producing a saturating firing rate (Carandini & Heeger, 2012). Abnormalities in saturation have been related to abnormal sensory functioning in epilepsy (Porciatti, Bonanni, Fiorentini, & Guerrini, 2000; Tsai, Norcia, Ales, & Wade, 2011), migraine (Nguyen et al., 2015) and autism (Rubenstein & Merzenich, 2003). Third, gain control governs how stimuli are combined in neural signals. Lowered gain control reduces suppressive effects in surround suppression (Petrov & Mckee, 2006), cross-orientation masking (Brouwer & Heeger, 2011), noise masking (Morrone et al., 1982), pedestal masking and binocular summation.

1.2.3 Measuring suppression

Gain control can be observed as suppression of signals in phenomena such as attentional modulation, adaptation, surround suppression and cross-channel masking. The latter two are traditionally employed for measuring suppressive gain control processes in contrast transduction. In surround suppression a stimulus is presented around the target stimulus (e.g. a sine- wave grating) outside the receptive field of the target channel. When the spatial properties (spatial frequency, orientation) are similar, the response to the target stimulus diminishes as the contrast of the surround is increased. In cross-channel masking, the mask is presented within the target receptive field and produces suppression when spatial properties of the mask are different from the target (Petrov, Carandini, & Mckee, 2005). These methods have been widely used psychophysically to measure masking and have also been applied to electrophysiology and neuroimaging.

Cross-channel masking has been widely used together with steady-state EEG as a sensitive tool in assessing excitation and suppression in vision (e.g. Tsai, Wade, & Norcia, 2012) and audition (Stapells, Linden, Suffield, Hamel, & Picton, 1984). Tsai et al. used a frequency tagging paradigm where a target stimulus is flickered at a specific temporal frequency (F1) and a superimposed mask is flickered at a different frequency (F2). The differences in amplitudes of electrophysiological responses at F1 between target only and target + mask conditions indicate the level of cross-channel suppression as described by the gain control model. This method provides a more direct measure of gain control compared to behavioural tasks and can be applied in a wide range of research, e.g. animal models (West, Furmston, Williams, & Elliott, 2015).

The effects of gain control (e.g. saturation, masking and tuning curves) are also often employed as measures of neural suppression using psychophysical and neuroimaging methodologies (Dickinson, Jones, & Milne, 2016). For example, Nguyen, McKendrick, & Vingrys (2015) estimated gain control abnormalities (E/I imbalance) in migraine patients by measuring saturation in their electroencephalographic (EEG) visually evoked potentials (VEPs). Another migraine study (Wilkinson, Karanovic, & Wilson, 2008) investigated E/I imbalance by behaviourally measuring binocular rivalry, another gain control

mediated neural phenomenon. Alternatively, a large body of ASD literature has used pitch, orientation, colour and other types of discrimination paradigms to infer changes in gain control (see Dickinson, Jones, & Milne, 2016 for review).

Finally, many studies suggest gain control as a proxy for measuring GABA levels and vice versa: measuring GABA markers as a proxy for suppression in sensory systems. For example, GABA concentration in human visual cortex was found to be correlated with binocular rivalry alternation rates, another suppression-dependent phenomenon (van Loon et al., 2013). However, as gain control depends on both excitatory and inhibitory connections in cortical and subcortical areas (Katzner et al., 2011), GABA-ergic synapses may only part of the picture.

1.3 Neural noise

1.3.1 What is noise?

Signal transduction is inherently stochastic. Noise can be observed at the scale of single neurons, as variations in neural firing rate during repeated presentations of a stimulus (Hubel & Wiesel, 1962, 1968). It also manifests at the whole organism scale as variable behavioural responses to repeated stimulation. Noise is an important part of signal detection theory (Green & Swets, 1974), which is routinely used to characterize signal transduction in neuroscience.

Neural noise was first observed in animal electrophysiology research as signal variability over repeated presentations of stimuli (Schiller, Finlay, & Volman, 1976). Neural noise results from many sources on several processing scales (Klein et al., 2015): (1) molecular fluctuations in ionic conductance and ion pump channel activity (Faisal, Selen, & Wolpert, 2008); (2) synaptic transmission noise (Schneeweis & Schnapf, 1999); (3) dynamic changes in conductance from short-term synaptic plasticity and adaptation (Clifford et al., 2007); (4) dynamic changes and interaction within networks (Turrigiano, 2011); (5) changes in internal states such as attention, arousal and top- down cognitive modulation (Fontanini & Katz, 2011). It is typically reported to be proportional to the mean firing rate of the neuron, such that the noise at a single unit level is multiplicative

(Tolhurst, Movshon, & Dean, 1983a). However, at the population level, the aggregate noise is approximately additive (signal-invariant; Chen, Geisler, & Seidemann, 2006).

In psychophysics, the neurophysiological 'neural noise' is often approximated by a model parameter representing 'internal noise', which is assumed to be late and additive. As the only certain difference in these terms is the scientific tradition from which they originally derive from (psychophysics or neurophysiology), they will be used interchangeably in this thesis.

1.3.2 Influence of noise

The effects of random activity in the brain can be observed both as fluctuations in behaviour (i.e. decisions) and in neurophysiological measurements, such as single- and multi-cell recordings, EEG, magnetoencephalography (MEG) and functional magnetic resonance imaging (fMRI). But how do we know that neural noise in visual cortex affects perception? For instance, how do we know that variations in responses on a contrast discrimination task are to do with neural noise in the visual cortex rather than finger errors or noise in prefrontal (executive function) areas?

Evidence for noise influencing behaviour comes from relating fMRI blood-oxygenation-level-dependent (BOLD) signal levels to perceptual decisions in a contrast detection paradigm (Ress & Heeger, 2003). If behaviour is not influenced by spontaneous activity in the detecting channel, we would expect that trials containing the target (both *hits* and *misses*) would invoke higher neural activation than trials that did not contain the target (*false alarms* and *correct rejections*). However, Ress & Heeger (2003) found that *hits* and *false alarms* were preceded by higher BOLD signal levels than *misses* and *correct rejections*: brain activation was more predictive of the percept rather than the stimulus. Higher activation in the instance of *false alarms* suggests that spontaneous neural activity (noise) has an important effect on perception and decision making.

However, other evidence on this is mixed. An MEG contrast detection study (Mostert, Kok, & Lange, 2015) confirmed the difference between *hits* and *misses*,

but did not find any difference in activation between *false alarms* and *correct rejections*. Furthermore, an EEG event-related potential (ERP) experiment, which used auditory signal detection in noise, found higher activation for *hits* than *misses*, *false alarms* and *correct rejections* (Hillyard, Squires, Bauer, & Lindsay, 1971). This implies that the brain is only responsive when the stimulus is present and consciously perceived. Such results contradict the findings of Ress & Heeger (2003) implying that early sensory noise does not play major a role in perception. However, these neuroimaging studies used crude designs where only the mean strength (or peak) of the signal was compared between trial categories. The controversy may be better settled by more sensitive machine learning classification algorithms and by taking into account activation changes over time.

1.3.3 Measuring neural noise

Unlike intracranial electrophysiology, EEG, MEG and fMRI measure responses of large populations of thousands of neurons. For neural noise to influence these measurements it has to be correlated between neurons, as unrelated spontaneous activity in individual neurons would average out in the BOLD response or when pooling neural activity with EEG electrodes or MEG sensors (Nienborg, Cohen, & Cumming, 2012). To measure neural noise specifically in the detecting channel of a stimulus (e.g. a neuron tuned to vertical orientations) measurements need to be much more fine grained. As intracranial recordings in humans are highly invasive and rarely possible, psychophysical measures of this noise may be preferential.

A substantial body of research has attempted to measure noise psychophysically for many different visual cues: luminance (Barlow, 1956), orientation (Jones, Anderson, & Murphy, 2003), shape (Sweeny, Grabowecky, Kim, & Suzuki, 2011), motion (Barlow & Tripathy, 1997) and contrast perception (Baldwin, Baker, & Hess, 2016; Burgess & Colborne, 1988; Lu & Dosher, 2008; Pelli, 1985). Furthermore, individual differences in contrast sensitivity for neurotypical adults have also been explained as being partly due to noise (Baker, 2013). Most commonly, the influence of neural noise on psychophysical task performance is

assessed by purposefully degrading the performance of the observer by adding external stimulus noise to the display.

1.3.4 Equivalent noise paradigm

Contrast detection in broadband white noise masks is commonly used to characterize noise in contrast transduction. The most well-known methodology for measuring internal noise is the equivalent noise (EN) paradigm (Legge, Kersten, & Burgess, 1987; Pelli, 1985). In this paradigm observers perform a two-alternative-forced-choice (2AFC) detection experiment with a white noise mask presented on both stimulus intervals and a target stimulus, such as a luminance modulated grating, added to one of the intervals. Target detection thresholds are obtained for several white noise contrast levels. It is assumed that performance on the detection task will start to decrease (thresholds will become higher) as a function of stimulus noise when the amount of stimulus (mask) noise surpasses the amount of internal noise in the detecting channel. The white noise contrast level at which performance starts to rapidly decline is assumed to be equivalent to the amount of internal neural noise in the system (Pelli, 1985).

The EN paradigm assumes a linear amplifier model of contrast transduction (LAM; Pelli, 1985), which can be defined as:

$$C_{thresh} = \frac{\sqrt{\sigma_{ext}^2 + \sigma_{int}^2}}{\beta} \qquad \text{(Eq. 1)}$$

where C_{thresh} is the threshold target contrast level, β is an efficiency constant (Lu & Dosher, 2008) and σ_{ext} and σ_{int} are the levels of external (stimulus) noise and internal noise respectively (Baldwin et al., 2016). The model features a linear relationship between stimulus input and signal output, with additive internal noise. External stimulus noise, such as the white noise masks in the EN paradigm, introduces variability into the detecting mechanism and impairs performance at high noise contrasts. When stimulus noise (σ_{ext}) is low, internal noise (σ_{int}) is

dominant and so C_{thresh} approximates $\frac{\sigma_{int}}{\beta}$. As σ_{ext} increases, the amount of internal noise in the system becomes negligible in comparison and so $C_{thresh} \sim \frac{\sigma_{ext}}{\beta}$, causing thresholds to increase in proportion to external noise contrast.

1.3.5 Issues with equivalent noise

Due to the broad frequency and orientation profile of white noise masks, adjacent channels may also be activated by the stimulus and in turn inhibit the target channel (cross-channel masking; Carandini, Heeger, & Senn, 2002). The strong suppressive effect of broadband white noise masks has been empirically demonstrated (Baker & Vilidaite, 2014). This suggests that impaired performance at high mask levels in the EN paradigm could be due to suppressive gain control effects and not noise (Baker & Meese, 2012; Baldwin et al., 2016).

One solution to this is to inject variability only into the detecting channel tuned to the target. This is possible by removing all off-channel spatial frequency and orientation information from the mask. The result is a mask that is spatially identical to the target grating, but with a randomly selected contrast – a 'zero-dimensional' (0D) mask (Baker & Meese, 2012). Similar noise masks have been previously used in luminance (Cohn, 1976), orientation (Dakin, Bex, Cass, & Watt, 2009) and auditory tone perception (Jones, Moore, Amitay, & Shub, 2013). The contrast level of the mask is randomly sampled from a Gaussian distribution to create interval-by-interval contrast jitter. It has been shown that this type of mask produces stronger masking effects than white or pink noise (Baker, 2013; Baker & Meese, 2012) and so offers a more suitable alternative to white noise masks.

In addition, as mentioned previously, the EN paradigm assumes a linear model which is at odds with contemporary accounts of contrast transduction (Baldwin et al., 2016). Evidence against linear processing of contrast has been found by several studies (Legge & Foley, 1980; Boynton, Demb, Glover, & Heeger, 1999; Baker & Vilidaite, 2014) as the relationship between stimulus contrast and visual response is accelerating at low contrasts and saturating at high contrasts (Baker,

2013; Tsai et al., 2012). Due to the nonlinearity of the human visual system a paradigm with an underlying nonlinear model or a model-free paradigm should be considered.

1.3.6 Double-pass paradigm

The 'gold standard' paradigm for measuring internal noise is the double-pass consistency paradigm (Burgess & Colborne, 1988; Green, 1964), as it estimates noise directly rather than inferring it from thresholds. When there is no variability in the stimulus, the variability in an observer's responses can only be due to internal noise. The most straightforward way of measuring it, therefore, is to present the exact same stimulus multiple times and look at the consistency of responses between presentations. In double pass, a 2AFC noise masking experiment (similar to EN) is run twice (pass 1 and pass 2) with the exact same examples of noise and target. The consistency of responses between the two passes (calculated as a proportion) indicates the level of internal noise in the system. Although this proportion does not directly relate to a physical quantity of neural noise, it is useful for comparison of noise levels between groups or viewing conditions and for investigating individual differences.

An accuracy measure can also be obtained from double-pass. Accuracy is most likely reflective of the amount of stimulus-related signal in the system (or sensitivity in the LAM framework) although correlation between accuracy and consistency would be expected: the more correct choices made on trials, the more consistently correct the answers will be. Nonetheless, accuracy could be used as a measure of signal strength – the inverse of suppression.

1.4 Modelling gain control and neural noise

The effects of contrast gain control and internal noise can be differentiated within the normalisation (gain control) model (Carandini & Heeger, 2012; Heeger, 1992; Legge & Foley, 1980). The neural response in the normalisation model can be defined as:

$$resp = \frac{C^p}{Z + C^q} + \sigma_{int} \qquad\qquad \text{(Eq. 2)}$$

where C is the stimulus contrast, σ_{int} is internal noise and Z is the saturation constant (the gain control parameter). The parameters p and q are exponents that produce the acceleration of the response at low contrast levels and saturation at high contrast levels. The normalisation model describes how the responses in the detecting channel are suppressed by activation in channels the gain pool (surrounding channels/neurons). The Z parameter achieves this in the model by controlling the amount of divisive inhibition and shifting the contrast response function (CRF) horizontally (Reynolds & Heeger, 2009; Tsai, Norcia, Ales, & Wade, 2011).

The differential effects of the noise (σ_{int}) and gain control (Z) parameters on contrast transduction are well illustrated by contrast discrimination threshold versus contrast (TvC) curves. In the contrast discrimination paradigm, a pedestal stimulus with a fixed contrast is presented in both intervals of a 2AFC experiment and a target contrast is added in one of the intervals. A staircase procedure is used to control the target contrast and focus trials around some threshold point. It is typical to obtain discrimination thresholds at several pedestal contrast levels to produce the TvC function, which takes the shape of a dipper (Nachmias & Sansbury, 1974). The pedestal produces a facilitation effect at low pedestal levels and threshold elevation from masking at higher levels of pedestal contrast. Changing internal noise (σ_{int}) produces vertical shifts of the dipper function: increased noise raises the whole curve upwards. Conversely, increased gain control (Z) shifts the function diagonally so that the thresholds increase at low pedestal contrast levels but remain unchanged at high pedestal levels (Figure 1.1).
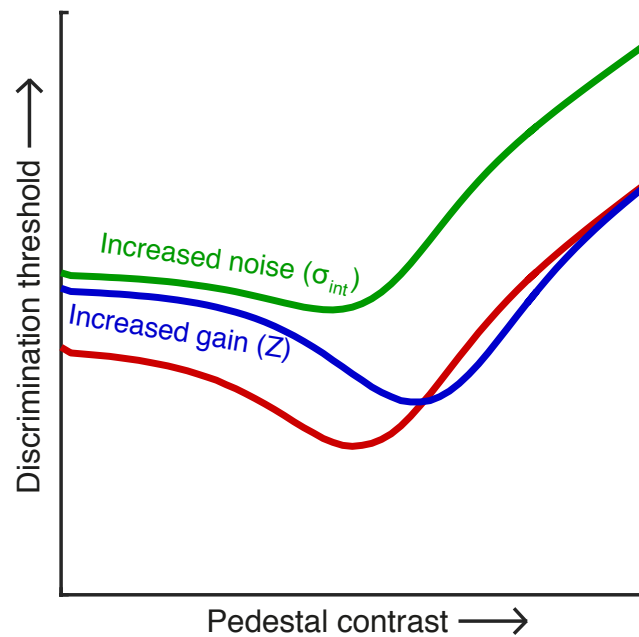
Figure 1.1. **Influence of internal noise and gain control on TvC curves.**

Although the pedestal masking paradigm is well-established and widely used, it has not yet been used to differentiate between internal noise and suppression. This paradigm, paired with the gain control model could be a useful alternative to equivalent noise.

1.5 Suppression and neural noise in TMS

1.5.1 TMS: introduction

In order to further investigate the influence of neural noise and suppression on sensory signals, it would be useful to establish causal links between these neural mechanisms and perception. Experimentally manipulating the level of neural noise or suppression would provide insight into the behavioural and neural effects of each mechanism. One way to affect neural processing in humans is to use brain stimulation such as TMS. TMS is a common noninvasive technique to establish links between brain areas and certain behaviours. Typically, TMS pulses are applied to a particular part of the cortex during or prior to a perceptual or

cognitive task and then the performance on this task is compared to baseline (no TMS). However, so far there has been little research into precisely how TMS affects neural signals.

For decades the effects of TMS have been likened to a 'virtual lesion' (Pascual-Leone, Walsh, & Rothwell, 2000) and assumed to suppress neural activity in the region of stimulation (Mckeefry et al., 2009). However, more recently it has been recognized that this view may be overly simplistic for several reasons (Silvanto & Muggleton, 2008). First, effects of TMS are not always inhibitory or disruptive: TMS can also enhance task performance. For example, single pulse TMS (spTMS) was found to facilitate the detection of masked objects (Grosbras & Hab, 2003). Secondly, TMS has also been shown to induce neural activity and subsequently involuntary motor movements when applied to the primary motor cortex (Moliadze, Fritzsche, & Antal, 2014; Ragert, Franzkowiak, Schwenkreis, Tegenthoff, & Dinse, 2008). In vision, phosphenes can be elicited by applying TMS to visual areas (Boroojerdi et al., 2002; Stewart, Walsh, & Hwell, 2001).

Lastly, the disruptive effects of TMS on neural processing are likely not due to simple suppression of neural activity. Elevated thresholds on perceptual tasks, as those often seen when using TMS to link sensory brain areas to perceptual processes, can be due to either signal suppression, or neural noise induction, or a combination of both factors (Ruzzoli et al., 2011; Schwarzkopf, Silvanto, & Rees, 2011). This implies that it may be possible to modulate neural noise and/or suppression with TMS in certain conditions.

The next two sections will cover the most notable findings on the neural mechanisms underlying TMS, focusing in particular on TMS of the occipital lobe. The protocols covered are the most commonly used TMS methods for establishing causal links between brain areas and behaviours at present day. Offline 1Hz repetitive TMS (rTMS) will not be covered as it has largely been replaced in the field by offline theta burst simulation (TBS). Furthermore, paired-pulse TMS is beyond the scope of this thesis as it involves measuring the effect of a TMS pulse on another TMS pulse, therefore complicating the interpretation of neural mechanisms.

1.5.2 Effects of online TMS

Online TMS refers to magnetic stimulation applied during a behavioural task. Most commonly, one (spTMS) or three pulses (repetitive, rTMS) are delivered on each trial of a task. Online TMS is the most commonly used type of TMS methodology in order to produce suppression of perceptual processing in the occipital cortex (Mckeefry et al., 2009). However, several studies have attempted to investigate whether online TMS protocols do suppress visual signals or whether they induce neural noise in the visual system.

The first study to investigate the neural mechanisms of TMS in humans used a contrast detection in broadband white noise masks (Harris, Clifford, & Miniussi, 2008) and a single pulse stimulation protocol. Harris et al. found multiplicative effects of V1 TMS stimulation on masking curves indicating that spTMS suppressed stimulus-related signals in the visual cortex. Steeper psychometric curves indicative of signal suppression by spTMS were also found when applying to V5 during a motion coherence task (Ruzzoli et al., 2011). On the other hand, Rahnev, Maniscalco, Luber, Lau & Lisanby (2012) suggested that TMS increases noise in the visual system as predicted by their single-channel model. However, this is a rather counterintuitive conclusion as their results showed lower accuracy and higher confidence ratings on an orientation discrimination task resulting from spTMS. Usually, confidence ratings are interpreted as being indicative of the amount of noise in the system, whereas accuracy as a measure of stimulus-related signal. Two other studies used similar paradigms and found that spTMS decreased both accuracy and confidence on symbol and orientation discrimination tasks (Koivisto, Harjuniemi, Railo, & Salminen-Vaparanta, 2017; Koivisto, Railo, & Salminen-Vaparanta, 2011). This contradicts Rahnev et al. (2012) and indicates that both neural noise and signal levels are affected by this protocol.

Interestingly, Rahnev et al. (2012) relate their findings to two other studies that found increased neural noise as a result of TMS stimulation: Ruzzoli, Marzi, & Miniussi, (2010) and Schwarzkopf, Silvanto, & Rees, (2011). However, both of these studies used three-pulse rTMS protocols, which are likely to affect neural signalling differently, perhaps affecting neural noise levels rather than suppressing sensory signals. Ruzzoli et al. (2010) found shallower motion coherence threshold

slopes, which suggest increased noise in area V5 when applying rTMS. Applying rTMS to V1 did not have any affect on thresholds. Schwarzkopf et al. (2011) also claim to demonstrate increased neural noise during motion coherence when using rTMS through a process called "stochastic resonance", in which noise can improve performance under specific conditions.

So far it seems likely that spTMS and rTMS suppress sensory signals and affect neural noise in differential ways. However, the findings so far are mixed and, in some cases, tenuous. For example, the findings of Harris, Clifford, & Miniussi, (2008) are based on the assumption that white noise masks increase the variability of neural signals, however, evidence suggests that broadband white noise suppresses signals (Baker & Meese, 2012; Baker & Vilidaite, 2014).

1.5.3 Effects of theta burst stimulation

A similar debate about underlying neural mechanisms exists for offline TMS protocols, i.e. theta burst stimulation. Unlike online protocols, theta burst stimulation is applied before a perceptual or cognitive task, and is presumed to have lasting effects of about 25-60 minutes (Cárdenas-Morales, Nowak, Kammer, Wolf, & Schönfeldt-Lecuona, 2010; Huang, Edwards, Rounis, Bhatia, & Rothwell, 2005). Two types of stimulation patterns (Cárdenas-Morales et al., 2010; Huang et al., 2005) are usually used (although some other variation also exist):

    (1) Continuous TBS (cTBS) – three pulses at 50Hz are delivered at 5Hz

    (2) Intermittent TBS (iTBS) – three pulses at 50Hz are delivered at 5Hz 10 times every 10 seconds (0.1Hz).

Although TBS is routinely used in to investigate sensory processing in low-level (Cai, Chen, & Zhou, 2014; Rounis et al., 2010) and high-level vision (Pitcher, Duchaine, & Walsh, 2014) as well as other senses (Ragert et al., 2008; Rai, Premji, Tommerdahl, & Nelson, 2012), research into the effects of TBS on stimulus-related signals is scarce.

Most of the research regarding the neural mechanisms of TBS used motor evoked potentials (MEPs) in a passive state (no task or action). The first TBS study (Huang et al., 2005) applied either cTBS, iTBS or intermediate TBS to the motor cortices of passive participants and subsequently measured MEPs in hand muscles to single TMS pulses. They found that cTBS suppressed subsequent activation, indicating overall suppression of neural activation in the motor cortex; whereas iTBS increased MEP amplitudes suggesting an overall increase in excitability. Similar conclusions on inhibitory cTBS effects and excitatory iTBS effects were made in other studies that used motor activation paradigms (Di Lazzaro et al., 2005, 2008; Moliadze et al., 2014). Two studies have extended these findings to perceptually-relevant neural signalling during sensory tasks. One study found that cTBS decreased accuracy on a visual orientation discrimination task (Rahnev et al., 2013), indicating that this stimulation protocol had suppressive effects. Another experiment measured the effects of iTBS on a tactile discrimination task and showed that iTBS improved task performance (Ragert et al., 2008), suggesting the enhancement of sensory signals.

However, these results have not always been replicated. Gentner, Wankerl, Reinsberger, Zeller, & Classen (2008) found that short cTBS durations (20 seconds) decreased MEPs, whereas longer durations (40 seconds) increased MEPs suggesting variability in TBS effects even within protocol. Another study that measured protein expression, intracranial multiunit somatosensory potentials and EEG gamma band power in the rat visual cortex, found that cTBS affected neither somatosensory potentials, nor gamma band power, whereas iTBS increased the strength of both. Both protocols affected protein expression but in different classes of inhibitory neurons. Besides differences between TBS protocols and stimulation lengths, different individuals seem to also experience different effects when stimulated using the same methodology. López-Alonso, Cheeran, Río-Rodríguez, & Fernández-del-Olmo (2014) applied iTBS and then measured resting and active motor thresholds: lowest intensity of spTMS to elicit 50μV a resting first dorsal interosseous muscle, and 200μV MEPs in an active muscle, respectively. Using cluster analysis the study found a bimodal split in subject muscle responses with 43% of individuals (total N = 56) showing increased resting and active MEPs and 57% showing no change or slightly lowered MEPs.

No significant change in MEPs was found when subjects were analysed as one group. These findings shed light on a previous study with a similar design (Hamada, Murase, Hasan, Balaratnam, & Rothwell, 2013), which found no significant change in mean group MEPs after cTBS or iTBS, although some subjects exhibited this change and there was high variability in the sample.

The findings of these studies suggest that there might be individual differences in whether or not and how individuals are affected by TBS, or perhaps TMS in general. It may be that some people have a natural susceptibility to TMS or that TBS effects are unpredictable or have highly complex underlying neural mechanisms which are yet to be understood.

1.5.4. TMS: summary

Previous research into the effects of TMS on sensory processing suggests the potential of affecting neural noise and/or suppression in particular conditions. However, so far only the offline TBS protocols have been compared to one another using the same paradigm. Previous research mostly indicates that spTMS suppresses neural signals (Harris et al., 2008; Ruzzoli et al., 2011) and rTMS affects neural noise (Ruzzoli et al., 2010; Schwarzkopf et al., 2011). However, so far sub-optimal behavioural paradigms have been used and there has not yet been a direct comparison of these TMS protocols. Uncovering how different types of TMS influence sensory processing could be useful for investigating the effects of neural noise and suppression in sensory systems.

1.6 Suppression and neural noise in ASC

Along with a host of social and language impairments, autism spectrum conditions encompass pervasive sensory symptoms (American Psychiatric Association, 2013). These include hyper- and hypo-sensitivity to intense stimuli such as bright lights and loud noises, unusual sensory interests and overstimulation (Ben-Sasson et al., 2009; Jones, Quigney, & Huws, 2003). Both impairments and enhancements of sensory processing in several sensory

modalities have been found (see Bennetto, Kuschner, & Hyman, 2007; Cascio et al., 2008; Haesen, Boets, & Wagemans, 2011 for reviews), including in vision (see Simmons et al., 2009 for review). As these symptoms seem to be due to differences in the sensitivity of the sensory systems, neural noise and gain control may be important factors underlying these hyper- and hypo-sensitivities.

1.6.1 Sensory differences in ASC

The visual processing differences in ASC have been explained by a great many theories. Particularly attractive in its simplicity was the suggestion that the differences are due to enhanced visual acuity. In fact, one study (Ashwin, Ashwin, Rhydderch, Howells, & Baron-Cohen, 2008) reported that visual acuity in ASC individuals was much higher than in controls and approaching the range of birds of prey. However, many technical faults have been identified in the study (Bach & Dakin, 2009) and the results were not replicated (Bolte et al., 2012). Furthermore, contrast sensitivity (Koh, Milne, & Dobkins, 2010) has been found to be normal in individuals with ASC, suggesting that the sensory abnormalities are not due to enhanced or diminished eye-sight, or an overall reduction in visual signalling. However, the idiosyncrasies become apparent early on in the visual processing stream. For example, orientation discrimination in first-order (luminance modulated) contrast stimuli are enhanced in ASC individuals but reduced in second-order (contrast modulated) stimuli (Bertone, Mottron, Jelenic, & Faubert, 2005). Amongst many other differences in low-level vision, motion perception has also been found abnormal with most studies suggesting higher motion coherence thresholds in ASC (Milne et al., 2002; Pellicano, Gibson, Maybery, Durkin, & Badcock, 2005; also see Simmons et al., 2009 for review).

Several alternative hypotheses explaining these as well as other low- and high-level visual processing differences in ASC have been suggested (Greenaway, Davis, & Plaisted-Grant, 2013; Pellicano et al., 2005; Rosenberg, Patterson, & Angelaki, 2015; Rubenstein, 2010). Of particular interest to this thesis is the suggestion that increased neural noise levels in ASC sensory systems could account for the wide variety of increased and decreased performance on visual tasks as well as the heightened variability in responses of ASC individuals

(Simmons et al., 2009). Another popular theory which this thesis will focus on is the imbalance of excitation and inhibition (E/I) which explains unusual changes in sensitivity as well as some of the findings in visual perception that seem to indicate a suppression-related impairment (Dickinson, Bruyns-Haylett, Smith, Myles, & Milne, 2016).

1.6.2 Abnormal levels of neural noise

Higher levels of neural noise in ASC brains were first suggested by Simmons et al (2009) and since have been investigated with EEG, fMRI and behavioural studies. Functional MRI BOLD responses were found to be more variable in ASC individuals during a motion coherence task (Dinstein et al., 2010, 2012) even though behavioural responses did not differ from the control group. Although the 2012 study has been criticized for having a small sample, the finding was replicated in motion perception as well as in somatosensory and auditory tasks using the same fMRI paradigm (Haigh, Heeger, Dinstein, Minshew, & Hall, 2016). Additional evidence comes from more variable P-100 ERP latency in response to Gabor patches, more variable α-band phase coherence within trials (Milne, 2011) and lower signal-to-noise ratios in VEPs (Weinger, Zemon, Soorya, & Gordon, 2014). However, a recent study with a larger sample of ASC individuals and well-matched control participants found no differences in either phase coherence or inter-trial responses (Butler, Molholm, Andrade, & Foxe, 2016).

Adding to the controversy, it has also been argued that individuals with ASC may in fact have lower internal noise than healthy controls (Davis & Plaisted-Grant, 2014; Greenaway et al., 2013). This hypothesis has been based on the observation that ASC individuals exhibit higher contrast discrimination thresholds in a pedestal masking paradigm (Greenaway et al., 2013). However, the current understanding of sensory processing posits that elevation of thresholds cannot be indicative of lower internal noise. Increased internal noise produces higher thresholds as the signal-to-noise ratio is lower, as predicted by both the gain control model and LAM (Manning & Baker, 2015). Furthermore, the hypothesis is based on the assumption that the stimuli (4AFC luminance modulated squares)

in the study by Greenaway, Davis & Plaisted-Grant introduced variability into the detecting mechanism although no aspect of the stimulus was variable. On the other hand, higher discrimination thresholds give indirect support to the high noise theory. In light of these arguments and previous findings, it seems more plausible that patients with ASC have higher internal noise.

The research on internal noise in ASC mostly suggests increased noise in the visual system and other parts of the brain, although the methods and models used have been inconsistent and have generated controversy. The hypothesis that ASC individuals exhibit behaviour indicative of higher internal noise would be best tested with a direct, sensitive measure of noise, such as the double-pass paradigm. Furthermore, with the large range of study designs and stimuli used to investigate this, it is also unclear what type of neural noise (if any) is implicated in ASC and at what stage of sensory processing (Simmons & Milne, 2014). As neural noise has a broad definition in many studies it often encompasses everything from cellular level noise in sensory systems to neural variability in response mechanisms, to changes in mental states and attention. An examination of neural noise in ASC vision at different levels of neural processing may be able to shed light on this subject.

1.6.3 Imbalance of excitation/inhibition

The balance of excitation/inhibition (E/I) has been suggested to differ between ASC and neurotypical populations (Markram & Markram, 2010; Rubenstein, 2010; Rubenstein & Merzenich, 2003), independently of the increased noise theory. As excitatory and inhibitory connections underlie gain control, it is reasonable to assume that ASC individuals would exhibit gain control abnormalities (Rosenberg et al., 2015). Rosenberg et al. (2015) suggests that lack of inhibition, and therefore reduced gain control, or normalisation, may explain the behavioural and perceptual impairments in ASC. This unifying theory of a system-wide impairment is compelling in light of the argument that normalisation is a canonical computation, replicated throughout the brain (Carandini & Heeger, 2012). Reduced inhibition is supported by findings of lower levels of GABA precursors (Harada, Taki, & Naa, 2011) and reduced $GABA_A$ receptor density

(Mori, Mori, Fujii, Toda, & Miyazaki, 2012) in the frontal lobes of ASC individuals. However, levels of both precursors and receptors were normal in other parts of ASC brains, which contradicts the hypothesis that E/I imbalance is system-wide. In fact, behavioural studies suggest that the balance of E/I may differ even within the visual-system. For example, luminance-modulated pattern orientation discrimination in ASC exhibits properties of higher inhibition (Dickinson, Jones, & Milne, 2014) whereas contrast-modulated texture orientation discrimination exhibits lower inhibition (Bertone et al., 2005).

So far the direction of the E/I hypothesis is unclear as all four possible causes (increased or decreased excitation; and increased or decreased inhibition) for an E/I imbalance have been suggested and supported by empirical studies, as summarized by several large scale reviews (Coghlan et al., 2012; Dickinson, Bruyns-Haylett, Smith, Myles, & Milne, 2016; Nelson & Valakh, 2015; Rosenberg, Patterson, & Angelaki, 2015; Rubenstein & Merzenich, 2003; Rubenstein, 2010). A recent account by Nelson & Valakh (2015) acknowledges the complexity and variability of empirical findings and suggest that E/I imbalance is variable throughout the brain and even within circuits. This has also been demonstrated empirically: GABA marker concentrations in different sensory cortices of ASC participants have been shown to be different (Gaetz et al., 2014), suggesting that the differences between brain areas and between neural channels may be due to the complex genetic nature of the disorder.

1.6.4 The role of genes in ASC

Autism spectrum conditions have a strong but complex genetic basis with a large number of genes implicated (Miles, 2011). The past several decades of family genetics studies have shown that ASC is strongly hereditary (Folstein, Rosen-Sheidley, & Street, 2001; Rutter, 2000): concordance rates in monozygotic twins are 60-90% (Rubenstein, 2010). The genetic aetiology of autism is far from being fully understood, however, current accounts suggest that ASC may be a "perfect storm" of genetic make up and environmental influences on the brain as well as on gene expression itself (Ciernia & Lasalle, 2016).

The genes implicated in ASC are typically involved in synapse formation (e.g. neuroligins), neurotransmitter and neuromodulator production (e.g. SLC6A4) and ion transportation (e.g. SLC9A3), amongst other signalling-level processes (Rubenstein, 2010). Genes encoding GABA receptors have also been linked to autism (Coghlan et al., 2012; Shao et al., 2003). It is not surprising, therefore, that the E/I imbalance, and by extension, gain control abnormalities in ASC can also be traced to genetic causes (Rosenberg, Patterson, & Angelaki, 2015; Rubenstein, 2010). This is also demonstrated by the finding that neurotypical parents of ASC children exhibit significantly more variable gamma-band oscillations than neurotypical controls without ASC children (Rojas et al., 2001), suggesting that subclinical populations that possess some of the ASC-related genotype also exhibit neurological differences (Robertson & Simmons, 2013).

Such synapse-level genetic influences would predict that people of the 'broader autistic phenotype', i.e. individuals that exhibit autistic traits but do not have clinical ASC, would also show some of the perceptual hyper- and hypo-sensitivities found in ASC. This has indeed been demonstrated by Robertson & Simmons, (2013) who correlated autism spectrum quotient (AQ) scores (Baron-Cohen, Wheelwright, Skinner, Martin, & Clubley, 2001) with a novel measure of sensory difficulties in the neurotypical population. The findings revealed a very high correlation (R = 0.78) between Sensory Questionnaire scores and AQ. This would predict that if gain control and/or neural noise are in fact implicated in autism, evidence of this may also be detectable in the neurotypical population.

1.6.5 Animal models of ASC sensory abnormalities

Amongst the many rodent and other animal models of autism and related disorders (Ey, Leblond, & Bourgeron, 2011), there is a distinct lack of sensory symptom models. There is, however, one exception to this. LeBlanc et al., (2015) recorded VEPs in heterozygous mutants of gene *Mecp2*, which causes Rett syndrome in humans, as well as VEPs in 34 human children with Rett syndrome. They found comparably reduced evoked potentials in both species. However, individuals with Rett syndrome do not usually exhibit hypo- and hyper-sensitivities typical to autism, meaning that the model may not be generalizable.

In this thesis I present a novel model of ASC in *Drosophila melanogaster*. The genetic model uses an ortholog of the human gene *SLC9A3* (or *NHE9*), which has been linked to several autism spectrum disorders (Kondapalli et al., 2013; Schwede, Garbett, Mirnics, Geschwind, & Morrow, 2013). Nonsense mutations of the gene in humans have been found in individuals with ASC and their parents but not in neurotypicals (Morrow et al., 2008). This model is a good candidate for research into sensory abnormalities in ASC as it is *not* related to GABA-ergic or glutaminergic systems, for which the findings in ASC individuals have so far been mixed. Rather, *SLC9A3* is a sodium-hydrogen ion exchanger and directly influences electrical neural signalling. Furthermore, this model is novel in linking an ASC-related genetic mutation to the sensory symptoms of autism.

The use of *Drosophila* as a model organism may provide a cheap, quick medium in which to carry out future sensory studies of autism. *Drosophila* have been successfully used to model several human neurological disorders, including Parkinson's, Alzheimer's, schizophrenia (Afsari et al., 2014b; Van Alphen & Van Swinderen, 2013) and autism (Hahn et al., 2013). Hahn et al. (2013) used a *dnl2* deficiency in fruit flies to model ASC social behaviour impairments. Mutant *dnl2* flies exhibited differences in acoustic communication, such as mating calls, and social interactions, such as male-male aggression. *Drosophila* are also particularly advantageous as sensory model organisms because of the similarities of neural dynamics and neural hierarchy to those of human visual systems (Behnia & Desplan, 2015; Borst & Euler, 2011; Clark et al., 2014).

1.7 Outline of thesis

The main aim of the empirical chapters of this thesis is to examine suppression and neural noise in the visual system under normal viewing conditions, when altering sensory signals using TMS and in ASC. *Chapter 2* investigates whether and how spontaneous activity in the visual cortex and the brain as a whole influences perception and perceptual decision making. Previous studies (e.g. Ress & Heeger, 2003) have already demonstrated crude differences in activation dependent on the subjects' percept rather than the physical stimulus, but the

evidence is mixed (Mostert et al., 2015). Furthermore, it is unclear what the origin of the neural noise affecting perception is: early sensory or late decision-making. In the experiments of *Chapter 2,* a machine learning algorithm is used to predict subjects' perceptual decisions from EEG and MEG data. The use of EEG and MEG also allows for the examination of the time-course of visual responses and spontaneous neural activity.

Chapter 3 addresses the psychophysical measurement of neural noise and attempts to separate its behavioural effects from neural suppression. So far it is unclear which psychophysical paradigm is best at measuring noise and dissociating it from gain control. This issue is addressed in *Chapter 3*, in which three psychophysical paradigms are empirically evaluated and refined for measuring internal noise. This chapter also investigates individual differences in neural noise and suppression, and develops two convenient and quick ways of measuring these neural processes.

Chapter 4 addresses the issue of distinguishing neural noise and suppression in the neural effects of TMS on perceptual task performance. The short form of the double-pass paradigm, developed in *Chapter 3,* is employed to compare four types of TMS stimulation: spTMS, online rTMS, cTBS and iTBS. This direct comparison of these protocols aims to inform future studies into artificial modulation of neural noise and suppression in sensory systems. Additionally, *Chapter 4* investigates differences in TMS susceptibility by comparing individuals who perceive and do not perceive TMS phosphenes.

The aforementioned methods are crucial for understanding the implications of noise and suppression in typical sensory processing. However, the novel psychophysical methodology can also be used to measure internal noise in relation to sensory symptoms in ASC. *Chapter 5* aims to measure neural noise as a function of number of autistic traits (AQ score) during several sensory and cognitive discrimination tasks: contrast, facial expression intensity and number summation. These tasks allow for the assessment of neural noise at low, mid and high levels of processing and in different areas of the brain and can inform the source of neural noise in sensory perception in ASC.

Chapter 6 explores the other main explanation of ASC sensory symptoms, which suggests that hyper- and hypo-sensitivity in ASC can be explained by differences in neural suppression. This is taken a step further to assess the genetic link to sensory signal processing in ASC by developing a *Drosophila* model of autism. Suppressive neural properties are measured using electrophysiology in neurotypical adults, individuals with ASC and the fruit fly model. Furthermore, *Chapter 6* addresses the development of sensory processing in ASC individuals by assessing VEPs of children/young fruit flies and adults/older fruit flies.

Finally, *Chapter 7* summarises the findings presented in this thesis and discusses the broader implications and future directions.

Chapter 2

Internal noise in contrast discrimination propagates forwards from early visual cortex

This chapter has been adapted from: Vilidaite, G., Marsh, E. & Baker, D. H. (submitted). Internal noise in contrast discrimination propagates forwards from early visual cortex. *Neuroimage.*[1]

2.1 Abstract

Human contrast discrimination performance is limited by transduction nonlinearities and variability of the neural representation (noise). Whereas the nonlinearities have been well characterised, there is less agreement about the specifics of internal noise. Psychophysical models assume that it impacts late in sensory processing, whereas neuroimaging and intracranial electrophysiology studies suggest that the noise is much earlier. We investigated whether perceptually-relevant internal noise arises in early visual areas or later decision

[1] The author, Greta Vilidaite designed the Experiment 2, collected and analysed the majority of the data, the results and wrote the manuscript under the supervision of Dr Daniel Baker. Experiment 1 was designed and some of the analysis was performed jointly with Dr Daniel Baker. Emma Marsh collected some of the data.

[2] The author, Greta Vilidaite collected the data, analysed the results and wrote the manuscript under the supervision of Dr Daniel Baker. The experiments were designed

making areas. We recorded EEG and MEG during a two-interval-forced choice contrast discrimination task and used multivariate pattern analysis to decode target/non-target and selected/non-selected intervals from evoked responses. We found that perceptual decisions could be decoded from both EEG and MEG signals, even when the stimuli in both intervals were physically identical. Above-chance decision classification started <100ms after stimulus onset, suggesting that neural noise affects sensory signals early in the visual pathway. Classification accuracy increased over time, peaking at ~700ms. Applying multivariate analysis to separate anatomically-defined brain regions in MEG source space, we found that occipital regions were informative early on but then information spreads forwards across temporal and frontal regions. This is consistent with neural noise affecting sensory processing at multiple stages of perceptual decision making. We suggest how early sensory noise might be resolved with Birdsall's linearisation, in which a dominant noise source obscures subsequent nonlinearities, to allow the visual system to preserve the wide dynamic range of early areas whilst still benefitting from contrast-invariance at later stages.

2.2 Introduction

Cortical responses to visual stimuli are largely invariant to changes in absolute luminance, being instead determined primarily by stimulus contrast –changes in relative luminance across a region of an image. Consequently, a widely studied perceptual task is the ability to discriminate between visual stimuli of different contrasts. Human contrast discrimination performance is constrained by the nonlinearity mapping physical contrast to internal response, and the intrinsic variability of the neural representation ('internal noise'). Psychophysical, neurophysiological and neuroimaging work have converged on a nonlinearity that is expansive at low contrasts and compressive at higher contrasts (Boynton et al., 1999; Busse, Wade, & Carandini, 2009; Legge & Foley, 1980). However, there is substantially less agreement regarding the details of performance-limiting internal noise.

Most psychophysical models make the assumption that the dominant source of noise for contrast discrimination is additive (i.e. independent of signal strength) and impacts late stages of processing. The primary justification for this arrangement is the observation that a dominant source of noise occurring before a nonlinearity will neutralise the effects of that nonlinearity, rendering it invisible to inspection (Klein & Levi, 2009; Smith & Swift, 1985). Since contrast transduction is observably nonlinear, any early sources of noise must be negligible in comparison to the magnitude of late additive noise. On the other hand, most electrophysiological and neuroimaging studies have suggested that perceptually relevant noise is located in early sensory areas (Campbell & Kulikowski, 1972; Carandini, 2004; Roelfsema & Spekreijse, 2001). Ress and Heeger (2003) demonstrated the influence of early sensory noise by measuring fMRI blood-oxygen-level dependent (BOLD) responses in areas V1-V4 during contrast detection. They found that *false alarms* evoked higher responses than *misses*, suggesting that these areas encoded conscious percepts of the stimuli rather than the presence of the stimulus itself. The origin of the spurious activity in the case of *false alarms* must be neural noise in these early areas. Similarly, several intracranial primate electrophysiology studies have been able to predict the perceptual decisions of monkeys from neural activity recorded in early visual areas (Britten, Newsome, Shadlen, Celebrini, & Movshon, 1996; Britten, Shadlen, Newsome, & Movshon, 1992; Michelson, Pillow, & Seidemann, 2017). This suggests that sensory decisions are influenced by neural noise at an early stage of processing.

In this study, we attempt to resolve this discrepancy by investigating whether the dominant source of neural noise is located in early sensory or later (more frontal) brain areas involved in making decisions. To do this we examined the timecourse of perceptual decision making in a two-interval-forced-choice (2IFC) contrast discrimination paradigm. We used multivariate pattern analysis to decode participants' percepts from EEG (Experiment 1) and MEG (Experiment 2) data. The high temporal resolution (~1ms) of both techniques enabled us to closely examine the timecourse of perceptual decision making, and the spatial resolution of MEG source space allowed us to investigate the involvement of discrete anatomical brain areas.

2.3 Methods

2.3.1 Participants

Twenty-two adults with normal or corrected-to-normal vision took part in Experiment 1 and ten took part in Experiment 2. All participants gave written informed consent. Experiment 1 was approved by the Ethics Committee of the Department of Psychology at the University of York, and Experiment 2 was approved by the York Neuroimaging Centre Ethics Committee.

2.3.2 Stimuli and psychophysical task

Stimuli were horizontally oriented sine wave gratings with a spatial frequency of 1c/deg and a diameter of 10 degrees. The edges of the gratings were blurred by a cosine function. On each trial, two stimuli were presented: a pedestal stimulus of 50% contrast (where percent contrast is defined as $100*(L_{max}-L_{min})/(L_{max}+L_{min})$, where L is luminance), and a pedestal+target stimulus consisting of the 50% contrast pedestal plus a target contrast increment. Five target contrast conditions were used in Experiment 1: 0% (no target), 2%, 4%, 8% and 16%. In Experiment 2 only the 0% (no target) and 16% target contrast conditions were used.

The two stimuli on each trial were presented sequentially for 100ms each, with an inter-stimulus interval between 400ms and 600ms. The inter-trial interval followed the participant's response, and was of variable length between 1000ms and 1200ms as to avoid entrainment effects. The order of target and non-target intervals within trials was counterbalanced. Trials of different target contrasts were intermixed and the order was randomized. Stimulus onsets and participant responses were recorded on the M/EEG trace by way of low-latency digital triggers.

2.3.3 EEG data collection

Event-related potentials were recorded using an ANT Neuroscan EEG system and a 64-channel Waveguard cap with electrodes arranged according to the 10/20

system. Data were digitised at 1kHz using the ASALab software. Stimuli were presented on a ViewPixx display (VPixx Technologies Inc., Quebec, Canada) with a mean luminance of 51cd/m^2 and a refresh rate of 120Hz.

Participants were seated in a darkened room 57cm away from the display. Instructions for the task were to 'indicate the grating that appeared higher in contrast'. They were asked to fixate on a central fixation cross throughout the task and used a mouse to indicate their responses. There were 200 trials per target contrast (1000 trials total). The task was run in 5 blocks of ~8min with short breaks in between.

2.3.4 MEG data collection

MEG signals were recorded using a 4D Neuroimaging Magnes 3600 Whole Head 248 Channel MEG scanner housed in a purpose-built Faraday cage. The data were recorded at 1017.25Hz, with 400Hz Bandwith using a High Pass DC filter. Nine channels were identified as having failed and were removed from all analyses. The location of the head inside the dewar was continuously monitored throughout the experiment using 5 position indicator head coils. Stimuli were presented on an Epson EB-G5900 3LCD projector (refresh rate 60Hz; mean luminance 160cd/m^2) with a 2-stop ND filter, using Psychopy v1.84 (Peirce, 2007).

Participants were seated in a hydraulic chair in front of the projector screen in a dark room. Prior to the task the three dimensional shape of the participant's head was registered using a Polhemus fast-track headshape digitization kit. Five fiducial points were used for this over two registration rounds. If the distance in location between the first and second round was >2mm, the registration was repeated. When successful, the headshape was then traced and recorded using a digital wand. This was later coregistered with T1-weighted anatomical MRI scans of each participant acquired in separate sessions using a 3T GE Signa Excite HDx scanner (GE Healthcare).

Participants fixated on a central fixation cross throughout the task. The experiment was completed in a single block consisting of 240 trials per contrast condition (480 trials in total), with a total acquisition duration of around 20

minutes. A single hand response pad was used to make responses in the experiment.

2.3.5 EEG data analysis

EEG recordings were bandpass filtered (from 0.1Hz to 30Hz) and then epoched into 1 second-long windows (200ms before stimulus onset to 800ms after) for each interval of every trial. Each epoch was then baselined at each electrode independently by subtracting the mean response over the 200ms preceding stimulus onset. ERPs were then sorted by target/non-target intervals for stimulus classification analysis and then again by selected/non-selected intervals for decision classification.

A support vector machine (SVM) with a linear kernel (implemented in Matlab) was used to classify the data independently at each sample point (i.e. in 1ms steps). A second stage of normalization was applied at each time-point and each electrode by subtracting the mean response across all intervals and conditions for that time/sensor combination. The data were then randomly averaged in five subsets of 40 trials for each category (target/non-target or selected/non-selected), of which four subsets were used to train the model and one was used to test it. The SVM algorithm creates a parameter space of all data points and then fits a hyperplane boundary that maximizes the distances between the support vectors of each category (see Figure 2.1). Classifier accuracy for categorising the test data was averaged across 100 repetitions of the analysis (with different random allocations of trials on each repetition), and was repeated for each target contrast condition. Timecourses of classifier accuracy were then averaged across participants, and periods of above-chance performance were determined using a non-parametric cluster correction procedure (Maris & Oostenveld, 2007).
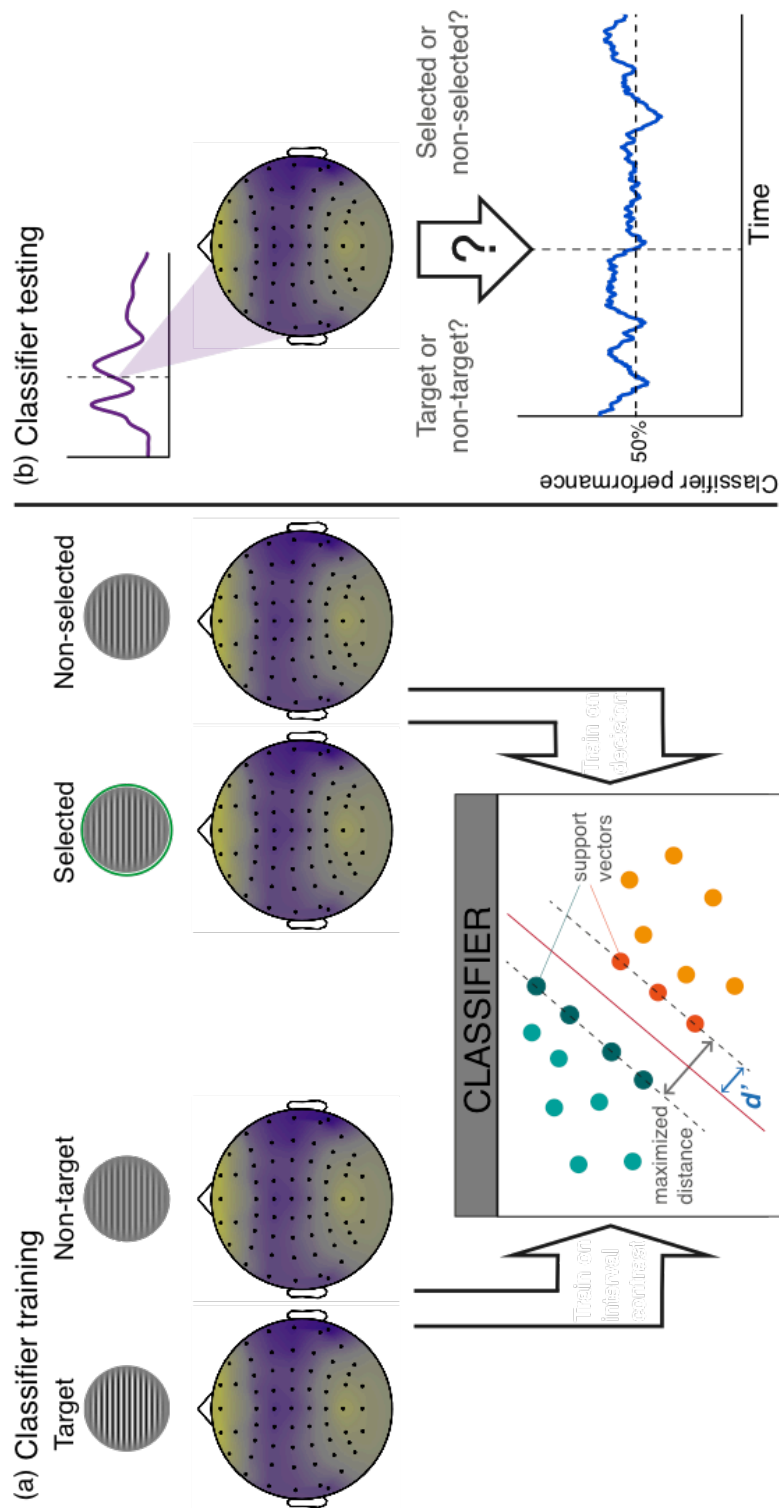
Figure 2.1. Classifier training and testing procedure. At each time point, a pattern of responses across all electrodes (or sensors/sources) for the target and non-target (or selected/non-selected) intervals was fed into the classifier algorithm (panel a, top). The classifier created a hyperplane boundary between the categories (panel a, lower plot). After training, a new pattern of responses at the same timepoint was presented to the algorithm for classification (panel b, top). This was repeated across all time points, and across 100 bootstrap resamples of the data, to build a timecourse of classifier accuracy (panel b, lower panel).

2.3.6 MEG data analysis

Cortical reconstruction and volumetric segmentation was performed with the Freesurfer image analysis suite (http://surfer.nmr.mgh.harvard.edu/) using each individual participant's anatomical MRI scan. Initial MEG analyses were then performed in Brainstorm (Tadel, Baillet, Mosher, Pantazis, & Leahy, 2011). First the MEG sensor array was aligned with the anatomical model of the participant's head using an automated error minimisation procedure. Covariance matrices were estimated from the data, and a head model comprising overlapping spheres was generated. A minimum norm solution was used to calculate a source model, with dipole orientations constrained to be orthogonal to the cortical surface. The model consisted of a set of linear weights at each location on the cortical surface that transformed the sensor space representation into source space.

MEG data were then imported into Matlab using Fieldtrip (Oostenveld, Fries, Maris, & Schoffelen, 2011), bandpass filtered and epoched. Pattern classification was performed in the same way as described for the EEG data in section 2.3.5. This was done using the sensor space representation (with 239 working sensors), the source space representation at approximately 500 vertices evenly spaced across the cortical mesh, and also within discrete regions of cortex defined by the Mindboggle atlas (Klein et al., 2017). The mean number of vertices in each cortical region is given in Table A.1 in the Appendix.
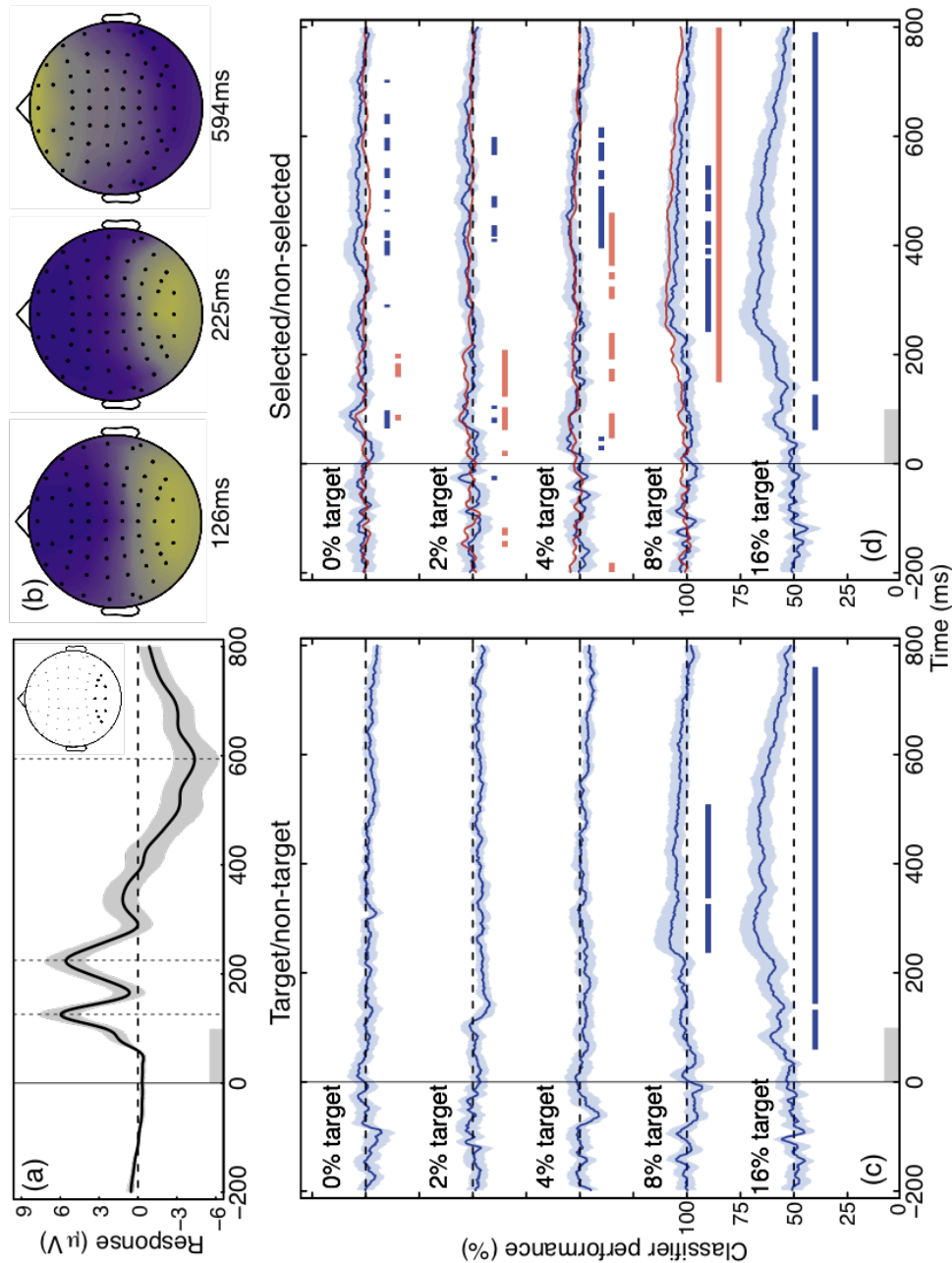
Figure 2.2. EEG data and classifier performance. Panel (a) shows the grand average ERP, pooled over 10 occipital electrodes (marked black in the inset), all contrast conditions and participants, with the shaded region showing bootstrapped 95% confidence intervals across participants. Dotted vertical lines indicate prominent time-points for which scalp topographies of voltages are displayed in panel (b). Target/non-target classification for the five contrast conditions is displayed in panel (c) and selected/non-selected classification in panel (d). Thin blue traces indicate the classifier performance as a function of time. Shaded regions indicate 95% correct confidence intervals across participants. Horizontal blue lines denote times when the classifier performed significantly above chance (determined using a nonparametric cluster correction procedure). The red traces in panel (d) indicate accuracy when the classifier was trained on the 16% target contrast condition data and tested on the remaining four conditions. Grey rectangles in (a,c,d) indicate the period of stimulus presentation.

53

2.4 Results

2.4.1 Experiment 1: EEG reveals above-chance classification of percepts

Task performance in the five target contrast conditions ranged from chance in the 0% target contrast condition (where there was no correct answer as the 'target' interval was determined arbitrarily) to close to ceiling in the 16% target contrast condition (94% correct). Mean event-related potentials (ERPs) averaged over ten occipital electrodes (where the changes in response from baseline were greatest) showed a typical response to brief visual stimulation (Figure 2.2a). Early time-points (126ms and 225ms after stimulus onset) displayed the largest positive response voltages over occipital electrodes. A later time-point (594ms) showed negative voltages in occipital areas and positive voltages in frontal electrodes (Figure 2.2b).

To test whether neural responses encoded stimulus contrast, we trained the classifier to discriminate between target and non-target intervals at each time point. Classification accuracy was not significantly above chance at any time-point in the 0%, 2% or 4% target conditions (Figure 2.2c). In the 8% and 16% conditions the classifier performance rose significantly above chance during several time windows, from 236ms at 8% contrast, and from 59ms at 16% contrast.

We then trained the classifier to discriminate between selected and non-selected intervals. In contrast to stimulus decoding, above chance classification of the decision was found in all five target contrast conditions (Figure 2.2d). Of particular interest was the 0% target condition, in which stimuli in both intervals were physically identical, but could appear different to the participant. In this condition, the choices of the participant could be classified above chance 64 - 98ms after stimulus onset as well as at several time windows after ~300ms. Similar timecourses of above chance classification were also observed in the 2% and 4% target conditions, although the early time cluster was less clear. The longest above chance classification window and highest classifier performance was observed in the 16% contrast condition. The significant time clusters in the

8% and 16% conditions were similar to those in the case of target/non-target classification (~220–300ms and ~50-750ms, respectively).

To test the robustness of decoding perceptual experience, we trained the classifier on responses from the highest target contrast condition and tested it on data from the other four target contrast conditions (red traces in Figure 2.2d). Once again, there were several above chance classification time windows in each target contrast condition, with increasing length and accuracy as a function of target contrast. This suggests that the patterns of neural activity associated with higher physical contrast (in the 16% target contrast condition) were similar to those associated with higher perceived contrasts when the target contrast was lower (e.g. 0%).

2.4.2 Experiment 2: source space decoding is more sensitive than sensor space decoding

In order to obtain better spatial resolution and a higher signal-to-noise ratio we repeated the experiment using MEG with 0% and 16% target contrast conditions. Similarly to Experiment 1, the mean ERPs, averaged over occipital sensors, showed two large early deflections (negative at 112ms and positive at 193ms; Figure 2.3a). Unsurprisingly, these two time-points showed dominant magnetic activity in occipital sensors (upper row of Figure 2.3b). A later sustained positive response that peaked at 583ms showed more wide-spread magnetic fields with a boundary between positive and negative amplitudes over frontal and parietal sensors. In source space, the early components are focussed around early visual regions at the occipital pole, with more widespread frontal activity evident at later time points (lower row of Figure 2.3b).
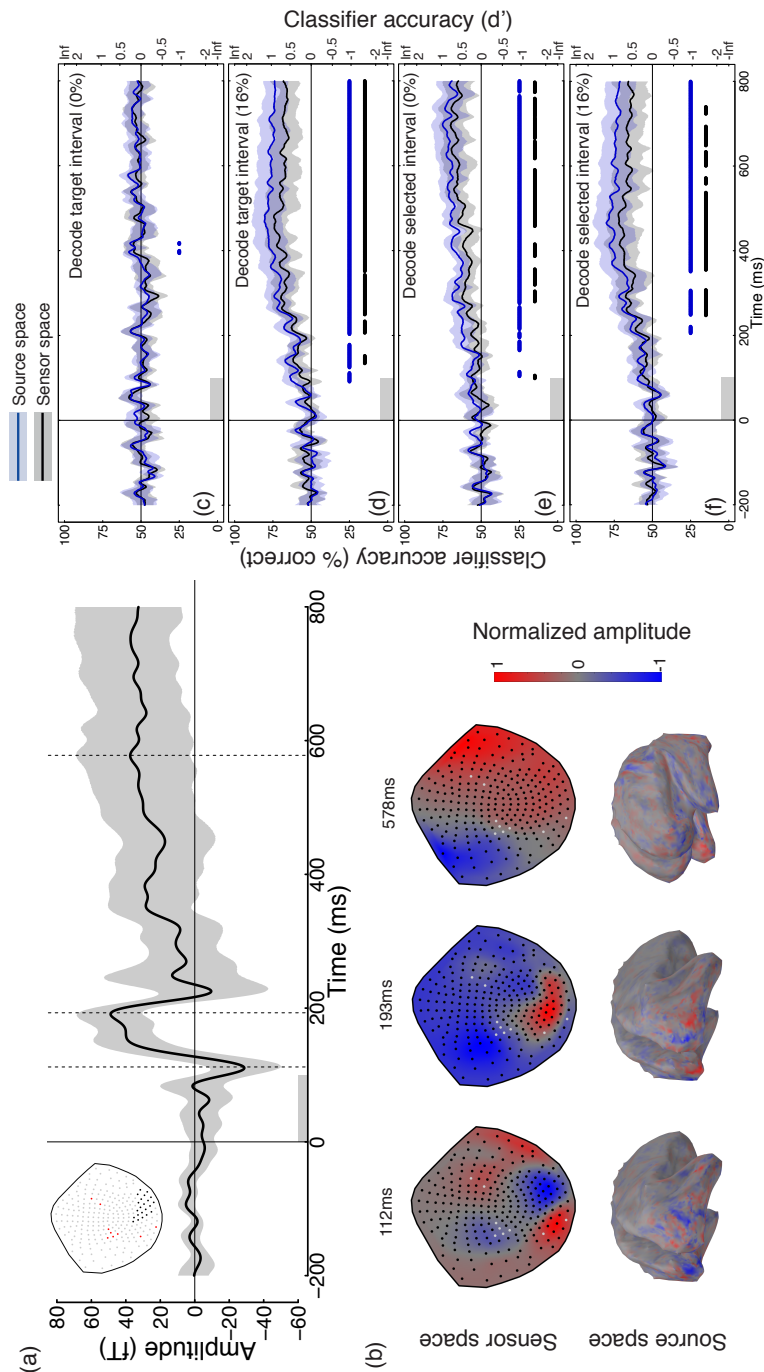
Figure 2.3. MEG data and classifier performance. Panel (a) shows the grand average ERP over the occipital sensors highlighted black in the upper left montage inset (red points indicate broken sensors). Shaded regions show bootstrapped 95% confidence intervals across participants, and dotted lines indicate three time-points for which activity is displayed in panel (b) both in sensor space (upper row) and in source space (lower row). Both representations are averages across participants, with the source space representations projected onto a standard reference (MNI152) brain inflated to 80% smoothness. Panels (c) and (d) show target/non-target classification in 0% and 16% target contrast conditions respectively, and panels e and f display selected/non-selected classification over time. Each panel shows sensor space (black) and source space (blue) classification (traces), 95% confidence intervals (shaded regions) and significant clusters (straight lines). Grey rectangles in (a, c-f) indicate the period of stimulus presentation.

56

The classification results replicated the key findings from Experiment 1. The target/non-target classification in the 16% target contrast condition showed a prolonged window of above chance performance, beginning at around 134ms (sensor space) or 91ms (source space) (Figure 2.3d). The target interval was not classified above chance in the 0% target condition apart from in two very brief time windows, which necessarily constitute Type 1 errors as this condition did not contain a target (and so the 'target' interval was arbitrarily assigned). The selected interval was decoded above chance during several time windows in both target contrast conditions (Figure 2.3e,f). Classification in the 0% target contrast condition reached 70% correct in sensor space and 75% correct in source space, with the earliest significant clusters beginning at 99ms (sensor space) and 104ms (source space).

2.4.3 Classification in anatomically-defined brain regions

We next asked which brain regions contribute information that can be used to determine perception and performance at different time points. We divided the cortex into 31 discrete non-overlapping anatomical regions using the Mindboggle atlas (Klein et al., 2017). Maximal evoked potentials in these regions showed clear differentiation (see Figure A.1). Because regions differed in size, each area contributed a different number of vertices on the cortical mesh for pattern classification (see Table A.1).

At early time points, around 100ms, information in three adjacent regions around the occipital pole (the peri-calcarine region, the cuneus and the lateral occipital cortex) could be used to decode the observer's percept in the 0% target contrast condition (final three traces in Figure 2.4a). Over time, this information spreads forward to frontal and temporal cortex (see Figure 2.4c). By 300ms following stimulus onset, almost the entire brain contains information relevant to the task. This includes regions that do not appear to respond directly to presentation of visual stimuli (i.e. there is no measurable evoked response, see Appendix A). A similar pattern of results is evident in the 16% target contrast condition (see Figure A.2), suggesting that differences in physical and perceived contrast are processed in a similar fashion.
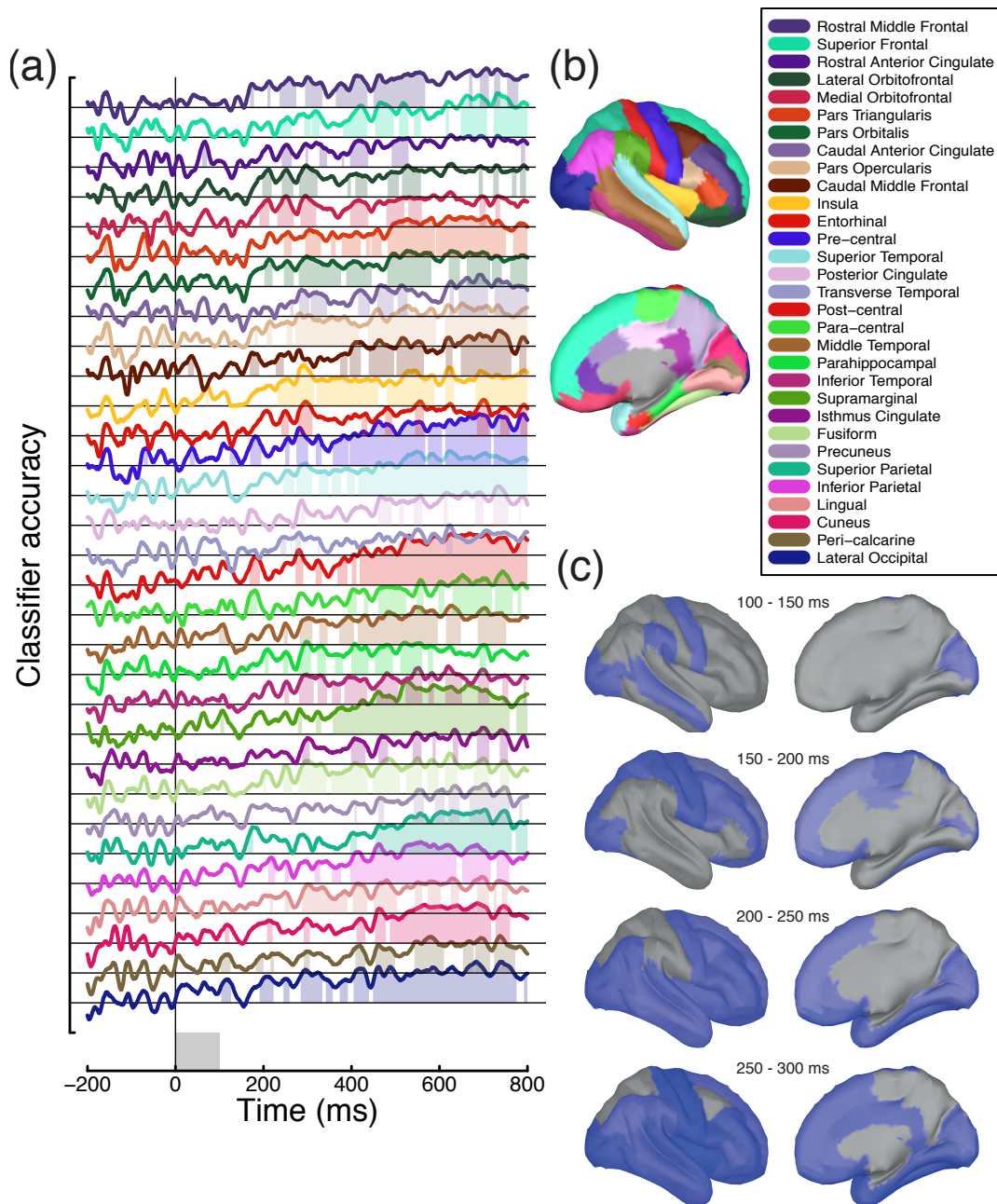
Figure 2.4. Atlas-based classification of decisions in the 0% target condition. Timecourses in panel (a) indicate classifier performance for each brain region, organised from anterior (top) to posterior (bottom) (see legend in panel b). Shaded regions in panel (a) indicate clusters in which classification performance was significantly above chance. In panel (c), regions containing significant clusters within a given time window are shown in blue.

2.5 Discussion

The present study investigated the timecourse and location of perceptually relevant neural noise in sensory processing, using multivariate classification of

58

EEG and MEG data. Our results show that perceptual decisions are encoded in early visual cortex even when the two stimuli in a discrimination task are physically identical. This indicates that perceptually relevant neural noise impacts at the initial stages of processing and affects stimulus encoding in the visual system. We will now discuss the implications of this finding for our understanding of how internal noise influences perceptual decisions.

2.5.1 Superior classification in MEG source space

Classifier performance overall was much higher for MEG data than for EEG data in identical conditions, despite the larger sample size of the EEG study (N = 22 for EEG vs. N = 10 for MEG). This is presumably due to the greater intrinsic sensitivity of MEG sensors, and the greater sampling density across the scalp (N = 64 for EEG vs. N = 239 for MEG). Classifier accuracy was also consistently higher in source space than in the sensor space representation primarily used in previous MEG studies (Cichy, Pantazis, & Oliva, 2014; Clarke, Devereux, Randall, & Tyler, 2015; Mostert et al., 2015). Since the source space representation is a weighted linear combination of activity at the sensors, this might be somewhat surprising. However, the source reconstruction presumably weights out signals from outside the brain (e.g. heart rate, breathing and blinking artefacts, and noise from outside of the scanner), resulting in a cleaner signal. Some form of source localisation may therefore be a useful processing step in future studies attempting multivariate classification of MEG signals. Additionally, combining the source space representation with atlas-based multivariate analysis permits questions to be asked about the information contained in specific brain regions at different points in time.

2.5.2 Single interval versus 2IFC

One distinction between this and most previous studies on the neural correlates of perceptual decision making is that previous work has used single interval (yes/no) paradigms (Hesselmann, Kell, Eger, & Kleinschmidt, 2008; Hillyard et al., 1971; Jolij, Meurs, & Haitel, 2011; Mostert et al., 2015; Ress & Heeger, 2003;

Schölvinck, Friston, & Rees, 2012; Squires, Squires, & Hillyard, 1975), whereas here we used a 2IFC design. Since most psychophysical studies of contrast discrimination have used 2IFC, this choice has more direct relevance to previous work. Additional benefits are that the number of evoked potentials in the selected and non-selected categories were necessarily balanced; and it was possible to compare neural responses to two physically identical stimuli. However in 2IFC participants must hold information about the stimulus from the first interval in memory until after the second stimulus has been presented. This process may account for the sustained patterns of activity that permit classification long after stimulus presentation (see Figures 2.2-2.4). Additionally, 2IFC cannot distinguish between hits and correct rejections (as these comprise 'correct' trials) or between misses and false alarms (incorrect trials), so direct comparisons of these trial categories is not possible in our design. Lastly, 2IFC designs avoid problems with differences in bias (or response criteria) between participants, as pairs of stimuli are compared directly on a given trial (rather than against an internal standard).

2.5.3 Multiplicative noise

An alternative account of contrast discrimination performance at high pedestal contrasts is that transduction is linear but internal noise is signal-dependent (Pelli, 1985). If the dominant source of noise were early and multiplicative, this would avoid any issues relating to Birdsall's theorem, as the transducer could be linear. It has proven difficult to distinguish between the multiplicative and additive noise accounts purely from contrast discrimination experiments (Georgeson & Meese, 2006; Kontsevich, Chen, & Tyler, 2002). At a single neuron level there is well-established evidence of multiplicative noise (Tolhurst, Movshon, & Dean, 1983b), yet it appears that across populations of neurons with different sensitivities the overall noise is effectively additive (Chen et al., 2006). Since evidence from fMRI (Boynton et al., 1999), EEG (Busse et al., 2009) and psychophysics (Kingdom, 2016) all argue strongly against a linear transducer, we think this explanation is unlikely to account for the body of available data.

2.5.4 Resolving early noise and Birdsall's theorem

Early noise has typically been considered at very early stages, including photoreceptor noise in the retina (Barlow, 1962). Late additive noise is often assumed (either implicitly or explicitly) to be added at the decision stage, long after the nonlinearities of early visual processing (Cabrera, Lu, & Dosher, 2015; Mueller & Weidemann, 2008). The results here point to a perceptually-relevant source of noise that is present in the early evoked response, at around 100ms or earlier. However we note that classification performance improves after this point in processing, reaching a maximum around 700ms after target onset (see Figure 2.3e). This is consistent with a cascade of multiple noise sources at different stages of processing. Since mathematical treatment of complex systems involving multiple nonlinearities and noise sources is currently lacking, it is unclear what implications this would have for the visibility of early nonlinearities.

One possibility is that a strong source of noise occurs immediately after the initial contrast transduction nonlinearity in V1, leaving that nonlinearity visible but obscuring later ones. This would explain why psychophysical contrast perception maps closely onto the neural response from early visual areas (Baker & Wade, 2017; Barlow, Hawken, Parker, & Kaushal, 1987; Boynton et al., 1999), but not the highly compressive contrast-invariant response in later regions (Avidan et al., 2002; Rolls & Baylis, 1986). Indeed, this might enable the visual system to harness the properties of Birdsall linearisation to preserve the dynamic range of early representations through later processing (that is more compressive) when making comparisons across stimuli (as in a discrimination paradigm). Object recognition, and other operations that benefit from invariance to features such as contrast, position and size, but do not require comparisons across multiple stimuli, would be immune to the Birdsall effect and benefit from the later nonlinearities. Furthermore, a strong early source of noise would make the study of later 'mid-level' visual processes much more challenging, perhaps explaining why vision research has typically focussed on earlier mechanisms and can be caricatured as being 'stuck' in V1 (Graham, 2011; Peirce, 2007).

2.5.5 Conclusion

To summarise, in this study we investigated the timecourse of the neural operations involved in contrast discrimination. We demonstrated that internal noise impacting early in time and in the visual pathway can affect sensory processing and perceptual decisions. Our novel application of multivariate analysis methods to spatially-parcellated MEG source space representations offers the capability of studying how the brain represents information in both space and time.

Chapter 3

Individual differences in internal noise are consistent across two measurement techniques

This chapter has been adapted from: Vilidaite, G., & Baker, D. H. (2016). Individual differences in internal noise are consistent across two measurement techniques. *Vision Research*, in press.[2]

3.1 Abstract

Internal noise is a fundamental limiting property on visual processing. Internal noise has previously been estimated with the equivalent noise paradigm using broadband white noise masks and assuming a linear model. However, in addition to introducing noise into the detecting channel, white noise masks can suppress neural signals, and the linear model does not satisfactorily explain data from other paradigms. Here we propose estimating internal noise from a nonlinear gain control model fitted to contrast discrimination data. This method, and noise estimates from the equivalent noise paradigm, are compared to a direct psychophysical measure of noise (double- pass consistency) using a detailed dataset with seven observers. Additionally, contrast discrimination and double-

---

[2] The author, Greta Vilidaite collected the data, analysed the results and wrote the manuscript under the supervision of Dr Daniel Baker. The experiments were designed jointly with Dr Daniel Baker.

pass paradigms were further examined with a refined set of conditions in 40 observers. We demonstrate that the gain control model produces more accurate double-pass consistency predictions than a linear model. We also show that the noise parameter is strongly related to consistency scores whereas the gain control parameter is not; a differentiation of which the equivalent noise paradigm is not capable. Lastly, we argue that both the contrast discrimination and the double-pass paradigms are sensitive measures of internal noise that can be used in the study of individual differences.

3.2 Introduction

Internal noise is intrinsic to the assumptions of signal detection theory (Green & Swets, 1974; Macmillan & Creelman, 2005) and signal degradation due to internal variability is evident in both electronic systems (e.g. amplifiers) and living organisms. Neural internal noise is inherent to sensory neurons and acts as a limiting factor in signal transduction (Faisal et al., 2008). In psychophysics, this leads to the psychometric function taking the shape of a sigmoid rather than transitioning sharply between sub-threshold and supra-threshold stimuli (Burgess & Colborne, 1988). A substantial body of research has attempted to measure noise psychophysically for many different visual cues, including luminance (Barlow, 1956), orientation (Jones, Anderson, & Murphy, 2003), shape (Sweeny et al., 2011), motion perception (Barlow & Tripathy, 1997) and contrast (Burgess & Colborne, 1988; Lu & Dosher, 2008; Pelli, 1985).

Differences in internal noise have been reported in normal human development (Skoczenski & Norcia, 1998) and ageing (Pardhan, 2004) and in clinical conditions such as amblyopia (Levi, Klein, & Chen, 2007), macular degeneration (McAnany, Alexander, Genead, & Fishman, 2013) and autism (Dinstein et al., 2012; Milne, 2011). Furthermore, individual differences in contrast sensitivity for neurotypical adults have also been explained as being partly due to noise (Baker, 2013). In order to assess differences in internal noise levels between observers it is crucial to use a paradigm that is capable of distinguishing internal noise effects from other performance-influencing factors (such as sensitivity, suppression,

uncertainty or efficiency). We now discuss several candidate psychophysical methods that might be used to achieve this aim.

3.2.1 Equivalent noise

Most commonly, the influence of internal noise on psychophysical task performance is assessed by purposefully degrading the performance of the observer by presenting external stimulus noise (such as 2D isotropic white noise; Pelli, 1985). The most widely adopted method is the equivalent noise (EN) paradigm (Legge et al., 1987; Pelli, 1985) which observers perform a two-alternative-forced- choice (2AFC) detection experiment with white noise masks shown in both intervals and a target stimulus added to one. Detection thresholds are obtained for several mask contrast levels, and the mask noise level at which performance begins to decline is taken as an estimate of the amount of internal noise in the system.

The EN paradigm assumes a linear amplifier model (Pelli, 1985), that defines thresholds as:

$$C_{thresh} = \frac{\sqrt{\sigma_{ext}^2 + \sigma_{int}^2}}{\beta} \qquad \text{(Eq. 3.1)}$$

where C_{thresh} is the threshold target contrast level, β is a parameter reflecting efficiency (Lu & Dosher, 2008) and σ_{ext} and σ_{int} are the levels of external (stimulus) noise and internal noise respectively. The model posits a linear relationship between stimulus input and signal output, with additive internal noise. External stimulus noise introduces variability into the detecting mechanism that impairs performance at high noise contrasts (when $\sigma_{ext} > \sigma_{int}$).

However, there is abundant evidence that the relationship between stimulus contrast and visual response is not linear but rather accelerating at low contrasts and saturating at high contrasts (Baker, 2013; Boynton et al., 1999; Legge & Foley, 1980; Tsai et al., 2012). Furthermore, due to the broad frequency and orientation profile of white noise masks, non-target channels will also be activated

by the mask and in turn inhibit the target channel. It has recently been demonstrated that broadband white noise has a strong suppressive effect similar to that of narrowband cross-oriented masks (Baker & Vilidaite, 2014). This suggests that impaired performance at high mask contrasts in the EN paradigm could be due to cross-channel suppression from white noise rather than within-target-channel noise (Baker & Meese, 2012).

One potential solution to this is to inject variability only to the detecting channel tuned to the target. This is possible by removing from the mask all off-channel spatial frequency and orientation information. The result is a mask that is spatially identical to the target grating, but with a randomly selected contrast – a 'zero-dimensional' (0D) noise mask (Baker & Meese, 2012). Similar approaches have been previously used in luminance (Cohn, 1976), orientation (Dakin et al., 2009) and auditory tone perception (Jones, Moore, Amitay, & Shub, 2013). The contrast level of the mask is randomly sampled from a Gaussian distribution to create interval-by- interval contrast jitter. It has been shown that this type of mask produces stronger masking effects than white noise (Baker, 2013; Baker & Meese, 2012), and does not show evidence of cross-channel suppression, so it may offer a more suitable alternative to white noise masks.

However, it has been pointed out (Allard & Faubert, 2013) that zero-dimensional noise masks tend to produce near perfect efficiency, implying that estimates of internal noise using this paradigm are determined entirely by detection thresholds in the absence of a noise mask! In addition, the EN paradigm still assumes a linear model that is at odds with contemporary accounts of contrast transduction (e.g. Baldwin, Baker, & Hess, 2016). In order to take into account the nonlinearity of the human visual system, paradigms and models that have more accurate underlying assumptions must be considered.

3.2.2 Pedestal masking

One possible alternative to the equivalent noise approach is to obtain an estimate of internal noise by measuring and modelling discrimination data. This type of noise estimate has been used in auditory research where the fitted noise parameter

was shown to be a good predictor of other measures of internal noise in the auditory system (Buss, Hall, & Grose, 2009; Jones, Moore, Amitay, & Shub, 2013). The same method can be implemented in visual contrast discrimination (Baker, 2013; Baldwin et al., 2016). In this paradigm, a fixed contrast pedestal stimulus is presented in both intervals of a 2AFC experiment with a target contrast increment added to one of the intervals. A staircase procedure is used to obtain discrimination thresholds at several pedestal contrast levels. The resulting function takes the shape of a dipper (Nachmias & Sansbury, 1974), with a facilitatory effect at low pedestal levels and threshold elevation from masking at higher levels of pedestal contrast. The contrast response function underlying the dipper (e.g. Boynton, Demb, Glover, & Heeger, 1999) is well described by a transducer nonlinearity (Legge & Foley, 1980; Tsai et al., 2012) adapted from the Naka-Rushton equation (Naka & Rushton, 1966):

$$resp = \frac{C^p}{Z + C^q} + \sigma_{int} \qquad \text{(Eq. 3.2)}$$

where C is the stimulus contrast, p and q are exponents that produce an accelerating response across low contrasts and a compressive response across high contrasts, Z is the saturation constant (the gain control parameter) and σ_{int} is proportional to the participant's internal noise. To simulate contrast discrimination experiments, a response (*resp*) is generated for each of the two intervals (with zero mean Gaussian noise added to each), and the interval with the larger response is selected. The influences of gain control and internal noise can be differentiated (see Figure 3.1): increasing the gain control parameter (Z) elevates thresholds only at low pedestal levels, whereas changing the noise parameter (σ_{int}) shifts the function vertically at all pedestal contrasts. Fitting the model to empirical contrast discrimination data will therefore provide an estimate of internal noise that is decoupled from estimates of sensitivity (or gain). However, it is currently unknown how accurate noise estimates using this method are, so it would be useful to compare it to a more direct measure.
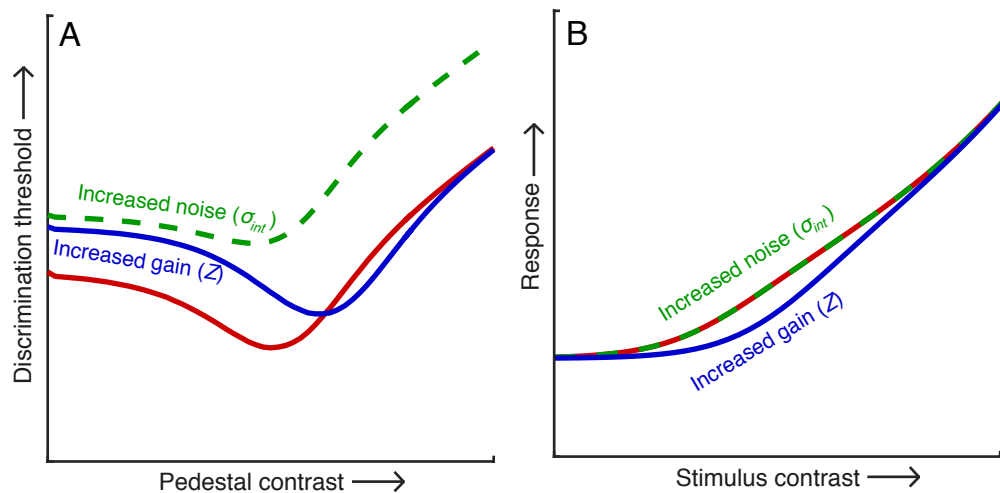
Figure 3.1. **Model predictions for contrast discrimination with different model parameters.** The red curve shows a typical dipper function for reference (parameter values: σ_{int} = 0.2, Z = 8); the green curve shows the vertical shift of the whole dipper function when the noise parameter (σ_{int}) is increased by a factor of 3.5; and the blue curve shows the diagonal shift of the function when the gain control parameter (Z) is increased by a factor of 4 (at low pedestal contrasts thresholds increase, but the dipper handles converge at high contrasts).

3.2.3 Double-pass consistency

When there is no variability in the stimulus, most variability in an observer's responses must be due to internal noise. One way of estimating internal noise, therefore, is to present a sequence of noisy stimuli multiple times and look at the consistency of responses across repetitions. This method is considered to be a direct way of measuring internal noise (Burgess & Colborne, 1988; Lu & Dosher, 2008), and is typically performed with two passes (and referred to as the double pass method). Double-pass methods are well established both in auditory (Green, 1964; Jones, Moore, Amitay, & Shub, 2013) and visual modalities (Burgess & Colborne, 1988; Hasan, Joosten, & Neri, 2012; Lu & Dosher, 2008), and have also been extended to more cognitive tasks (Diependaele, Brysbaert, & Neri, 2012). To estimate double pass consistency for contrast transduction, a 2AFC detection-in-noise experiment is run twice with identical sequences of noise in the two passes. If the consistency of responses between passes is high, there is low internal noise, if the consistency is low, the internal noise is high.

3.2.4 Aim

All three of the above-mentioned paradigms are widely used in contrast perception research, with double-pass and equivalent noise specifically aimed at estimating internal noise. There has been some attempt to compare pedestal masking and EN paradigms (Baker, 2013; Baldwin et al., 2016) as well as EN and double-pass (Baker & Meese, 2012; Lu & Dosher, 2008). However, estimates of internal noise from pedestal masking and double-pass consistency experiments are yet to be compared. Given that internal noise is an important limiting factor in signal transduction and an underlying cause of individual and, in clinical research, group differences it is of importance to determine the most accurate way of measuring it. This paper compares all three methods with detailed data sets for seven observers and a further investigation of double-pass and pedestal masking paradigms with a larger sample.

3.3 Methods

3.3.1 Observers

Seven observers (three males) completed Study 1 and 46 observers (16 males) completed Study 2. Six of the 46 observers were excluded from the analysis as their performance was at chance for most or all of the conditions, suggesting either poor understanding of the task or an inability to follow instructions. All participants were reportedly neurotypical adults and reported normal or corrected to normal vision. Informed consent was obtained from all observers.

3.3.2 Materials

The stimuli were displayed on a gamma corrected Iiyama VisionMaster Pro 510 monitor running at 100Hz. To enable accurate rendering of low contrast stimuli, we used a ViSaGe device (Cambridge Research Systems Ltd., Kent, UK) running in 14- bit mode. Responses were made using a computer mouse.

The stimuli were patches of 0.5c/deg sine-wave grating with horizontal stripes, windowed by a circular raised cosine envelope (i.e. a circle blurred by a cosine function, with a full-width at half-height of 2.4 degrees, and blur width of 0.6 degrees, see Figure 3.2 for examples). The equivalent noise and double-pass experiments used zero-dimensional (0D) noise masks (see Baker & Meese, 2012). The mask was identical to the target and had a contrast level randomly drawn from a Gaussian distribution of contrasts centred around 0% (negative contrasts constitute a polarity inversion). Stimuli flickered sinusoidally between zero and their maximum contrast at a rate of 7Hz (three cycles, lasting 430ms), preserving the phase polarity of the stimulus during presentation. Contrast levels were expressed as percent Michelson contrast ($C_\% = 100*(\frac{L_{max}-L_{min}}{L_{max}+L_{min}})$, where L_{max} and L_{min} are the maximum and minimum luminances of the grating), or in decibels (dB), defined as $C_{dB} = 20*\log_{10}(C_\%)$.

3.3.3 Procedure

Experiments in Study 1 were completed over several days in sessions lasting 30-60 minutes. All observers completed the experiments in the same following order: pedestal masking, noise masking and double-pass experiment. Study 2 was completed by each individual in a single 50-60 minute session. The pedestal masking took approximately 20 minutes and the double-pass experiment took 30-35 minutes to complete with short breaks in between blocks. For all experiments, the observers sat in a darkened room 105cm from the monitor with their heads supported by a chin rest. The instructions for all experiments were to 'Choose the interval in which the bar in the middle looks brighter'. The stimuli were presented foveally, along with a continuously presented central fixation cross. Each interval within a trial was presented for 430ms with an inter-stimulus interval of 400ms.
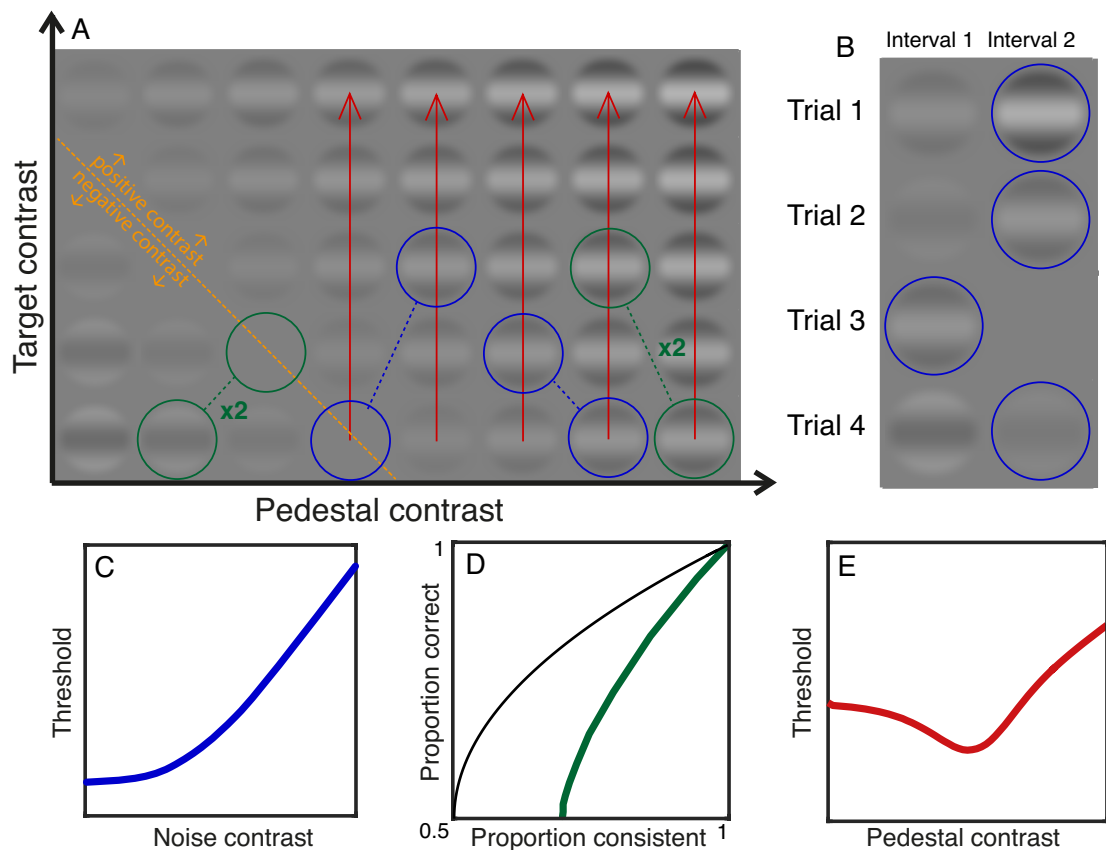
Figure 3.2. Illustration of methods used in the study with relation to a common contrast intensity space (panel A). For the equivalent noise paradigm (model curve shown in panel C) two independent mask contrast samples are selected for each trial with the target contrast being added to one sample. Example selections for two trials can be seen in blue circles (panel B) with blue dotted lines connecting intervals within a trial. The same procedure applies for the double-pass paradigm (model curve shown in panel D) with green circles and dotted lines showing example stimuli used. Each pair of contrasts in the double-pass experiment was presented twice. Panel B shows four more examples of trials for both EN and double-pass experiments with blue circles indicating the higher positive contrast that the observer would be expected to select. The red arrows in panel A indicate the range of possible target values for each pedestal contrast in the pedestal masking experiment. The orange dotted line indicates 0% contrast below which the sine-wave gratings reverse in phase polarity. Thresholds for contrast discrimination experiments follow a characteristic dipper shape (panel E).

3.3.3.1 Study 1 methods

3.3.3.1.1 Equivalent noise experiment

Each trial contained a mask only interval and a mask + target interval (example in Figure 3.2B). The mask contrast was drawn from a normal distribution with a mean of 0 and standard deviations of 0, 0.5, 1, 2, 4, 8, 16 and 32% Michelson contrast. Negative contrast values reversed the polarity of the stimulus. A 3-down-

1-up staircase procedure with a step size of 3dB controlled the target contrast. The staircase terminated after the lesser of 12 reversals or 70 trials and was repeated 3 times. We used Probit analysis (Finney, 1971) to fit a psychometric function to the pooled data across all repetitions, to estimate a threshold at 75% correct.

3.3.3.1.2 Double-pass experiment

The method of constant stimuli was used in these experiments. The stimuli had the same temporal and spatial configuration as in the equivalent noise experiments, with the mask and target + mask intervals presented in a random order on each pass (see Hasan, Joosten, & Neri, 2012). In the second pass, the samples of noise used in the first pass were repeated. Three levels of noise standard deviation were used with six target contrast levels each: i) 0% mask, target levels 0.5, 0.7, 1, 1.4, 2 and 3%; ii) 2% mask, target levels 1, 1.4, 2, 3, 4 and 5.6%; iii) 32% mask, target levels 8, 11, 16, 22, 32, 45%. Each mask standard deviation also had a target absent condition where the target contrast was set to 0% (21 conditions in total). Each condition had 200 trials (100 trials in each pass). The accuracy of responses was calculated as the proportion of correct responses out of all 200 trials in a condition; the consistency scores were calculated as the proportion of consistent responses across the two passes (Burgess & Colborne, 1988). For target absent trials nominal accuracy was calculated relative to an arbitrarily determined 'target' interval.

3.3.3.1.3 Pedestal masking experiment

Pairs of three-down-1-up staircases (terminating after 12 reversals or 70 trials) were used to obtain 75% correct thresholds (estimated using Probit analysis) for 9 pedestal contrasts (0.25, 0.5, 1, 2, 4, 8, 16, 32, 64%) and also in a detection condition where the pedestal contrast was set to zero. Participants completed four repetitions of each condition.

Equivalent noise data were fitted with the linear amplifier model (Eq. 3.1) with two free parameters (β and σ_{int}) for each observer and for the average data across

observers. The gain control model (Eq. 3.2) was also used to simulate and predict EN masking data (100,000 stimulated trials for each condition) with p and q parameters fixed at 2.4 and 2 (Legge & Foley, 1980) in order to keep the same number of free parameters as for the LAM. The two free parameters were the saturation constant (Z) and the internal noise (σ_{int}) parameters. Data from each observer and the average were fitted 50 times each with random starting values and the model that produced the lowest mean square error was chosen. This same procedure was used for fitting dipper data in Study 2. All models were fitted using a downhill simplex algorithm.

Pedestal masking data were fitted with the gain control model using a downhill simplex algorithm with the same two free parameters. The parameters obtained from modelling EN with LAM and pedestal masking with the gain control model were then used to simulate the double-pass experiment (100000 simulations with the gain control model and 1000000 simulations with LAM) and compare the predictions to the empirical data.

3.3.3.2 Study 2 methods

In Study 2, a smaller selection of the most informative conditions from the pedestal masking and double-pass experiments were run on a large number of observers in order to further compare the two methodologies. For pedestal masking, the same procedure and stimuli were used as in Study 1, albeit with pedestal contrast levels of 0, 2, 8 and 32%. Staircases for each condition were repeated 3 times. The double-pass procedure in Study 2 was kept the same, however, there were only two conditions: no target and 4% contrast target. In both conditions the noise standard deviation was 4% contrast. All observers completed the pedestal masking experiment first.

3.4 Results

The raw data are available online at:
https://dx.doi.org/10.6084/m9.figshare.3824250

3.4.1 Study 1

3.4.1.1 Equivalent noise

Results for the equivalent noise paradigm had the typical form, with thresholds increasing as a function of noise contrast, and the upper limb of the masking functions having a slope of 1 (Figure 3.3).
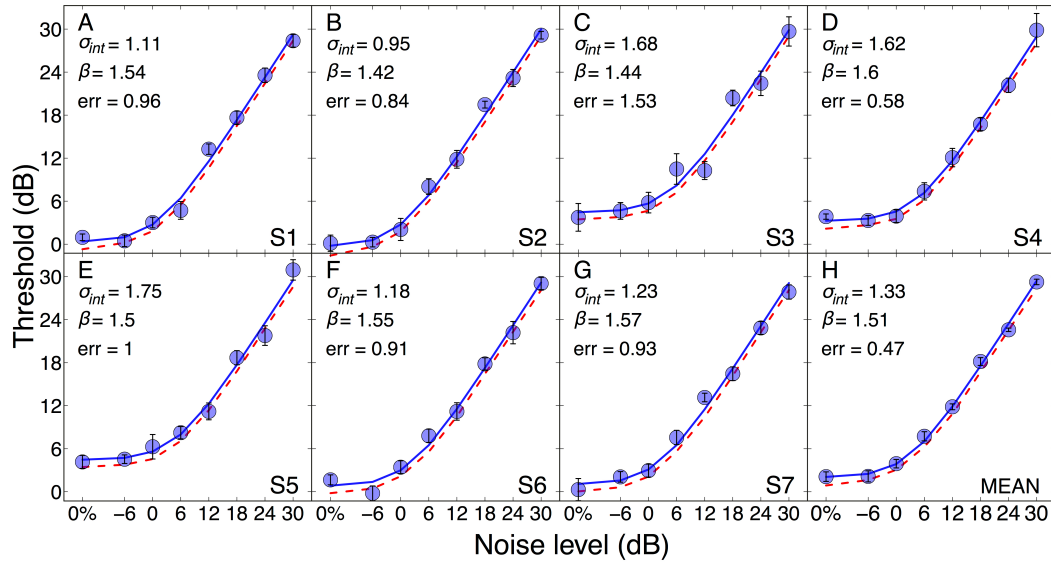
Figure 3.3. **Noise masking thresholds from the equivalent noise experiment plotted as a function of noise contrast level.** Blue dots show data points for all observers (panels S1-S7) with error bars indicating the standard error of the Probit fits. In panel H data points show the mean data averaged across observers (error bars show ±1SE across observers). Blue curves in all panels show simulated fits of the linear amplifier model and red dashed curves show simulated predictions of the gain control model. Values of parameters σ_{int} and β and the RMS error is shown at the top left corner of each panel.

The largest differences between participants can be seen at low noise levels (up to 0dB) where thresholds range between 0 and 5dB. At higher mask contrasts, all thresholds converge on the line of unity, x = y, consistent with previous reports that observer efficiency is near perfect for this task (Allard & Faubert, 2013). Best fits of the LAM (blue curves) described the data well (all RMS errors < 1.54dB), but estimates of the efficiency parameter (β) were similar across subjects (see values in each panel of Figure 3.3). This means that the only meaningful degree of freedom in this model was the internal noise parameter (σ_{int}), which determined both detection threshold and the inflection point on the noise masking function.

3.4.1.2 Pedestal masking

Figure 3.4 shows contrast discrimination data for 7 observers and their average, all of which display the characteristic 'dipper' shape first reported by Campbell & Kulikowski (1966).
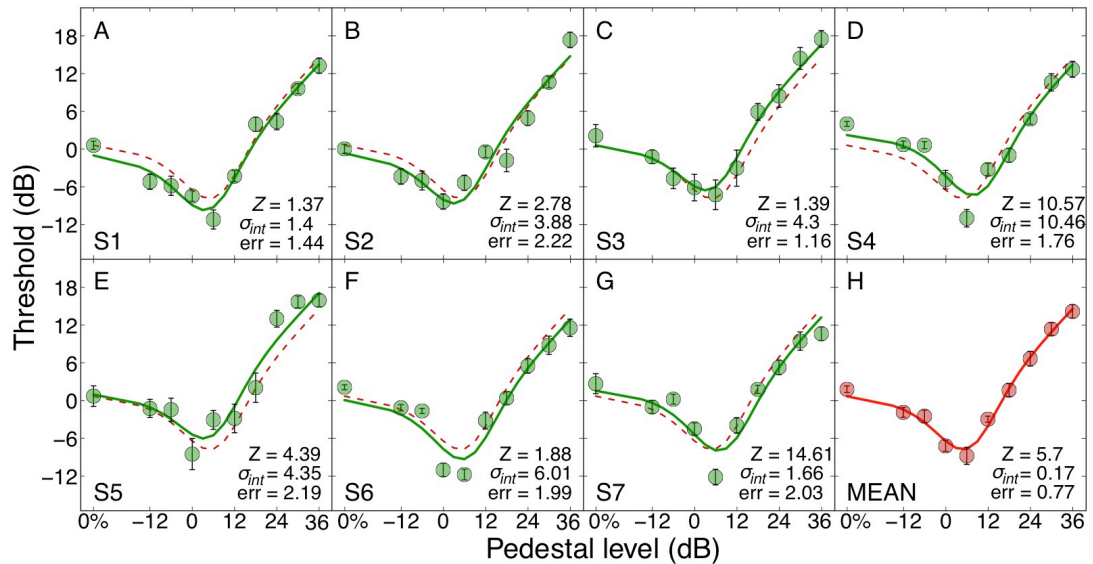
Figure 3.4. **Individual and mean contrast discrimination curves.** Thresholds at 75% correct plotted against the levels of pedestal contrast for each observer (green dots) and the mean data across observers (red dots, right-most bottom panel). Error bars in panels S1-S7 show ±1SE of the Probit fit; error bars in panel H show ±1SE across observers. Green curves are the gain control model fits with two free parameters for each observer separately; red dashed curves are the model fit to the mean data and can be used as a reference for how different values of saturation constant (Z) and internal noise (σ_{int}) influence the curves. Values of both parameters used for each model are indicated in the lower right of each panel along with the RMS error in dB units.

The gain control model with two free parameters was fitted to each observer's data individually and also to the mean data (fits to the mean data are duplicated in each panel with a red dashed curve, for comparison with the data of each observer). The model provided good fits to the data for all subjects (root mean square errors of less than 2.3dB). There is a noticeable influence of the gain control parameter (Z) on the threshold at the first four levels of pedestal contrast. For example, S4 with $Z = 10.57$ has a much higher threshold at low pedestal conditions compared to the mean whereas S2 with a lower $Z = 2.78$ has lower thresholds at those pedestal levels.

3.4.1.3 Double-pass consistency

Accuracy and consistency scores were calculated for each noise mask and target contrast condition in the double pass experiment (Figure 3.5). Increasing the variance of external noise produced increasingly consistent responses, whereas increasing target contrast levels produced increasingly accurate responses. Simulated predictions for double-pass data were made using LAM fits to the EN data and gain control model fits to the pedestal masking data individually for each observer. For the majority of the observers the predictions for 0% and 2% mask contrasts were reasonably accurate from both the LAM and the gain control model. Both models produced comparatively poorer predictions for the 32% mask contrast conditions, tending to overestimate the level of consistency relative to that in the data (see also Lu & Dosher, 2008). The errors between double-pass data points and model predictions were calculated and averaged over conditions for each observer. A paired-samples t-test showed the gain control model predictions had significantly smaller errors (mean = 0.11, SD = 0.03) than the LAM predictions (mean = 0.14, SD = 0.01, t = -4.14, p = 0.004).
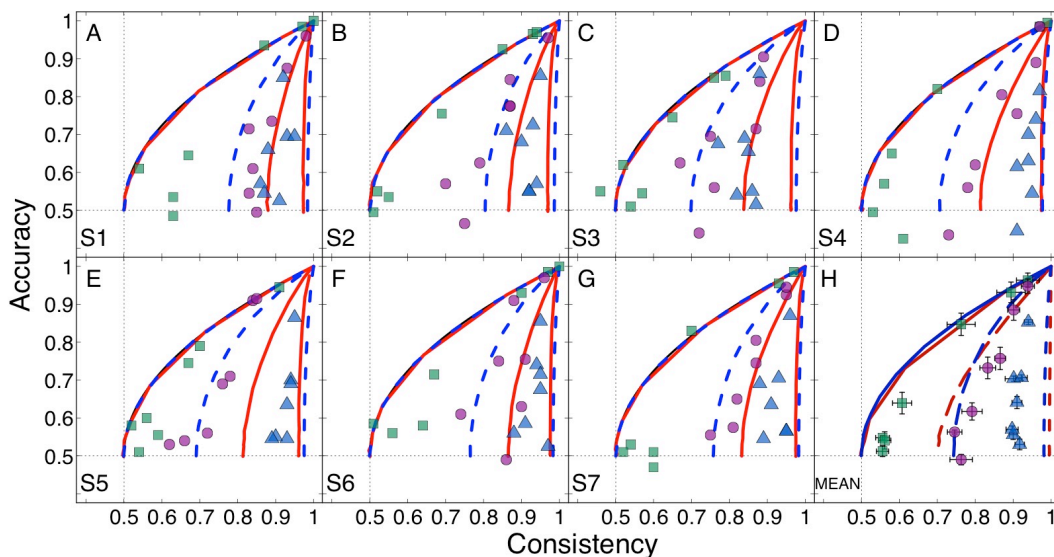
Figure 3.5. **Double-pass consistency and accuracy for the seven observers and their average** (panel H) at (i) 0% (green squares), (ii) 2% (purple circles) and (iii) 32% mask standard deviation (blue triangles). Target contrast levels are not specified on the plots but generally follow an upward trend with increasing target contrast. Red curves show gain control model predictions for the three mask contrast levels for each observer and mean data; blue curves show LAM predictions. The error bars in panel H indicate ±1SE of the mean for accuracy (vertical) and consistency (horizontal) across observers.

Akaike's Information Criteria (AIC = n * log(RMS) +2p, where n is the number of data points modelled, RMS is the root mean squared error and p is the number of free parameters in the model) were calculated for these the two original models as well as for LAM with a single free parameter (β fixed at 1) and for a four free parameter gain control model (exponents p and q were also free). The gain control model with two free parameters performed best (AIC = 20.17) compared to other models even when the number of free parameters is taken into account.

As it is difficult to draw population-level inferences about the consistency of noise measurements on a between observer basis with only seven observers, the conditions that seemed to show the strongest individual differences were selected for a follow up experiment with 40 observers.

3.4.2 Study 2

3.4.2.1 Pedestal masking

Using similar methods to Study 1, contrast discrimination thresholds were obtained for 40 observers (Figure 3.6A) and the same modelling procedure was implemented as described above. Thresholds varied between observers by 12dB (a factor of 4) or more at all pedestal levels. Pearson's correlations were carried out between the Z and σ_{int} parameters obtained from the gain control model fits and the thresholds at each pedestal level of the dipper function in order to examine the influence of these parameters at different pedestal contrasts.

Scatterplots for these correlations are shown in Figure 3.7, however, most importantly, the Z parameter significantly correlated with individual thresholds at detection (no pedestal condition; R= 0.60, p < 0.0001) and at low pedestal contrast (R = 0.56, p = 0.0002) but did not significantly correlate at higher pedestal contrasts of 18 and 30dB (R = -0.13, p = 0.426 and R = -0.17, p = 0.283 respectively). This is in line with the prediction (see Figure 3.1) that changes in gain produce changes in threshold only at low pedestal contrasts. Conversely, the internal noise parameter σ_{int} significantly correlated with thresholds throughout the dipper function (0.69 ≤ R ≥ 0.87, p < 0.0001) demonstrating that changes in the internal noise parameter shift the whole dipper function vertically in

proportion to the magnitude of internal noise.
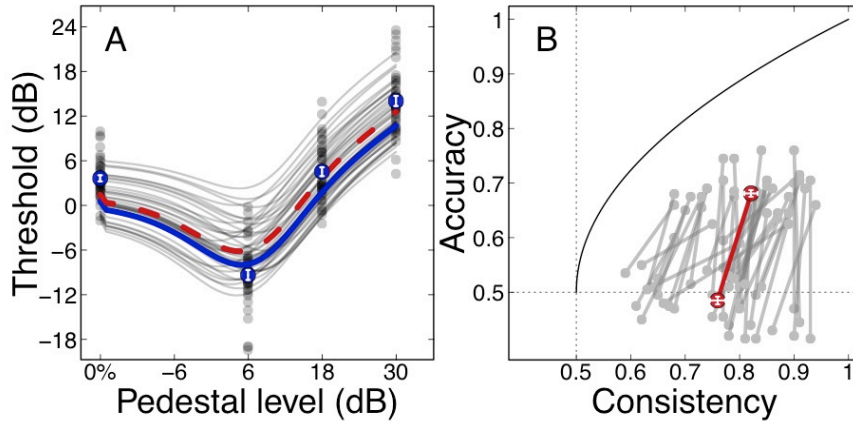
Figure 3.6. **Contrast discrimination and double-pass data in Study 2.** Panel A. Contrast discrimination thresholds as a function of pedestal contrast. Grey dots show data points for each of the pedestal levels for all 40 observers and grey lines show the gain control model fits to each observer's data. Blue dots show the mean of 40 observers with white error bars signifying inter-observer standard error of the mean. Thicker curves show the model fit for the 40 observers (blue) and model fit for 7 observers from Study 1 (red dashes). Panel B. Accuracy and consistency scores from the double-pass experiment of Study 2 for all 40 observers (grey dots and lines) and mean scores (red), with white error bars showing inter-observer standard error of the mean. Dotted lines show chance performance levels and the black curve shows the expected performance with no external noise (Klein & Levi, 2009).
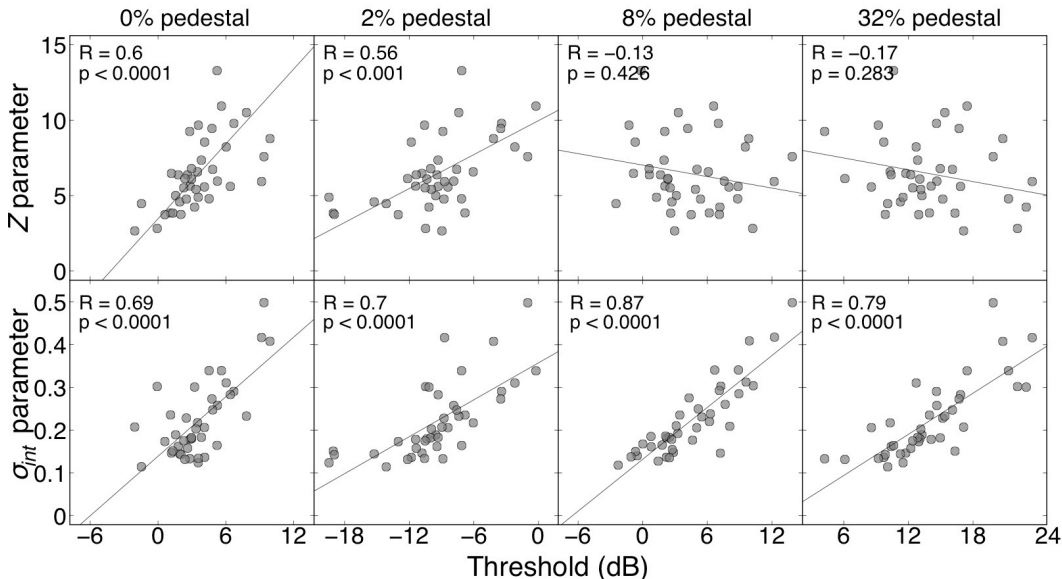
Figure 3.7. **Correlations between parameters and dipper thresholds.** Correlations between the gain control parameter Z and pedestal masking (dipper) thresholds (top row); and correlations between the internal noise parameter σ_{int} and thresholds (bottom row). Black lines represent Deming regression lines. R and *p* values from the Pearson's correlations are shown in the top left hand corner of each plot.

3.4.2.2 Double-pass consistency

Double-pass consistency and accuracy scores for the target and no target conditions were calculated in the same manner as in Study 1 with data from all individual observers and their mean plotted in Figure 3.6B. For comparison with other variables, we averaged the consistency scores across the two target contrast conditions, with high levels of consistency implying low levels of internal noise. This measure was then correlated with the four pedestal masking thresholds and Z and σ_{int} parameters from the fits shown in Figure 3.8A. The double-pass consistency and the fitted internal noise parameter (σ_{int}) showed a significant strong negative correlation (R = -0.68, $p < 0.0001$) indicating consistency between these two methods of estimating internal noise. On the other hand, double-pass consistency did not significantly correlate with the gain control parameter Z (R = -0.14, $p = 0.378$) indicating that contrast gain control estimated from pedestal masking data is not a measure of internal noise, and does not confound double pass consistency estimates.
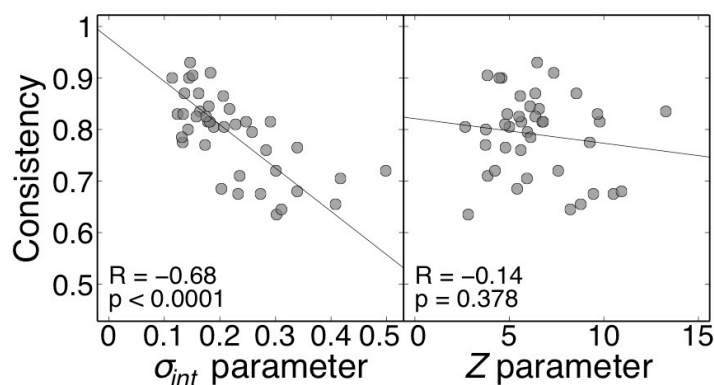
Figure 3.8. **Correlations between parameters and consistency.** Scatterplots showing correlations between fitted parameters σ_{int} (left panel) and Z (right panel) and double-pass consistency scores averaged over the no target and target present conditions. Black lines represent Deming regression lines. R and p values from the Pearson's correlations are shown at the bottom left hand corner of the scatterplots.

Pearson's correlations showed that double-pass consistency was negatively correlated with dipper thresholds at all pedestal contrasts (-0.65 ≤ R ≥ -0.44, $p < 0.005$), see Figure 3.9. This reiterates the point that internal noise has an influence across the entire contrast discrimination function.
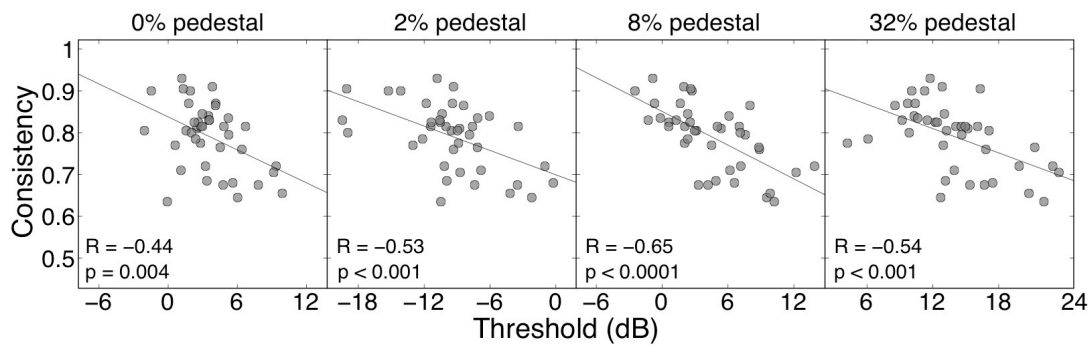
Figure 3.9. **Correlations between consistency and discrimination thresholds.** Scatterplots showing correlations between double-pass consistency scores averaged over the no target and target present conditions and pedestal masking thresholds at pedestal contrasts of 0, 2, 8 and 32% (from left to right). Black lines represent Deming regression lines. R and *p* values from the Pearson's correlations are shown at the bottom left hand corner of the scatterplots.

3.5 Discussion

We compared three different techniques for estimating internal noise. In our first study, we showed that a nonlinear model fitted to contrast discrimination data was able to predict performance in both an equivalent noise experiment and a double pass consistency experiment. In our second study, we showed that the noise parameter from a model fitted to contrast discrimination data was strongly correlated with double pass consistency, indicating that these two paradigms measure the same internal variable. We now discuss further details of the methods, and the practicalities of running experiments to estimate internal noise.

3.5.1 Comparing 2AFC discrimination with yes/no tasks

The suggestion to use contrast discrimination paradigms as a measure of internal noise is reasonably novel (Baker, 2013; Baldwin et al., 2016), and may seem surprising to some. However, the general approach is entirely orthodox in studies that use a yes/no paradigm, where it is equivalent to measuring the slope of the yes/no psychometric function, or a just-noticeable-difference (JND). In such experiments, stimulus intensity (contrast, luminance, pitch, facial expression etc.)

for a single target is typically compared to a standard (either explicit or implicit), with participants indicating whether the target appears higher ('yes') or lower ('no') in intensity than the standard. The results are plotted on a linear x-axis, with steep psychometric functions indicating low internal noise (good discriminability), and shallow functions indicating high internal noise (poor discriminability). Often a JND 'threshold' is also estimated at some criterion performance level (typically 25% and 75%). Two example simulated psychometric functions for this paradigm are shown in Figure 3.10A, illustrating that individuals with higher internal noise produce shallower functions with larger JNDs.
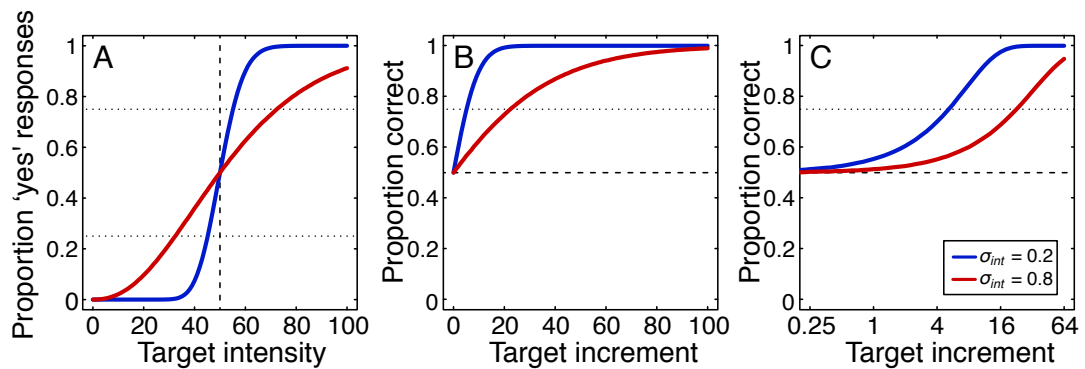
Figure 3.10. **Illustration of the relationship between yes/no and 2AFC paradigms for intensity discrimination experiments.** Panel A shows simulated yes/no psychometric functions for an intensity discrimination task in which a target was compared to a standard with an intensity of 50 units (given by the vertical dashed line). A low noise participant (blue) will have a steep psychometric function, with small just noticeable differences (JNDs) at the 25% and 75% points. A high noise participant (red) will have a shallower psychometric function and larger JNDs. Panel B shows psychometric functions for a 2AFC discrimination task, with a pedestal level of 50 units, and a range of target increments, which are always added to the pedestal. Again, the functions are shallower for the higher noise observer when plotted on a linear x-axis, and the 75% correct threshold is higher. Panel C shows the same data replotted on a logarithmic x-axis. Now the psychometric functions are approximately parallel, and the high noise observer is differentiated only by having a higher threshold. All simulations used the gain control model given by Eq. 3.2, with parameters fixed at $p = 2.4$, $q = 2$, $Z = 1$, and involved 1000000 simulated trials per target level.

In two alternative forced choice discrimination experiments, such as those described here, a pedestal is presented in one interval, and a pedestal plus target increment in the other. The pedestal level is fixed, and target stimuli constitute an increment to the pedestal contrast (though some studies have also examined decrements, i.e. (Foley & Chen, 1999). As such, effectively only the upper portion of the yes/no function is measured, as shown in Figure 3.10B. However, for contrast discrimination experiments the target values are conventionally plotted on a logarithmic x-axis (or alternatively converted to logarithmic units, such as the dB units used here). The log scaling of the target contrast values means that a zero point is not present, and the functions do not change in slope with changes in internal noise (see Figure 3.10C). Instead, only the threshold (at 75% correct) varies as noise increases. Given the close relationship between these paradigms, estimating noise levels from the dipper function is not particularly radical, and we are somewhat surprised that it has rarely been attempted.

3.5.2 Why is consistency overestimated?

We attempted to predict the double pass consistency data using models fit to either the equivalent noise thresholds or the contrast discrimination thresholds (see Figure 3.5). Both models overestimated the empirical double-pass consistency, especially at high mask levels. This is similar to findings from previous studies using white noise, which also found that a linear model fitted to threshold data overestimated consistency (Lu & Dosher, 2008). One possible solution is to invoke additional processes, such as induced multiplicative noise that is caused by the mask. However direct tests of this approach have not provided evidence for changes in consistency via such mechanisms (Baker & Meese, 2013). Alternatively, lower than predicted response consistency could be explained by several biases and higher level decision strategies that are relatively independent of perception, such as interval bias, finger error (lapsing), and 'superstitious' behaviours (i.e. choosing the opposite interval to the one selected on the previous trial). These low frequency events are difficult to isolate, particularly for binary decision tasks. Future work could use reports of confidence (e.g. Baker & Cass, 2013), involve an explicit mechanism for remediating trials

on which an observer believes they have lapsed (Meese & Harris, 2001), or measure eye movements or other physiological variables to provide a basis for rejecting some trials. For our zero-dimensional noise, it is conceivable that observers might erroneously make judgments based on absolute contrast (ignoring phase polarity) on some trials, which would further reduce consistency estimates.

3.5.3 What is the best way to measure internal noise?

As previous studies have demonstrated, detection in white noise experiments is confounded by suppression from the mask (Baker & Meese, 2012; Baker & Vilidaite, 2014). However, using a zero-dimensional noise mask to avoid this problem results in near-perfect efficiency (Allard & Faubert, 2013), so that the inflection point of the noise masking function merely reflects detection threshold (see Figure 3.3). One alternative presented here and elsewhere (Baker, 2013; Baldwin et al., 2016) is to estimate internal noise using a discrimination paradigm. This is feasible for well-characterised processes such as contrast transduction, and previous findings can be reinterpreted in this context. For example, Greenaway, Davis, & Plaisted-Grant (2013) recently reported a contrast discrimination deficit in autism spectrum disorders, that could well be a consequence of increased internal noise in this population (Dinstein et al., 2012; Milne, 2011).

However, discrimination paradigms may not be suitable for more complex stimulus domains, in which the mapping between stimulus and internal representation is unknown, and perhaps nonmonotonic. In such cases, the double pass method can still be applied, as it is relatively invariant to differences in the underlying transfer function, since the addition of external noise causes 'Birdsall linearisation' (Smith & Swift, 1985) that neutralises nonlinearities. For example, Baker & Meese (2013) recently showed that double pass consistency is unaffected by strong gain control suppression from a narrowband mask. The method has been successfully adapted to lexical decision tasks (Diependaele et al., 2012) and pitch discrimination (Jones, Moore, Amitay, & Shub, 2013), and we have recently run experiments using faces that vary in emotional expression, as well as value judgement tasks (Vilidaite, Yu, & Baker, 2016). Data can be obtained without prohibitively large numbers of trials (here we used 200 trials per target level), and

the interpretation of results is reasonably straightforward. Additionally, double-pass shows good internal reliability with split-half analysis showing a very high correlation (R = 0.88, $p < 0.0001$).

3.5.4 Implications for understanding individual differences

A previous analysis of 18 studies concluded that individual differences in gain control could account for more of the variance in contrast sensitivity than could internal noise (Baker, 2013). To see if this was also the case here, we conducted a further analysis of study 2. Individual observer data from the dipper experiment (Figure 3.6A) were fitted as before but allowing only one free parameter, either Z or σ_{int}, fixing the other to the value obtained from modelling the average data. This procedure should reveal which of the free parameters can explain the largest proportion of the population variance. A paired samples t-test was used to compare mean RMS errors between these two fits, and revealed that RMS errors were significantly lower when σ_{int} was a free parameter (mean = 2.89dB, SD = 1.34dB) than when Z was a free parameter (mean = 3.86dB, SD = 1.75dB, $t(39)$ = 5.52, $p < 0.001$). This suggests that internal noise had a larger influence on individual differences in contrast discrimination in this study than did gain control.

The discrepancy between studies could be due to the fixed, low spatial frequency (0.5c/deg) used here, and the variety of spatial frequencies included in the analysis by Baker (2013). This seems a plausible explanation given that differences in sensitivity caused by changes in spatial frequency are largely due to differences in gain control, and not internal noise (Baldwin et al., 2016). This could imply that noise accounts for a greater proportion of inter-individual variation at some spatial frequencies than others, perhaps because optical and neural factors limit sensitivity more at higher spatial frequencies. Indeed, previous work that has addressed individual differences in contrast sensitivity has revealed independently varying factors that likely relate to channels tuned to different spatiotemporal scales (Peterzell & Teller, 1996; Peterzell, Werner, & Kaplan, 1995). Although it may be tempting to relate these channels to magnocellular and parvocellular

systems, we note that disambiguating these psychophysically is fraught with problems (e.g. Goodbourn et al., 2012; Skottun, 2000).

In general, we take the theoretical position that internal noise is a stable and measureable property of the visual system that could, in principle, vary across individuals and clinical groups. Our aim here was to determine which experimental techniques might best be used to measure internal noise, with the intention of applying them in specific contexts (i.e. with different clinical groups). Because they are highly correlated with each other, double pass consistency and contrast discrimination appear to be suitable measures. Future work might use these tools to focus on how internal noise changes as a function of both genetic and environmental factors (e.g. ageing, diet, visual experience etc.), and how noise in one system (i.e. vision) relates to noise in other senses and tasks, or measured using different methodologies.

3.5.5 Conclusions

We compared three methods for estimating internal noise in contrast processing. Estimates from contrast discrimination and double pass consistency paradigms were highly correlated, and so are likely to be measuring the same underlying phenomenon. Depending on the dimension of interest, one or both of these methods appear to provide a good measure of internal variability, and could be used in individual differences research, or with different clinical groups.

Chapter 4

The effects and non-effects of TMS on contrast perception

This chapter has been adapted from: Vilidaite, G., & Baker, D. H. (under review). The effects and non-effects of TMS on contrast perception. *Journal of Cognitive Neuroscience*.[3]

4.1 Abstract

TMS is widely used to establish causal relationships between brain areas and behaviors, but the effects on task performance are not fully understood and have never been directly compared between protocols. The impairments in task performance due to TMS may be due to signal suppression, neural noise induction or a combination of both. Here we compare the effects of four common stimulation protocols: single-pulse (spTMS), online repetitive (rTMS), continuous (cTBS) and intermittent theta burst stimulation (iTBS) during a low-level visual task. We dissociate the effects of neural noise and neural suppression during perception using psychophysics and computational model predictions. Double-pass contrast discrimination was used to estimate neural noise by measuring response consistency between two repetitions of the task for each TMS protocol

---

[3] The author, Greta Vilidaite, designed the experiment, collected the data, analysed the results and wrote the manuscript under the supervision of Dr Daniel Baker.

and control condition. The strength of stimulus-related neural signals was also measured as task accuracy. Single pulse TMS suppressed sensory signals and did not change the level of neural noise in the visual system. Conversely, rTMS increased neural noise but did not change the strength of stimulus-related signals. Theta burst stimulation did not have any effect on task performance. Furthermore, spTMS and rTMS only influenced task performance in the group of subjects who were able to perceive phosphenes during screening. We conclude that care is needed when choosing the exact stimulation protocol when assessing functionality of brain areas. Furthermore, individual differences in overall TMS susceptibility may be a large factor in the TMS reproducibility crisis.

4.2 Introduction

Transcranial magnetic stimulation (TMS) is widely used to establish causal links between behavior and anatomy by targeting a brain area during an associated behavioral task (Beauchamp, Nath, & Pasalar, 2010; Moser et al., 2002; Silson et al., 2013). Although the 'virtual lesion' metaphor of TMS (Pascual-Leone et al., 2000) has been largely dismissed, the neural mechanisms by which TMS influences behavior and perceptual processing are still poorly understood. Furthermore, different types of TMS protocols (e.g. online, offline, repetitive, single pulse) can have vastly different effects on neural signals and behavior (Cárdenas-Morales et al., 2010; Ragert et al., 2008; Ruzzoli et al., 2011). Despite this, these TMS protocols are often used interchangeably.

Within the framework of signal detection theory (Green & Swets, 1974), decreases in accuracy on psychophysical tasks, such as those observed when applying TMS, can be attributed to either (a) suppression of stimulus-related neural signals; (b) increased random activity, i.e. neural noise; or (c) a combination of both (also see Vilidaite and Baker, 2016). In the case of online TMS, some studies using single-pulse TMS (spTMS) have found that stimulation suppresses stimulus-related signals (Harris et al., 2008; Ruzzoli et al., 2011). Contrastingly, other studies using repetitive protocols (rTMS) showed that TMS influences task performance by increasing neural noise (Ruzzoli et al., 2010;

Schwarzkopf et al., 2011). One explanation of this is that spTMS and rTMS affect neural signaling in distinct ways. However, another spTMS study in rats found both suppressive and noise inducing effects (Moliadze, Zhao, Eysel, & Funke, 2003).

The two widely used offline TMS protocols, continuous (cTBS) and intermittent TBS (iTBS), have also been shown to have different effects on neural signals (Huang et al., 2005). Huang et al. claimed cTBS suppressed neural signals whereas iTBS enhanced them. This has been supported by several subsequent studies (Di Lazzaro et al., 2005, 2008; Moliadze et al., 2014; Ragert et al., 2008; Rahnev et al., 2013). Conversely, other studies showed that TBS had variable (Harada et al., 2011) or even bimodal (López-Alonso et al., 2014) effects on motor evoked potentials between subjects as well as between exact stimulation protocols (Gentner et al., 2008), whereas Benali et al., (2011) found no effect of cTBS.

The discrepancies in the findings are likely due to the use of different tasks (contrast masking, orientation discrimination, motion coherence or no task) and different brain areas. Furthermore, some paradigms, such as white noise masking, used by Harris et al. (2008), cannot adequately distinguish between signal suppression and neural noise induction (Baker & Vilidaite, 2014). Furthermore, although TBS is widely used for perceptual research, most studies on the neural mechanisms of TBS were conducted using electromyographic motor evoked potentials (Di Lazzaro et al., 2005, 2008; Moliadze et al., 2014). The lack of task in these studies means it is impossible to dissociate TMS effects on behaviorally relevant signals and effects of overall activity, including neural noise.

Here we directly compared the neural effects of four most commonly used TMS protocols (spTMS, rTMS, cTBS and iTBS) on a well-understood neural computation – contrast transduction. We compare all stimulation protocols using the same paradigm and brain area. We use a highly sensitive double-pass paradigm (Burgess & Colborne, 1988; Vilidaite, Yu, & Baker, 2017) to dissociate TMS induced changes in stimulus-related signal strength (i.e. suppression) and in neural noise. As a secondary objective, we investigated natural TMS-

susceptibility by comparing subjects who could and could not perceive phosphenes to address inter-subject variability in TMS effectiveness.

We simulated predictions using a linear amplifier model (LAM) (Pelli, 1985) which indicated that if TMS reduced neural signal strength (lowered sensitivity β), we would observe a steep drop in task accuracy but no change in double-pass consistency (see section 4.3.5 on double-pass). Alternatively, if TMS increases neural noise (σ_{neural}), we would see a small reduction in accuracy and a larger drop in consistency. Finally, if TMS both reduces stimulus-related signals and increases noise, we would observe a large reduction in both measures (Figure 4.1).
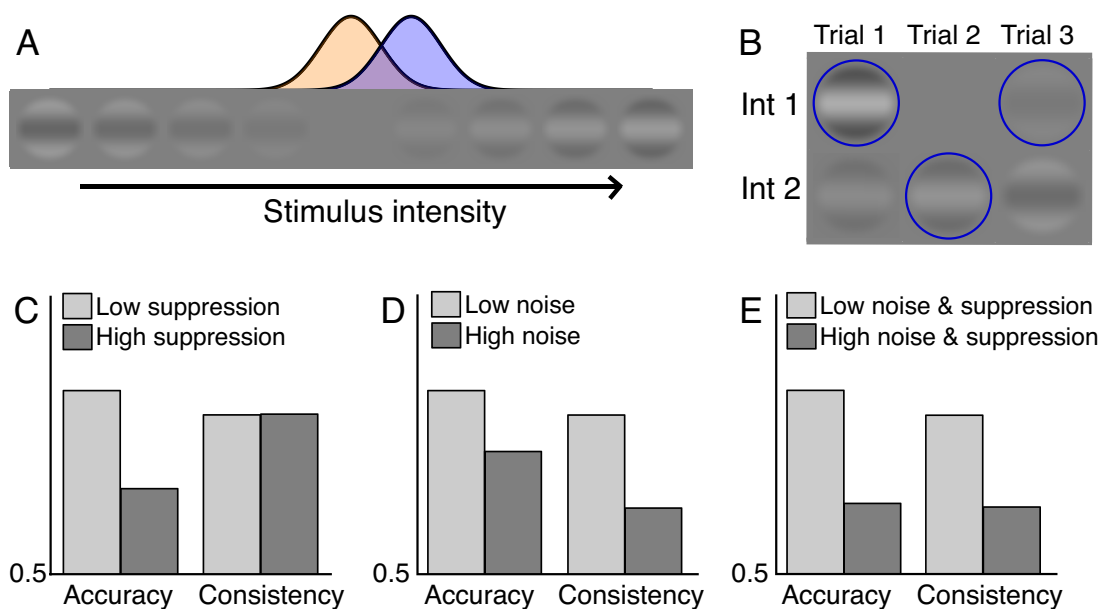
Figure 4.1. **Stimuli and model predictions for changes in noise and suppression.** Each interval during a trial was drawn from the target (blue) and non-target (yellow) stimulus distributions (A). Subjects were asked to choose the interval with the more positive contrast (B; example correct intervals are shown with a blue circle). Stochastic simulations were used to generate model predictions of double pass data (C-E). Light bars in all panels indicate a system with low neural noise ($\sigma_{neural} = 4\%$) and low suppression (high sensitivity) in the system ($\beta = 1$). Dark bars model an increase in either suppression, noise, or both. If TMS suppresses neural signals (lowers sensitivity, $\beta = 0.5$) then we should expect double pass data to be similar to the prediction in panel C. On the other hand, if TMS increases neural noise ($\sigma_{neural} = 4\%$) the data should resemble panel D. If both suppression and neural noise are increased we would expect data to be similar to panel E.

4.3 Methods

4.3.1 Subjects

Twenty-five subjects were initially screened for perception of phosphenes in order to precisely place the stimulus in the stimulated region of the visual field. Six subjects (4 females, age range 22 - 34) were initially recruited due to consistent perception of phosphenes and made up the 'phosphene group'. Another six subjects (3 females, age range 23 - 55) were then recruited without phophene localization and made up the 'no phosphene group'. Five of these subjects were previously tested for phosphene perception and found not to perceive phosphenes during screening. All twelve subjects had normal vision and no neurological or psychiatric conditions. The subjects met all criteria for TMS safety and gave informed consent.

4.3.2 TMS protocol

A Magstim Rapid 2 with a 'figure of 8' coil was used throughout the study. Four TMS protocols were used: online spTMS, online rTMS, offline cTBS and offline iTBS. Online spTMS and rTMS were applied at 70% stimulator output. Either one (spTMS) or three (rTMS) pulses were delivered 50ms after stimulus onset during each interval of each trial (see Figure 4.2C). In the case of rTMS, a train of 3 pulses at 20Hz was presented at stimulus onset so that the pulses were timed at 0, 50 and 100ms. The length of the stimulus presentation was 200ms and the inter-stimulus interval (ISI) was 1100m. The minimum length of the inter-trial interval (ITI) was 2000ms with each new trial triggered by the subject's response (the ITI was longer if they responded after 2000ms). The coil was swapped 1-2 times during each session to avoid overheating. During the task, subjects fixated on a central fixation cross whilst stimuli were presented in the peripheral location of the phosphenes.
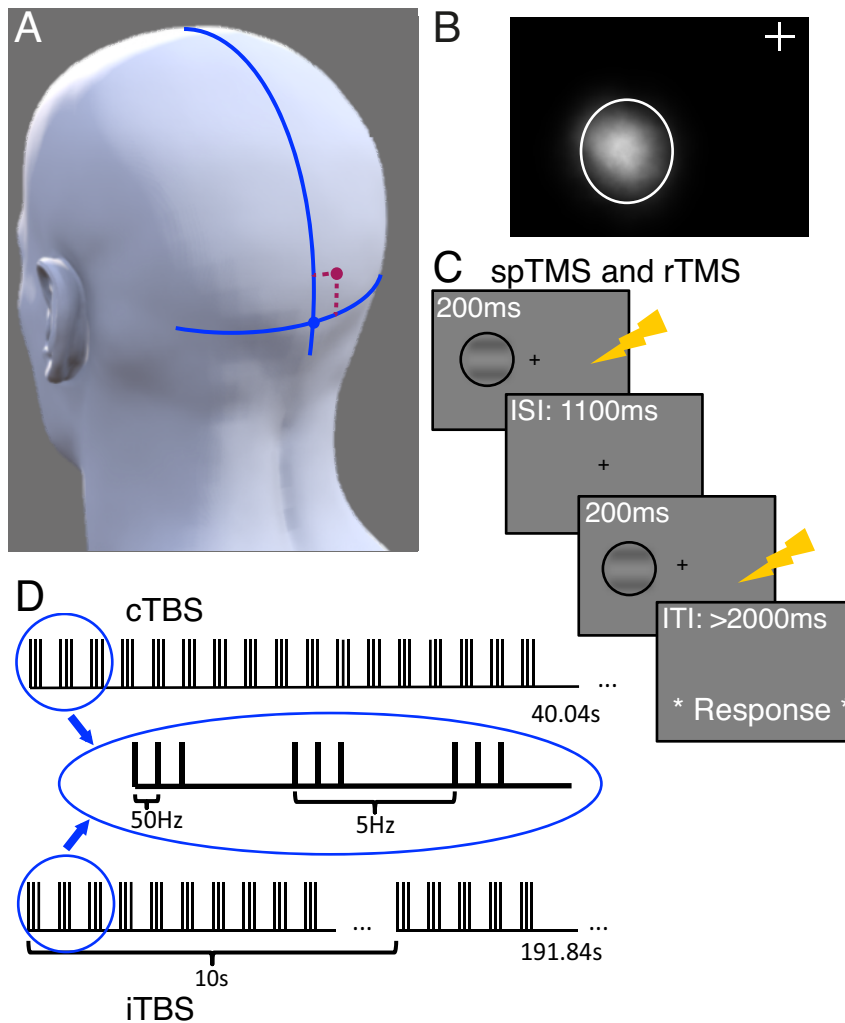
Figure 4.2. Stimulation protocols and phosphene localization. The TMS coil was positioned (red dot) approximately 2cm above and 1cm to the right of the inion (blue line intersection) to induce phosphenes (A). Before phosphene localization subjects were trained to indicate the location and shape of a simulated phosphene on the screen (B; see section 4.3.3). During spTMS and rTMS protocols either one or three pulses were delivered during each stimulus interval (C; see section 4.3.2 for more details). Pulses during offline cTBS and iTBS were delivered as shown in D.

For offline cTBS and iTBS protocols, stimulation was performed before the start of the task but after phosphene localization. Standard TBS protocols were employed (Cárdenas-Morales et al., 2010; Huang et al., 2005; see Figure 4.2D) at a typical intensity (30% stimulator output).

4.3.3 Phosphene localization

Task stimulus location was determined for each subject in the phosphene group separately using phosphene localization. Subjects were first trained to use an in-house developed interface (Matlab) for reporting perceived phosphenes. They were asked to position a circle around a simulated phosphene (a patch of pink noise windowed by a Gaussian envelope) on the screen several times.

Subjects were then asked to wear a rubber swimming cap and position their heads in front of the screen against a chin and forehead rest. The experimenter positioned the TMS coil approximately 2cm above and 1cm to the right of the inion (Figure 4.2A). Seven TMS pulses at 20Hz (70% stimulator output) were delivered whilst subjects looked at a dark blank screen. They were asked to then adjust the position and size of a circle on the screen to match their perceived phosphene. This was repeated up to 9 times or until five phosphenes were perceived consecutively. If phosphenes were not perceived during the first few attempts, the coil was repositioned slightly.

For subjects in the no phosphene group phosphene localization was not performed (or was unsuccessful) and so the stimuli were presented in the average location of phosphenes from the other six subjects. The location of the phosphenes was similar for all subjects in the phosphene group (left visual field, see Figure 4.3A) and so it is reasonable to assume that a similar area of the visual field was stimulated in the cases where no phosphenes were perceived.
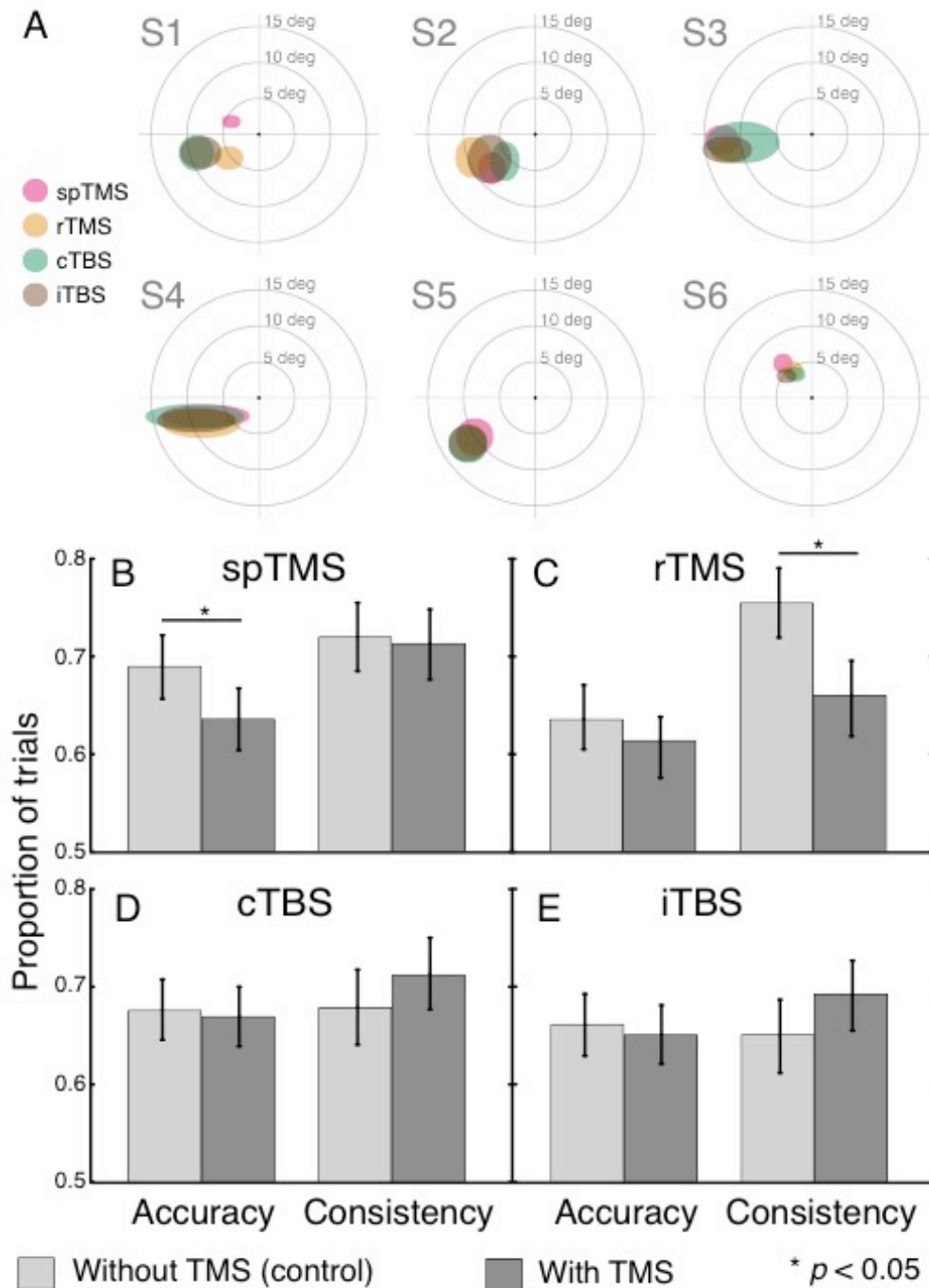
Figure 4.3. **Phosphene locations and double-pass accuracy and consistency for the phosphene group.** Phosphene locations were similar for all six subjects, centered around the midline of the left visual field (A), within 15 degrees of the fixation cross. The four stimulation protocols: spTMS (pink), rTMS (yellow, averaged over four sessions), cTBS (green) and iTBS (brown) produced similar phosphenes within subjects, as indicated by filled ovals. For the phosphene group, single pulse TMS (B) significantly reduced the mean accuracy scores with TMS stimulation (dark bars) compared to the no-TMS condition (light bars) but not consistency scores which indicates increased suppression resulting from TMS stimulation. Repetitive TMS (C) significantly reduced consistency but not accuracy on the task, indicating a TMS-induced increase in neural noise. Neither cTBS (D) nor iTBS (E) produced any significant change in task performance. Error bars indicate bootstrapped 95% confidence intervals (see section 4.3.7).

4.3.4 Stimuli

The stimuli were sinusoidal gratings of 0.5 cycles/degree spatial frequency in cosine phase with the stimulus centre. They were presented in the previously established phosphene location, determined individually for each subject and each TMS session. The size of the gratings was 3 degrees of visual angle (at 57cm viewing distance). The stimuli were surrounded with a black circle to decrease spatial uncertainty. The contrast of the gratings were expressed in percentage Michelson contrast: defined as $C_{\%}=100*(\frac{L_{max}-L_{min}}{L_{max}+L_{min}})$, where L_{max} and L_{min} are the maximum and minimum luminances of the grating. Negative contrast values reversed the polarity of the grating (bright bars became dark and vice versa). Stimuli were presented with 14-bit luminance resolution on a gamma corrected Diamond Pro 2070SB monitor (Mitsubishi) with a refresh rate of 86Hz using a ViSaGe stimulus generator (Cambridge Research Systems Ltd., Kent, UK) controlled by a PC.

4.3.5 Double-pass consistency

The psychophysical estimates of neural noise and signal suppression were acquired using a variation of the double-pass consistency paradigm (Burgess & Colborne, 1988; Vilidaite & Baker, 2016; Vilidaite et al., 2017). In this paradigm, noisy stimuli are presented to an observer twice (pass 1 and pass 2) and the consistency of responses to these stimuli is calculated between the passes. As the stimuli and conditions are kept the same, any differences in responses between pass 1 and pass 2 must be due to random activity in the observer's brain (neural noise). The lower the consistency between passes, the more neural noise there is in the system. A measure of accuracy, calculated over both passes, is a function of the intensity of neural response to the stimuli. For example, a decrease in accuracy when applying TMS compared to the control condition would indicate signal suppression. Accuracy and consistency were calculated as a proportion of trials (chance level being 0.5).

Here we used a two-interval-forced-choice (2IFC) contrast discrimination task, where subjects were asked to choose the interval with the more positive contrast

(Figure 4.1B). The instruction given to the subjects was: "Choose the stimulus which is brighter in the middle". On each trial (200 trials per pass), two luminance-modulated gratings were presented sequentially, for 200ms each, with a 1100ms inter-stimulus interval. There were two stimulus conditions: target absent and target present. In the target absent condition, both stimuli had contrast values that were randomly drawn from a Gaussian distribution of contrast values centered around 0% Michelson contrast (Figure 4.1A). The standard deviation (σ_{stim}) of the distribution was 4%. In the target present condition, a 4% contrast increment was added to one of the stimuli. Accuracy on the task was calculated from the target present condition, as the target absent condition had no correct answer. Consistency was calculated from the target absent condition. The order of the intervals in each trial and the order of the trials were randomized in pass two.

4.3.6 Procedure

Each TMS stimulation type was administered in a separate session. Online rTMS was split into four sessions (100 trials each) due to restrictions on the amount of TMS stimulation that can be safely administered in a session (Rossi et al., 2009; Wassermann, 1998). Online TMS sessions were counterbalanced between subjects, i.e. the spTMS session occurred first for S1, whereas for S2 the first session was rTMS, then spTMS, then rTMS again, etc. Each of the four rTMS sessions had separate phosphene localization. For each online TMS session, the control conditions (no TMS) were performed in the following session before the new TMS condition was administered. Each session after the first one followed this sequence: control task (no TMS condition using phosphene locations of the previous session), TMS set up, phosphene localization for current session, psychophysical task for current session. The control conditions did not differ from TMS conditions, except that no TMS was applied and the stimuli were presented in the previously established phosphene location.

TBS sessions were also counterbalanced: half of subjects received cTBS first and the other half received iTBS first. TBS sessions always followed after online TMS sessions. During the task, the minimum inter-trial interval in these conditions was 500ms. The psychophysical task was split into four blocks, ~5min each in length,

between which subjects were able to have a short break. In the phosphene group, these blocks were interspersed with passive viewing of flickering gratings whilst EEG was recorded (~4min each, data not presented here). In these cases EEG cap set up took place immediately after TBS stimulation and took 3-4min. Control sessions (no TBS) were done on a different day.

The task was performed in a dark room in all cases. Subjects were able to rest with the lights turned on during dedicated breaks in TBS sessions or when the coils were swapped during online TMS sessions. All sessions were 25-70min long, including set up time. There were gaps of at least 24 hours between sessions and no more than three sessions occurred in any one week. Subjects were debriefed after the last session about the purpose of the experiment.

4.3.7 Model predictions

Predicted double-pass accuracy and consistency scores were obtained by simulating the double-pass experiment using a linear amplifier model. Neural responses were simulated for the target and the null intervals:

$$resp = \sigma_{neural} + \sigma_{stim} + \beta * C_{targ} \qquad \text{(Eq. 4.1)}$$

where *resp* is the numerical representation of a neural response to each interval; σ_{neural} is neural noise; σ_{stim} is stimulus noise; β is sensitivity (the inverse of suppression); C_{targ} is the contrast of the target. For null intervals C_{targ} was set to zero. Low and high internal noise (σ_{neural}) as well as sensitivity (β) values were used to model three possible outcomes of TMS stimulation (Figure 4.1 C-E).

4.4 Results

4.4.1 With phosphene localization

All six subjects in the phosphene group perceived phosphenes in similar locations of the center-left visual field, consistent with the stimulation of the right visual cortex (Figure 4.3A). The centers of the phosphenes, and therefore the locations of the presented stimuli, were within 15 degrees of visual angle from the central fixation cross for all subjects. The variation in phosphene location was ~10 degrees visual angle between subjects and <5 degrees within subjects.

We performed statistical analyses (t-tests) between accuracy and consistency scores within each stimulation protocol (TMS versus no TMS conditions). Bayes Factors (BFs) were calculated to quantify probabilities of the experimental (there is a difference between TMS and control conditions) and null hypotheses (there is no difference between TMS and control conditions). BFs >1 indicated support for the experimental hypothesis, whereas BFs < 1 indicated support for the null hypothesis.

As shown in Figure 4.3B, a significant drop in accuracy (t(5) = 2.83, p = 0.037, BF = 2.83) is seen when spTMS is applied compared to the control condition but no change in consistency was observed (p = 0.601, BF = 0.29). This indicates a suppressive effect of spTMS on stimulus-related neural signals but no effect on neural noise. This pattern of data closely resembles our LAM model predictions (Figure 4.1C) for an increase in neural suppression. Conversely, applying rTMS shows a small non-significant change in accuracy p = 0.848, BF = 0.33) compared to the no-TMS condition and a significant decrease in consistency (t(5) = 2.74, p = 0.041, BF = 2.38; Figure 4.3C) – consistent with model predictions for an increase in neural noise, as predicted by model simulations (Figure 4.1D). Neither protocol produced data consistent with change in both suppression and neural noise (Figure 4.1E).

No effects on the accuracy (p = 0.790) or consistency (p = 0.132) were observed when applying cTBS (Figure 4.3D; Table 4.1), indicating that the stimulation protocol did not change the level of neural noise or the amount of signal in the visual system. Similarly, no change in accuracy (p = 0.773) or consistency (p =

0.244) was observed when applying iTBS (Figure 4.3E). Bayes Factors for these conditions were all below 1, indicating support for the null hypothesis.

4.4.2 Without phosphene localization

None of the four TMS protocols had any significant effect on accuracy or consistency scores in the no phosphene group (Figure 4.4). All comparisons between no-TMS and TMS conditions were non-significant ($p > 0.05$) and produced Bayes Factors around 0.3, indicating support for the null hypothesis (see Table 4.1).
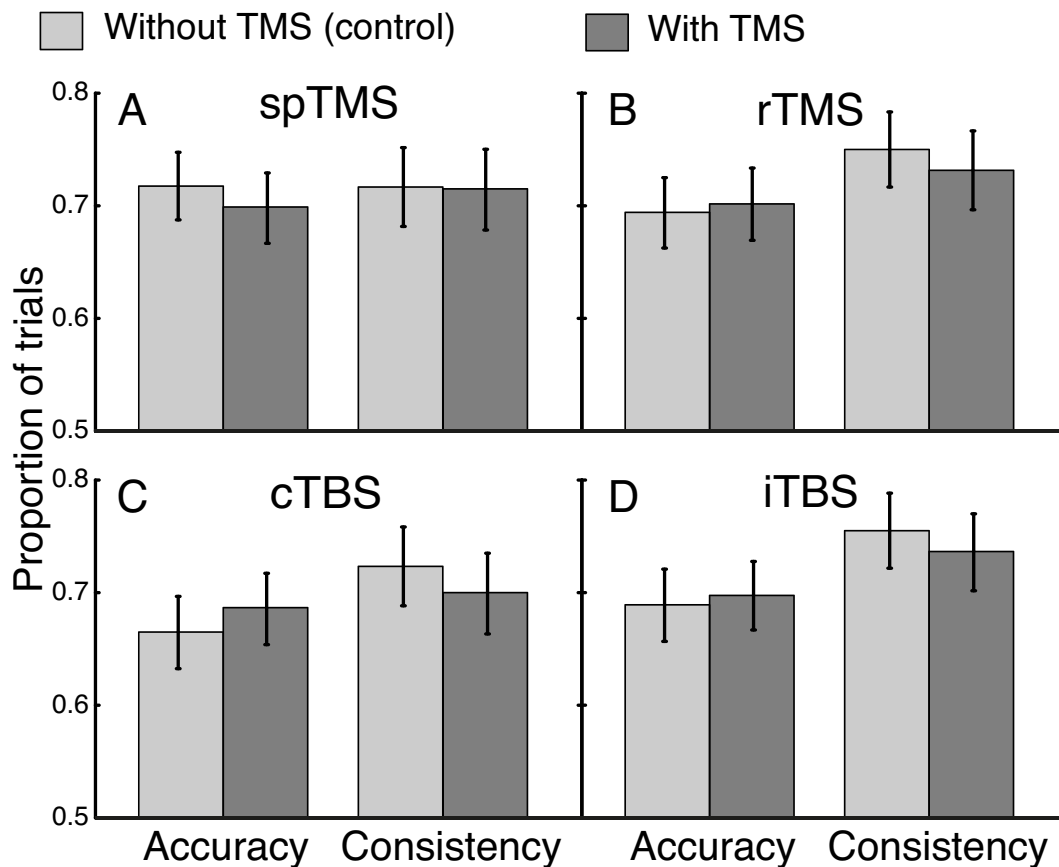
Figure 4.4. Double-pass accuracy and consistency for the no phosphene group. No significant change was observed when using spTMS (A), rTMS (B), cTBS (C) or iTBS (D) when phosphene localization was not used. Error bars indicate bootstrapped 95% confidence intervals (see section 4.3.7).

To compare the phosphene and no phosphene groups, we calculated control-TMS condition differences. Figure 4.5A shows that bootstrapped 95% confidence intervals of the no phosphene group were overlapping the 'no change' line (where the difference between no-TMS and TMS conditions was equal to zero) for all TMS protocols. As expected, confidence intervals of spTMS for this group were above the line for accuracy and not consistency and vice versa for rTMS (Figure 4.5B).

Table 4.1. Statistical analysis outcomes comparing no-TMS and TMS conditions

		Accuracy			Consistency		
		p	t	BF	p	t	BF
With phosphenes	spTMS	**0.037**	**2.83**	**2.61**	0.848	0.2	0.29
	rTMS	0.591	0.57	0.33	**0.041**	**2.74**	**2.38**
	cTBS	0.79	0.28	0.3	0.132	-1.8	0.93
	iTBS	0.773	0.3	0.3	0.244	-1.32	0.58
Without phosphenes	spTMS	0.601	0.56	0.33	0.975	0.03	0.29
	rTMS	0.794	-0.27	0.3	0.399	0.92	0.42
	cTBS	0.39	-0.94	0.42	0.509	0.71	0.36
	iTBS	0.474	-0.77	0.38	0.63	0.51	0.33
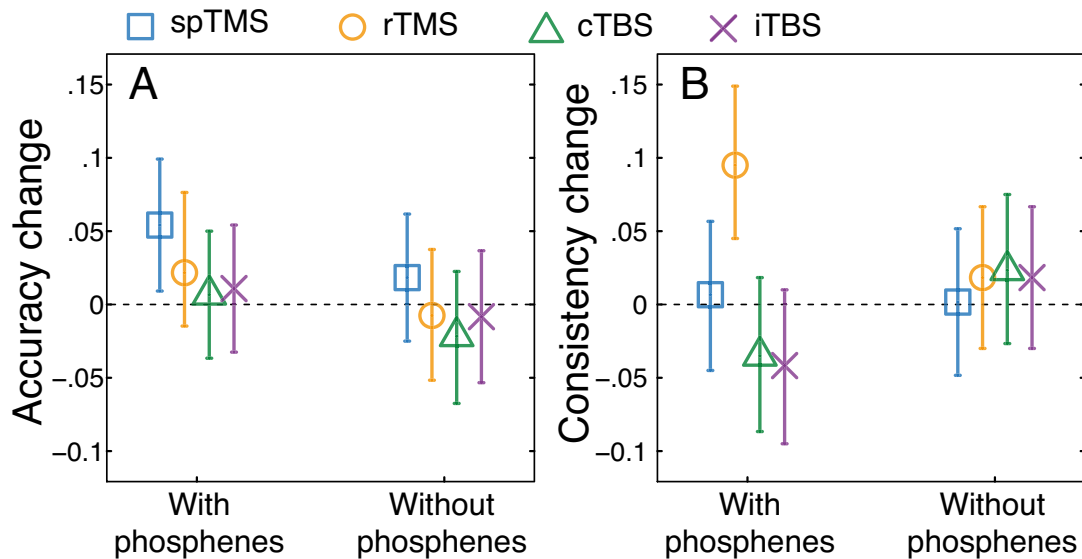
Figure 4.5. Change in accuracy and consistency between no TMS and TMS conditions. The 95% confidence intervals for the differences between no-TMS and TMS conditions in accuracy (A) were above zero (the 'no-change' line) only for spTMS and only in the phosphene group, compared to other protocols in both subject groups. This was also true for no-TMS to TMS change in consistency (B) for the rTMS protocol in the no phosphene group but none of the other protocols

4.5 Discussion

The results indicate that spTMS reduced accuracy in the double-pass paradigm by suppressing stimulus-related neural signals, as predicted by the low sensitivity (β) model simulations. Conversely, rTMS did not significantly change the accuracy but reduced consistency, indicating neural noise induction, predicted by the high noise (σ_{neural}) model simulations. No change in accuracy or consistency was observed when applying cTBS or iTBS. Furthermore, none of the stimulation protocols affected task performance in subjects that were not able to perceive phosphenes.

The suppressive effects of spTMS and the noise induction observed using rTMS are in accordance with previous literature using these protocols (Harris et al., 2008; Ruzzoli et al., 2011, 2010; Schwarzkopf et al., 2011). Previously these findings were considered to be opposing, as online TMS was assumed to have similar neural effects regardless of the stimulation protocol. The current direct comparison between single- and triple-pulse protocols suggest suppressive and noise-inducing mechanisms are protocol-specific. It may be that a single pulse

100

induces synchronous neural firing in non-detecting channels which then inhibit the stimulus-selective channel (Silvanto & Muggleton, 2008; Silvanto, Muggleton, Cowey, & Walsh, 2007). Contrastingly, three pulses in succession may affect interconnected neurons variably thus creating a noisy cascade of neural activity and interrupting the brain's endogenous rhythms.

Although spTMS and rTMS have distinct underlying neural mechanisms, both protocols only affected subjects who were able to perceive phosphenes, which suggests individual differences in TMS susceptibility. It is important to note that the stimulation intensity used for eliciting phosphenes was the same as that used for spTMS and online rTMS during the task. Indeed, previous research found a bimodal distribution of TMS effectiveness in the population (López-Alonso et al., 2014). These differences are most likely due to differences in skull thickness or folding of the visual cortex, as this would determine the distance between the coil and the targeted visual area. Stokes et al. (2013) demonstrated computationally that the TMS-induced electric field strength is linearly dependent on the distance between the coil and the brain. Although the justification for using rTMS is often the increased strength of neural effects, therefore increasing the number of subjects exhibiting behavioral change, here we show that individual differences, rather than choice of protocol, determine if TMS has an effect.

Offline TBS was found to not influence subjects' behavior regardless of phosphene perception or stimulation pattern (continuous or intermittent). At first glance, this contradicts the original TBS study's findings that cTBS suppresses neural signals whereas iTBS is excitatory (Huang et al., 2005). Other studies have also found suppressive cTBS (Di Lazzaro et al., 2005, 2008; Rahnev et al., 2013) and excitatory iTBS effects (Di Lazzaro et al., 2008; Moliadze et al., 2014; Ragert et al., 2008). However, most of the research into TBS effects measures motor evoked potentials (MEPs), which reflect an overall increase or decrease in neural activity whilst the subject is passive. It may be that TBS changes overall activation levels of the cortical neurons but does not have particular effects on perceptually-relevant signals that would affect task performance or consistency of responses.

Alternatively, the effectiveness of TBS may be overstated in the literature as indicated by a recent large scale meta-analysis (Chung, Hill, Rogasch, Hoy, & Fitzgerald, 2016), which found a large positive publication bias in the TBS literature. TBS has been shown to have highly unreliable effects on MEPs (Hamada et al., 2013; López-Alonso et al., 2014; Martin, Gandevia, & Taylor, 2006) and, in a large-sample study, no overall effects at all (Hamada et al., 2013). Similarly, an empirical study measuring several different neurophysiological outcomes of cTBS showed poor reproducibility of effects (Vernet et al., 2014). Experiments in which TBS has shown no significant effects often succumb to the 'file drawer' problem and remain unpublished, whereas experiments showing significant TBS effects have a much higher chance of getting published (Héroux, Taylor, & Gandevia, 2015).

Another possibility is that TBS produces long-term effects through synaptic plasticity but is not effective immediately. Recent literature suggests TBS as an effective treatment for several neurological disorders (Lorenzo et al., 2013; Nyffeler, Cazzoli, Hess, & Muri, 2009; Talelli, Greenwood, & Rothwell, 2007), in particular, depression (Bakker et al., 2015; Li et al., 2014). Typically, the positive therapeutic effects in depression appear after several sessions of regular treatment suggesting a long-term change in brain function and connectivity. However, it is perhaps not surprising that TBS would not produce immediate changes in sensory signaling as the stimulation intensities are below the neural activation threshold (Huang et al., 2005). Therefore, although TBS is a valuable clinical tool, the applicability of TBS to basic research of brain function is questionable.

In sum, the inter-subject and inter-protocol differences in TMS effects shed light on the interpretation of findings in the existing TMS literature as well as informing future methodological choices. The individual differences in responsivity, demonstrated in the current experiment, as well as the use of different stimulation protocols in the literature may be some of the major factors in the TMS 'replication crisis'. Here we suggest that screening for overall TMS susceptibility in subjects (such as phosphene perception) may be crucial for successful TMS research and reproducibility because of previously discussed anatomical differences. However, screening for a *specific* behavioural effect should be strictly avoided. Furthermore, the effectiveness of TBS stimulation

protocols as alternatives to online TMS for linking behavior to brain function should be evaluated appropriately in the light of current findings and previous meta-analyses.

Chapter 5

Internal noise estimates correlate with autistic traits

This chapter has been adapted from: Vilidaite, G., Yu, M. & Baker, D. H. (2017). Internal noise estimates correlate with autistic traits. *Autism Research, 10*, 1384-1391.[4]

5.1 Abstract

Previous neuroimaging research has reported increased internal (neural) noise in sensory systems of autistic individuals. However, it is unclear if this difference has behavioural or perceptual consequences, as previous attempts at measuring internal noise in ASD psychophysically have been indirect. Here we use a 'gold standard' psychophysical double-pass paradigm to investigate the relationship between internal noise and autistic traits in the neurotypical population (n = 43). We measured internal noise in three tasks (contrast perception, facial expression intensity perception and number summation) to estimate a global internal noise factor using principal components analysis. This global internal noise was positively correlated with autistic traits ($r_s = 0.32$, $p = 0.035$). This suggests that increased internal noise is associated with the ASD phenotype even in subclinical

---

[4] The author, Greta Vilidaite, designed the experiment, analysed the results and wrote the manuscript under the supervision of Dr Daniel Baker. Some of the data was collected by Miaomiao Yu. Yu also designed one of the tasks.

populations. The finding is discussed in relation to the neural and genetic basis of internal noise in ASD.

5.2 Introduction

Internal variability (noise) is an inherent property of neural systems and a limiting factor in neural signal transduction. Internal noise results from many sources at several processing scales from molecular and synaptic fluctuations (Faisal, Selen, & Wolpert, 2008; Schneeweis & Schnapf, 1999; Clifford et al., 2007) through to changes in internal states such as attention, arousal and top-down cognitive modulation (Fontanini & Katz, 2011). The collective internal noise resulting from these sources can be observed in electrophysiology and neuroimaging studies as signal variability (see Dinstein, Heeger, & Behrmann, 2015 for review) and behaviourally as varying responses to multiple presentations of a stimulus.

It has been proposed that internal noise is higher in Autism Spectrum Disorders (ASDs). This idea could account for a variety of abnormal sensory experiences associated with the condition (Horder, Wilson, Mendez, & Murphy, 2014; Robertson & Simmons, 2013; Simmons et al., 2009). Consistent with this theory, visual event-related potentials were found to be more variable in ASD individuals (Milne, 2011). Similarly, fMRI BOLD responses in the visual and auditory systems (Dinstein et al., 2012) are also more variable compared to neurotypical controls. Conversely, it has also been argued that internal noise may be unaltered (Butler, Molholm, Andrade & Foxe, 2017) or reduced (Davis & Plaisted-Grant, 2014) in ASD. In support of this latter idea, a study using a luminance increment paradigm targeting the magnocellular pathway found increased discrimination thresholds in individuals with high-functioning autism compared to neurotypical controls (Greenaway et al., 2013). Greenaway et al. attribute this to stochastic resonance, a process by which low levels of internal noise would yield worse performance on the task, although evidence for this phenomenon is tenuous (Manning & Baker, 2015). Additionally, as Manning & Baker point out, increased discrimination thresholds are indicative of increased rather than decreased internal noise since higher neural variability degrades the neural signal during processing, impairing performance. As this should increase discrimination thresholds, the

Greenaway et al study could be interpreted as evidence for increased internal noise in ASD.

Furthermore, mixed evidence for internal noise levels comes from motion coherence studies some of which show increased motion coherence thresholds indicating higher internal noise (Manning, Tibber, Charman, Dakin, & Pellicano, 2015; Milne et al., 2002; Pellicano, Gibson, Maybery, Durkin, & Badcock, 2005); and some show decreased thresholds suggesting lower noise (Manning et al., 2015). However, interpretation of motion studies is complicated by the possibility that participants might use different strategies, such as different sized pooling windows, in order to perform the task, and not all studies take this into account. So far, straightforward evidence for increased internal noise comes from EEG and fMRI research, however, it is unclear if and how increased variability in these measures affects perception and behaviour in ASD. It is therefore important to measure internal noise with a direct psychophysical paradigm.

One consequence of internal noise is that responses to the same stimulus over multiple repetitions will be inconsistent. This can be measured quantitatively using the 'double-pass' method, that was originally developed in auditory psychophysics (Green, 1964) and has subsequently been used to estimate noise in the visual system (Burgess & Colborne, 1988; Lu & Dosher, 2008), as well as in higher level cognitive tasks (Hasan et al., 2012). The double-pass method has mostly been used in contrast perception research using white pixel noise to inject variability (Burgess & Colborne, 1988). However, white pixel noise confounds adding external noise with increased cross-channel suppression (Baker & Meese, 2012), and so poses limitations on the accuracy of internal noise estimation (Baldwin et al., 2016) and is not applicable outside of low-level visual properties. An alternative way to render a stimulus 'noisy' (and so able to induce variability into the detecting neural system) is to jitter the intensity of the stimulus along a continuum (Baker & Meese, 2012, 2013), such as contrast, tone, frequency, facial expression intensity, etc.

The double-pass paradigm measures internal noise by repeating noisy stimuli twice (two passes) and calculating the consistency of responses between the passes (Burgess & Colborne, 1988; see Figure 5.1). In a two-alternative forced-

choice design two stimulus samples are drawn for each trial from a continuous normal distribution of stimulus intensities (e.g. contrast, tone frequency, etc.). The participant is asked to choose the more intense stimulus every time (first pass). This same procedure is then repeated again (second pass) with the exact same stimuli in each trial, and the consistency of responses across the first and second passes is calculated. The lower the consistency between passes, the higher the internal noise of the participant, because strong internal noise results in more highly variable responses.

Given the complexity and range of symptoms in ASD, the novel method (Baker & Meese, 2012, 2013) of introducing noise into the stimuli paired with the double-pass method can be applied to many perceptual and cognitive tasks in which internal noise may be implicated. To date, very little is known about internal noise throughout the brains of ASD individuals as research has been limited to low level visual properties. It is also not known how internal noise relates to autistic traits in subclinical populations. The current study investigates three tasks in which ASD individuals' performance has been reported to be differential from neurotypical individuals: contrast perception (CP; Bertone, Mottron, Jelenic, & Faubert, 2003, 2005; Greenaway et al., 2013), facial expression intensity (FE; see Harms, Martin, & Wallace, 2010 for review) and mathematical number summation (NS; Iuculano et al., 2015). The study aimed to investigate the relationship between autistic traits as measured with the Autism Spectrum Quotient (AQ; Baron-Cohen, Wheelwright, Skinner, Martin, & Clubley, 2001) and internal noise in three neural systems. We hypothesised that if internal noise is a general factor associated with autistic traits, there would be a relationship between AQ and a global estimate of internal noise in all three tasks.

5.3 Methods

5.3.1 Participants

Forty-five neurotypical participants (aged 18-39, 16 males) with normal or corrected-to-normal vision were recruited for the study. Two of the participants were not included in the analysis because of missing data in one or more of the tasks.
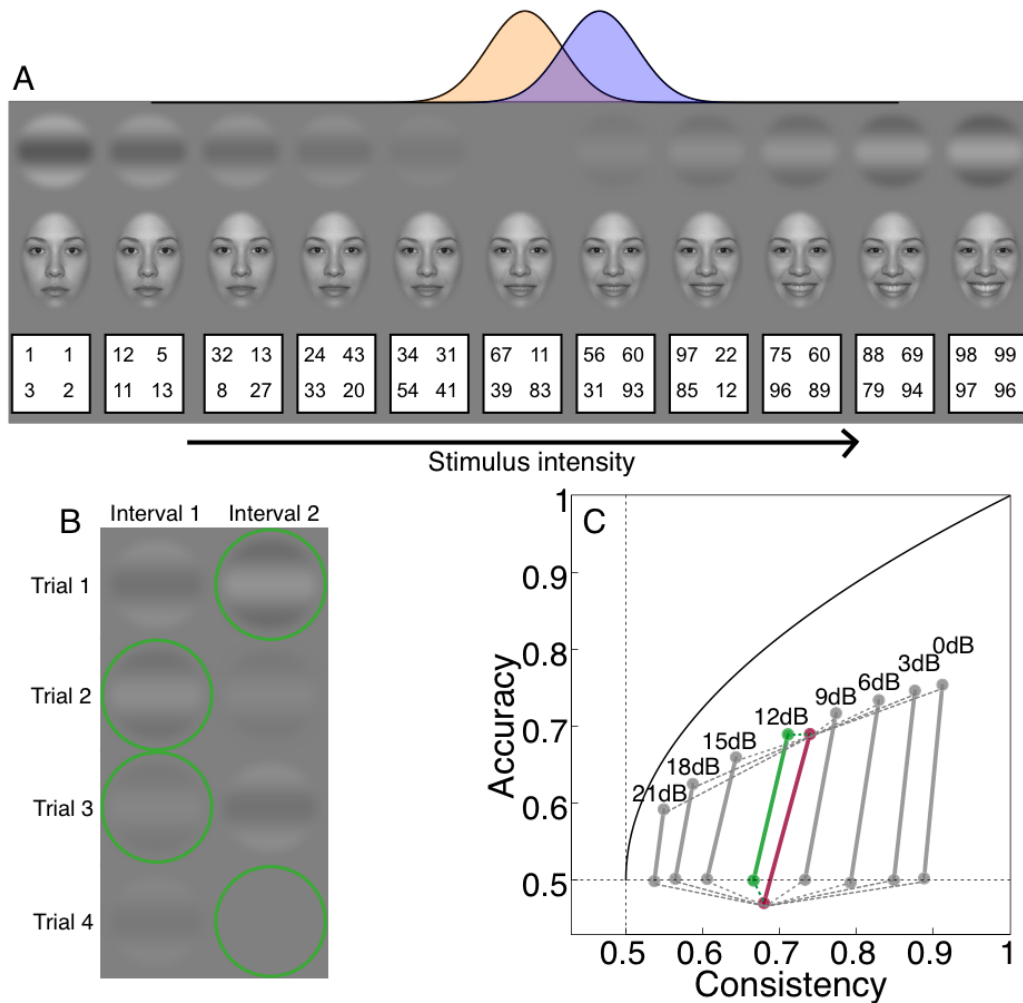
Figure 5.1. Stimuli and model predictions used in the study. Panel A. Stimuli used for the double-pass 2AFC discrimination tasks: contrast (top row), facial expression intensity (middle row) and number summation (bottom row). In 50% of trials (no target condition) a stimulus was drawn for each of the two intervals from a stimulus intensity distribution (orange) centered around 0% contrast, 50% facial expression morph and 200 sum for the numbers task. In the other 50% of trials (target present condition) one of the intervals was drawn from a higher stimulus intensity distribution (e.g. 4% contrast), shown in purple. Panel B. Examples of the two intervals in four hypothetical trials of the CP task with correct choices indicated by green borders. The same trials are repeated in a double pass experiment, with interval order randomized. Panel C. Estimation of internal noise by model simulations. The red dots and connecting line shows accuracy and consistency scores from an example participant for the two conditions (target present condition at the top). The green and grey dots and solid lines show simulated curves (see text for details) for an example range of internal noise levels (expressed in dB). Errors between participant scores for each condition were calculated (shown as dotted lines) and the internal noise level which produced the smallest error (averaged over conditions) was assigned to the participant (in this case green, 12dB). In the main analysis, we used a finer sampling of internal noise levels (0.1dB steps) than depicted here. The solid black line represents the expected performance in the absence of external noise (Klein & Levi, 2009) and the dashed lines show chance levels.

5.3.2 Materials

Stimuli for all tasks were presented on a gamma corrected Iiyama VisionMaster Pro 510 CRT monitor running at 100Hz, with a mean luminance of 32 cd/m^2. To enable accurate rendering of low contrast stimuli in the CD experiment, we used a ViSaGe device (Cambridge Research Systems Ltd., Kent, UK) running in 14- bit mode. Participants used a computer mouse to make their responses. The AQ questionnaire was delivered and scored automatically by computer.

5.3.3 Stimuli and paradigm

Examples of the stimuli are displayed in Figure 5.1. Stimuli were presented in pairs in each trial and the participants were asked to pick the more intense stimulus. CD stimuli were horizontal sine-wave gratings with a spatial frequency of 0.5c/deg in cosine phase. Stimuli flickered between 0 and their maximum intensity (on/off flicker) at 7Hz for 429ms (3 cycles). The stimulus intensity for CD was the contrast level of the stimulus. There were two conditions, target present and target absent. In the target absent condition, the stimuli in the two intervals of each trial had random contrast levels drawn from a Gaussian distribution centred around 0% Michelson contrast (defined as $C_\% = 100*(\frac{L_{max} - L_{min}}{L_{max} + L_{min}})$, where L_{max} and L_{min} are the maximum and minimum luminances of the grating), with a standard deviation of 4%. Negative values reversed the polarity of the grating so that it became dark in the centre. In the target present condition, a positive contrast increment of 4% was added to one of the intervals in each trial, so that the distribution in that interval had a mean and standard deviation of 4%.

Similarly to CD, facial expression intensity was drawn from a Gaussian distribution of a continuous morph between a neutral and an expressive face (Figure 5.1), with a mean of 32% and a standard deviation of 16%. In the target absent condition both intervals within a trial were selected from the same Gaussian distribution whereas in target present an expression increment of 16% was added to one of the intervals (we imposed a floor of 0% so that expressions could not become negative). Six emotional expressions (anger, sadness,

happiness, fear, surprise and disgust) were used and data were collapsed over expressions. The RMS contrast of each expression was equated before morphing, ensuring that all stimuli had equal contrast. Facial stimuli were within-gender averages of from the NIMSTIM face database (Ekman & Friesen, 1971), with 23 male models and 19 female models (Adams, Gray, Garner, & Graf, 2010). Face gender was randomly determined on each trial, but was constant for both intervals of each trial. The faces were windowed by an oval raised cosine envelope, and spanned 10x16 degrees of visual angle. Face stimuli were presented for 100 ms.

In the NS task, two boxes, each containing four double-digit numbers were presented. In the target absent condition the four numbers in each box on each trial were selected from a distribution centred around 50, with a standard deviation of 10 (and an average sum of 200). In the target present condition one of the boxes had a mean of 50 and the other had a mean of 60.

For all tasks, each trial was repeated twice (pass one and pass two), preserving the exact samples of stimulus intensity, once in each half of the experiment.

5.3.4 Procedure

The method of constant stimuli was used. There were 100 trials in each target condition in each pass (400 trials in total per participant in each experiment). All experiments were carried out in a dark room at 57cm distance from the computer monitor using a chin-rest. Participants had breaks between sessions and the entire experiment took approximately two hours in total per participant.

5.3.5 Estimating noise from model

Accuracy and consistency scores were used to obtain accurate estimates of internal noise for each participant. In order to obtain a single measure of internal noise that averages out measurement error, double-pass accuracy and consistency scores were simulated for different levels of internal noise using a noisy linear model. We then determined the level of internal noise that best described the data

for each observer. Simulated responses to the target and the null intervals within a trial were given by:

$$resp_{target} = \sigma_{int} + \sigma_{ext} + C_{mean} + C_{target}$$

$$resp_{null} = \sigma_{int} + \sigma_{ext} + C_{mean}$$

where $resp_{target}$ and $resp_{null}$ are the responses in the target and null intervals respectively, σ_{int} and σ_{ext} represent internal and external noise, C_{mean} is the mean intensity of the stimulus and C_{target} is the target intensity added in the target interval. The noise variables (σ_{int} and σ_{ext}) were drawn on each simulated trial from Gaussian distributions with a mean of zero, and the appropriate standard deviation for each experiment. The interval with the larger response was selected. This was repeated twice with identical values of σ_{ext}, but different values of σ_{int}, in order to simulate both accuracy and consistency scores. There were 100000 simulated trials for each internal noise level and this was done for 801 noise levels (ranging from -40dB to 40dB in steps of 0.1dB). The errors between the model simulations and empirical data points in each condition (in the accuracy-consistency space) were calculated for each participant. The internal noise level that produced the smallest absolute error (averaged over conditions) was then assigned to that participant. This was repeated for each of the three experiments.

5.4 Results

Mean accuracy in the target present condition was 0.67 (SD = 0.06) for CP, 0.67 (SD = 0.05) for FE and 0.68 (SD = 0.06) for NS, indicating participants were performing above chance. The consistency scores were also above chance for CP (mean = 0.81, SD = 0.10), FE (mean = 0.70, SD = 0.08) and NS (mean = 0.69, SD = 0.06) tasks. We used these values along with the modelling approach described above to derive an estimate of internal noise for each participant in each experiment. The noise estimates from the CP and FE tasks were not normally distributed when tested with the Shapiro-Wilk test of normality ($p < 0.001$ and $p =$

0.009 respectively) therefore two-tailed Spearman signed rank correlations were used throughout the analysis.

Internal noise was significantly correlated with AQ in the CP ($r_S = 0.34$, $p = 0.028$) and NS ($R = 0.31$, $p = 0.042$) but not the FE task ($r_S = 0.26$, $p = 0.091$). There were strong significant positive correlations between noise estimates across all three tasks ($r_S \geq 0.60$, see Figure 5.2 for r_S and p values). Since this suggested the presence of a single underlying factor, we performed principal component analysis (PCA) on the model estimates of internal noise. PCA is a dimension-reduction technique that attempts to condense a multivariate dataset of correlated variables into a smaller number of uncorrelated factors. Internal noise estimates from the CP, FE and NS tasks loaded onto a single factor, 'global internal noise', which was extracted by Keiser's criterion (eigenvalue of 2.30) explaining 76.81% of the variance. Factor loadings were extracted for participants and the inverse values were taken as a global measure of noise (such that small values indicate low noise).
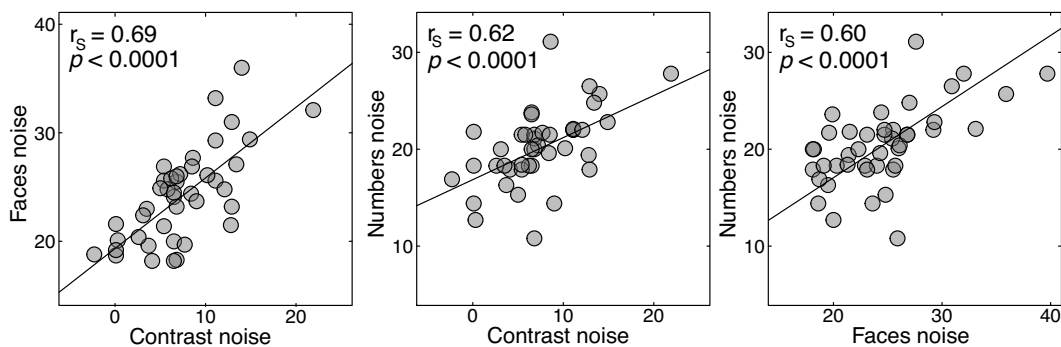
Figure 5.2. Scatterplots showing correlations between the estimated noise levels in all three tasks, expressed in logarithmic (dB) units. Black lines represent best-fit Deming regression lines.

The global internal noise factor was positively correlated with AQ scores ($r_S = 0.32$ $p = 0.035$) suggesting that higher internal noise is related to higher levels of autistic traits. As raw double-pass consistency scores are sometimes used as a measure of internal noise (low consistency means high internal noise), the PCA was repeated on mean consistency scores (averaged over the two target conditions). The internal noise factor extracted in this way explained 77.13% of

112

variance and was also significantly correlated with AQ ($r_S = 0.33$, $p = 0.032$). This suggests higher levels of autistic traits are related to higher internal noise (see Figure 5.3). However, as the accuracy scores in the NS task were significantly correlated with AQ (R = -0.43, $p = 0.004$), the modelled estimates of internal noise which take into account both the accuracy and consistency are preferred. AQ was not significantly correlated with accuracy in CP (R = -0.14, $p = 0.384$) or in FC (R = -0.14, $p = 0.364$).
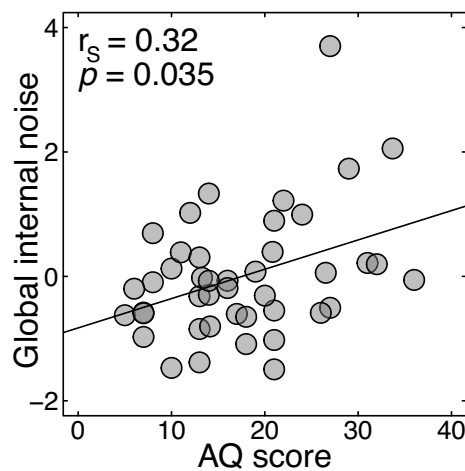
Figure 5.3. Scatterplot showing the significant positive correlation between AQ scores and internal noise. The black line represents a Deming regression line.

5.5 Discussion

The current study reports the first direct psychophysical estimate of internal noise in relation to autistic traits. Using the double-pass method in three different tasks we found a positive relationship between autistic traits in the neurotypical population and overall levels of internal noise. Individual differences in internal noise in the CP, FE and NS tasks were largely accounted for (76.81% of the variance) by a single internal noise factor suggesting a common noise source. This factor was positively correlated with autism spectrum quotient (AQ) scores. We suggest that this factor is either global internal noise affecting perception and behaviour regardless of task complexity or neural mechanism involved, or it is late decision making noise.

5.5.1 Neural basis of internal noise in ASD

The current finding of increased internal noise being associated with more autistic traits supports previous electrophysiological and neuroimaging studies that found more variable responses to sensory stimuli in clinical ASD populations (Dinstein et al., 2010, 2012; Milne, 2011). Increased internal noise can also manifest as decreased coherence in natural neural oscillations such as γ-band activity. Rojas, Maharajh, Teale, & Rogers (2008) found reduced phase-locking in γ-band oscillations, indicative of increased neural noise, in adults with ASD and also in neurotypical parents of ASD children compared to controls. Increased neural variability in neurotypical first-order relatives of ASD individuals suggests a genetic influence of an ASD genotype on the level of internal noise in the brain. This is not surprising as ASD has a complex but strong genetic basis (see Miles, 2011 for review) which may, at least in part, be mediated by neural noise factors. The finding of the present study, as well as Rojas et al. (2008), suggest that internal noise is intrinsic to the ASD phenotype and extends beyond clinical ASD populations. As others have proposed, noisier sensory processing throughout development could plausibly lead to several of the social difficulties (i.e. facial expression perception) typically associated with ASD (Simmons et al., 2009).

5.5.2 Early versus late noise

It is unclear from the current study whether the internal noise we measured affects the neural signal early or late in processing. Noise in early sensory regions will be passed forward to decision making processes and so produce variable responses. As we find that internal noise is common across our three tasks, this type of noise would need to span multiple regions of the brain to account for our data. Autistic traits may be related to early sensory noise as previous research suggests increased neural variability in several sensory regions of the brain (Dinstein et al., 2012). Alternatively, the internal noise we measured may be a late decision-making noise that influences behaviour at the level of executive processing. This possibility is consistent with research showing poorer executive function (Hughes, Russell, & Robbins, 1994; Kenworthy, Black, Harrison, della Rosa, & Wallace, 2009) and abnormal connectivity of white matter in frontal lobes (Sundaram et al.,

2008) in clinical ASD populations. In either case, internal noise may pose a limitation on brain function for individuals high on the autistic spectrum.

5.5.3 Innovation in noise measurement

This study benefits from a novel implementation of the double-pass paradigm for measuring internal noise. The application of intensity jitter rather than traditional white pixel noise (as often used in contrast detection experiments; Burgess & Colborne, 1988) extends the viability of double-pass methods to other sensory and cognitive modalities. We have also developed accurate model-based estimates of internal noise that take into account any sensitivity differences between individuals. Previous studies (Burgess & Colborne, 1988) used raw consistency scores as a measure of internal noise. However, we observed a high correlation between accuracy and consistency scores in our data ($r_S \geq 0.41$, $p \leq 0.006$). This is not surprising since it follows that higher performance on a task would yield more consistent responses (in the limiting case of perfect performance, consistency is necessarily 100%). The modelled estimates of noise take into account both accuracy and consistency scores and so are not biased by individual differences in sensitivity.

The current methodology measures noise more directly than previous psychophysical studies (Greenaway et al., 2013; Manning et al., 2015). The equivalent noise approach used in other work (Manning et al., 2015; Manning, Charman, & Pellicano, 2013; Milne et al., 2002; Pellicano et al., 2005), relies on a specific (usually linear) model of the underlying mechanism that may not accurately reflect how stimuli are processed, and cannot disambiguate differences in noise from differences in sensitivity (see Baldwin, Baker & Hess, 2016). Double-pass techniques avoid these problems, and additionally have high internal reliability and produce internal noise estimates consistent with those from another psychophysical paradigm (*Chapter 3*). As this study investigated the relationship between internal noise and autistic traits in neurotypical individuals, it would be of great interest to use the double-pass method to measure internal noise in clinical ASD. Considering current findings and previous studies we would expect higher internal noise in ASD individuals when compared to controls.

5.5.4 Summary and conclusions

Neurotypical individuals exhibiting higher levels of autistic traits had higher internal noise, measured using three psychophysical tasks. This finding supports previous studies that found higher internal noise in ASD populations using neuroimaging methods. Increased internal noise seems to be a fundamental feature associated with ASD in clinical and subclinical populations, and may explain some of the symptoms and traits of ASD (Simmons et al., 2009). We suggest that a genetic link between the autistic phenotype and internal noise could account for the current findings.

Chapter 6

Autism sensory dysfunction in an evolutionarily conserved system

This chapter has been adapted from: Vilidaite, G., Norcia, A. M., West, R. J. H. Elliott, C. J. H., Pei, F., Wade, A. R. & Baker, D. H. (under review). Autism sensory dysfunction in an evolutionarily conserved system. *PNAS.*[5]

6.1 Abstract

Individuals with Autism Spectrum Disorder (ASD) report a host of sensory symptoms, which suggests a fundamental, genetic (Miles, 2011) neural signaling deficit in autistic brains (Rubenstein & Merzenich, 2003). However, neither animal models nor previous theories explaining sensory symptoms have been able to predict neurophysiological data in autistic humans. Here we show a strikingly similar trajectory of visual development in a genetic Drosophila Nhe3 model of autism and in autistic human participants. We report a dissociation between first-

---

[5] The author, Greta Vilidaite, designed the adult human and fruit fly experiments under the supervision of Dr Daniel Baker, Prof Alex Wade and Dr Chris Elliott. Greta Vilidaite collected all of the data except for the children's data, which were collected by Dr Francesca Pei. Greta Vilidaite analysed the results and wrote the manuscript under the supervision of Dr Daniel Baker and Prof Anthony Norcia and with advice from other co-authors.

and second-order electrophysiological visual responses to steady-state stimulation in adults with ASD as well as a large sample of neurotypical individuals with high numbers of autistic traits. We also report a strikingly similar impairment in the adult fruit fly model of ASD. We explain this as a selective signaling abnormality in the transient response mechanisms in the visual system. In contrast to adults, autistic children show decreases in both first- and second-order responses, which are closely matched by the fruit fly model, suggesting a compensatory change in processing occurs over the course of development. Our results provide the first animal model of autism comprising a developmental sensory pathway phenotype.

6.2 Significance statement

Autism Spectrum Disorder exhibits strong and widespread sensory symptoms that have not yet been explained by previous research. Here we have developed a novel *Drosophila* model of sensory deficits in autism that is highly predictive of electrophysiological visual data in both autistic adults and children. Both the animal model and human data, from three samples (total N = 154), point towards a deficit of a fundamental signaling mechanism in early parts of the sensory system. This deficit shows signs of change during development indicating a possible partial rescue of function at later stages of life. Our findings can explain previous inconsistencies in research into visual perception in autism. The *Drosophila* model can be used in future biomarker and treatment development.

6.3 Introduction

Autistic individuals report a host of sensory symptoms including unusual sensory interests, overstimulation and hyper- and hyposensitivity to intense stimuli such as bright lights or loud noises (Ben-Sasson et al., 2009; Jones et al., 2003). Several theories have been proposed to account for sensory abnormalities in autism – one of the most common proposing an imbalance in excitation/inhibition (E/I) (Rubenstein & Merzenich, 2003). The E/I imbalance theory of autism has gained mixed but largely supportive evidence from neurochemical, neurobiological and

genetic investigations (Green et al., 2013; Hahn et al., 2013; Nelson & Valakh, 2015), implicating GABA-ergic mechanism deficits (Gao & Penzes, 2015). Alternatively, a vision-specific theory has linked visual processing abnormalities in ASD to a selective deficit in the magnocellular pathway (Milne et al., 2002; Plaisted, Swettenham, & Rees, 1999). Such signaling-level impairments indicate a genetic cause of ASD sensory symptoms (Miles, 2011). However, neural measurements that can convincingly delineate these competing explanations are yet to be reported.

One attempt in mice to model a related developmental condition, Rett syndrome, found similar cross-species decreases in visual neural responses and poor visual acuity (LeBlanc et al., 2015). However, Rett syndrome lacks the pervasive sensory symptoms characteristic of autism, thus it is difficult to link cellular and genetic abnormalities to ASD sensory deficits (Burd & Gascon, 1988). As an alternative to rodents, *Drosophila* have provided successful models of human neurological disorders such as Parkinson's (West et al., 2015) and Alzheimer's (Moloney, Sattelle, Lomas, & Crowther, 2009). Fruit flies share 75% of human disease causing genes (Reiter, Potocki, Chien, Gribskov, & Bier, 2001) and have a visual system exhibiting similar nonlinear neural properties, including a color- and luminance-selective module as well as a motion-selective module (Fischbach & Dittrich, 1989). The neural dynamics of these modules closely resemble those of the transient and sustained neural populations in humans (Afsari et al., 2014; Behnia & Desplan, 2015; Clark et al., 2014). This provides an excellent framework for modeling low-level changes in sensory neuronal signaling (Clark et al., 2014) which may lie behind sensory abnormalities in autism.

In this study we aimed to develop an animal model of sensory abnormalities in human ASD and to investigate the mechanism underlying these impairments. We measured visual neural responses both in autistic humans and in *Drosophila* with a genetic mutation linked to autism. In humans, loss-of-function mutations in the gene *SLC9A9* have been linked to ASD (Kondapalli et al., 2013). Here we used a *Drosophila* orthologue of *SLC9A9 – Nhe3*. A homozygous P-element insertion loss-of-function mutants (*Nhe3^{KG08307}*) and *Nhe3* hemizygotes *(Nhe3^{KG08307}*/Df(2L)BSC187) were used to inhibit *Nhe3* function in fly. To assess the functionality of sustained and transient pathways in these species, we

measured two steady-state electrophysiological responses: first harmonic (stimulation) and second harmonic frequencies, in both humans and fruit flies. The use of two Nhe3 mutations in different genetic backgrounds ruled out the possibility of other mutations influencing the flies' visual responses. The dynamics of the sustained pathway manifest in the electrophysiological stimulation frequency (first harmonic) response whereas the dynamics of the transient pathway can be observed in the second harmonic response (Afsari et al., 2014; Skottun & Skoyles, 2007). Furthermore, to investigate the progression of ASD sensory abnormalities over the course of development, we also measured visual responses at two stages of fruit fly maturation and acquired similar responses from autistic children. Finally, as the ASD phenotype is complex and non-binary, we validated our sensory model with a large sample of neurotypical participants with high and low numbers of autistic traits.

6.4 Results

6.4.1 Increased sustained/transient response ratio in Nhe3 fruit flies

Using a steady-state visual evoked potential (ssVEP) paradigm (West et al., 2015) (see Figure 6.1) we measured fruit fly visual responses to flickering stimuli via an electrode on the fly's eye. Wild type, eye-color matched flies (a cross between isogenic and Canton-S) were used as controls (+). Flies from each genotype (n = 12) were tested at three days (when the flies are young) and at 14 days post eclosion (older). First harmonic (12Hz) and second harmonic (24Hz) response amplitudes were derived by fast Fourier transform (see *Methods,* section 6.6). Although the first harmonic responses of mutant and wild-type flies were the same, the second harmonic response was significantly reduced in the *Nhe3* mutants (Figure 6.2A, 6.2B).
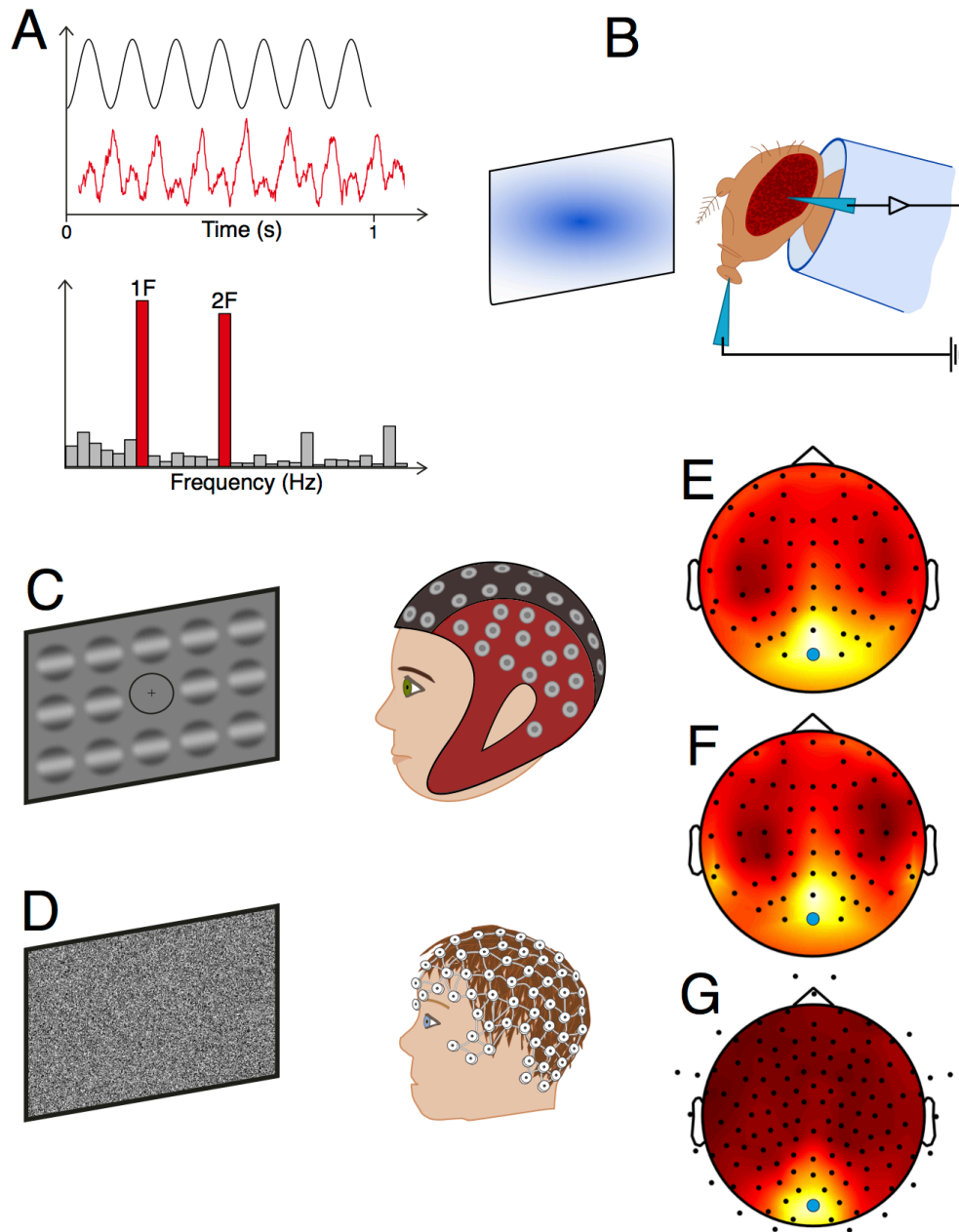
Figure 6.1. Human and *Drosophila* steady-state electrophysiology methods. Panel A illustrates an example of electrophysiological responses (in the adult AQ dataset) as a function of time (red trace) in response to stimulus flicker (black trace). Two peaks can be observed after each increase in stimulus contrast giving rise to the first (1F) and second (2F) responses, which are evident in the frequency domain after Fourier transform (lower panel A). Adult subjects (for both the ASD vs. neurotypical dataset and the neurotypical AQ dataset) were presented with a grid of sinusoidal gratings flickering at 7Hz whilst SSVEPs were recorded using a 64-channel EEG cap (C). Children were tested with a binary noise stimulus flickering at 5.12Hz and a 128-channel EEG cap (D). SSVEPs were measured from the occipital electrode Oz (indicated by green dots in e, f, g) where the highest first harmonic amplitude was centered, indicated by the heatmaps for the adult AQ data set (E), adult ASD data set (F) and child data set (G). Fruit fly electrophysiological data was acquired as shown (B) using square wave stimulus flicker; see *Methods* (section 6.6) for more details.
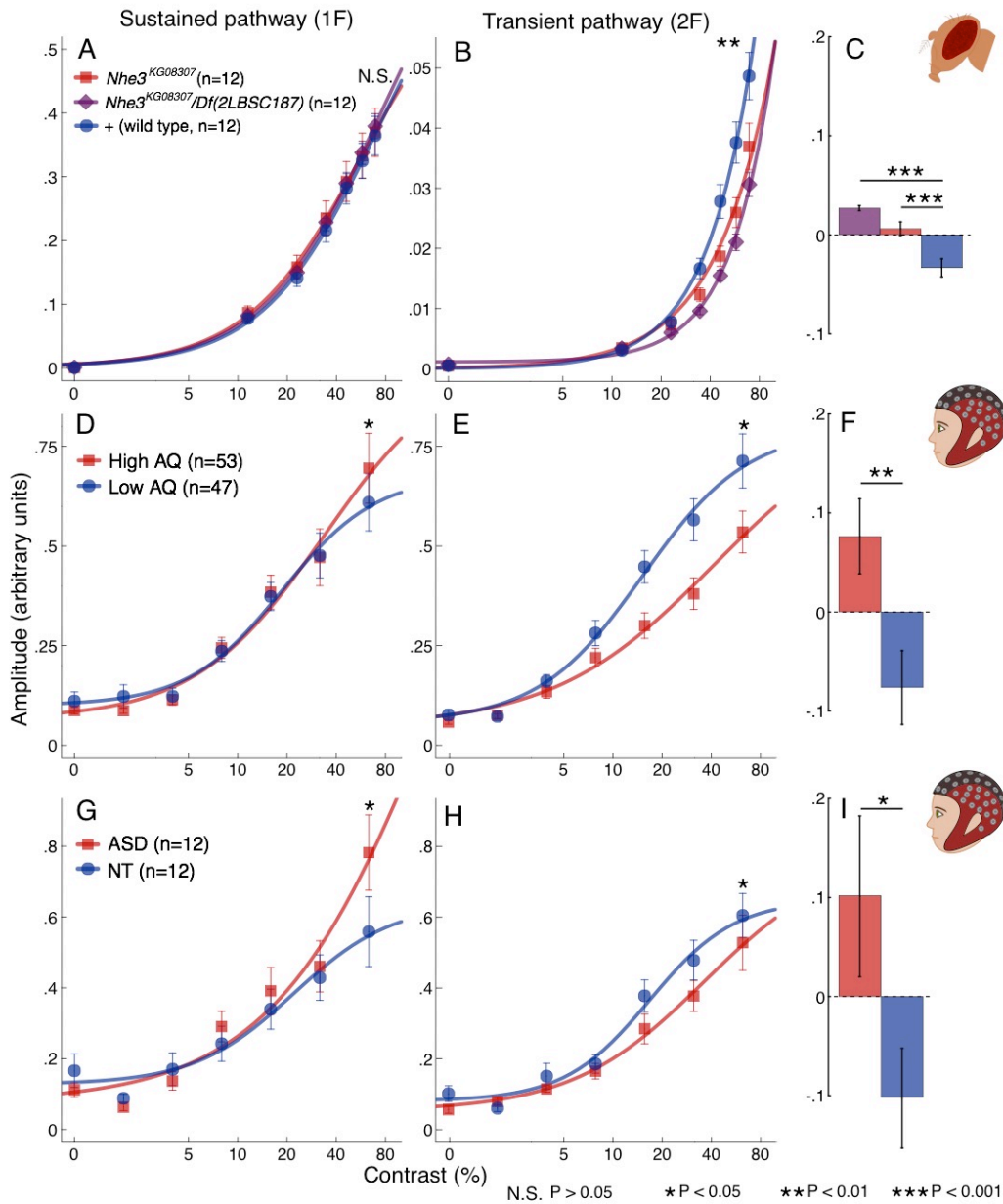
Figure 6.2. Older ASD-mimic flies and autistic humans have visual deficits in the transient pathway. Contrast response functions for adult *Nhe3* mutant flies (*Nhe3^{KG08307}* homozygotes, red squares and *Nhe3^{KG08307}* /*Df(2L)BSC187*, purple diamonds) were similar at the 1st harmonic (a one-way ANOVA showed no effect of group $F_{2,33} = 0.05$, P = 0.95, panel A) but responses were reduced for P/P (simple contrast, P = 0.025) and P/Df mutants compared to controls at the 2nd harmonic (simple contrast P = 0.001; ANOVA group effect $F_{2,33} = 6.71$, P < 0.01; panel B). Ratios between frequencies ($\frac{1F-2F}{1F+2F}$) were significantly higher for P/P (P < 0.001) and for P/Df (P < 0.0001) than for the control genotype (C). First harmonic responses were also similar for the high AQ and low AQ groups (panel D) and for adults with and without ASD (panel G). However, 2nd harmonic responses were reduced for both adults with high AQ (panel E) and with ASD compared to controls (panels H). The ratio between harmonics was also higher in both experimental groups compared to controls (panels F and I, P = 0.005 and P = 0.04, respectively). Curved lines are hyperbolic function fits to the data. Frequency ratios are baselined in respect to the mean over groups of each comparison for display purposes.

122

To quantify this functional dissociation between the two response components we calculated a normalized ratio between first (1F) and second (2F) harmonics $(\frac{1F-2F}{1F+2F})$ and averaged over the highest contrast conditions (where the response rises above the noise floor, see *Methods,* section 6.6). This allowed us to measure the differences between sustained and transient responses whilst normalizing for overall responsiveness of the visual pathway. The ratio was significantly higher in both mutant strains than in the controls (ANOVA, $F_{2,33} = 20.53$, $P < 0.0001$, both paired contrasts $P < 0.001$; Figure 6.2C). These data suggest an impairment in the post-receptoral neural pathways (structures downstream of the photoreceptors) of the older mutant flies.

Interestingly, unlike the older flies, the young 3 day old flies showed a reduced response at both frequencies (see Figure 6.3A, 6.3B) relative to controls. Importantly, there was no effect of genotype on the ratio between harmonics ($F_{2,33} = 1.38$, $P = 0.27$; Figure 6.3C). These results suggest a deficit in the sustained visual module of young mutant flies, which most likely causes a cascading impairment in the transient module. These differences between visual responses at two stages of life suggest a change in visual processing over the course of development.
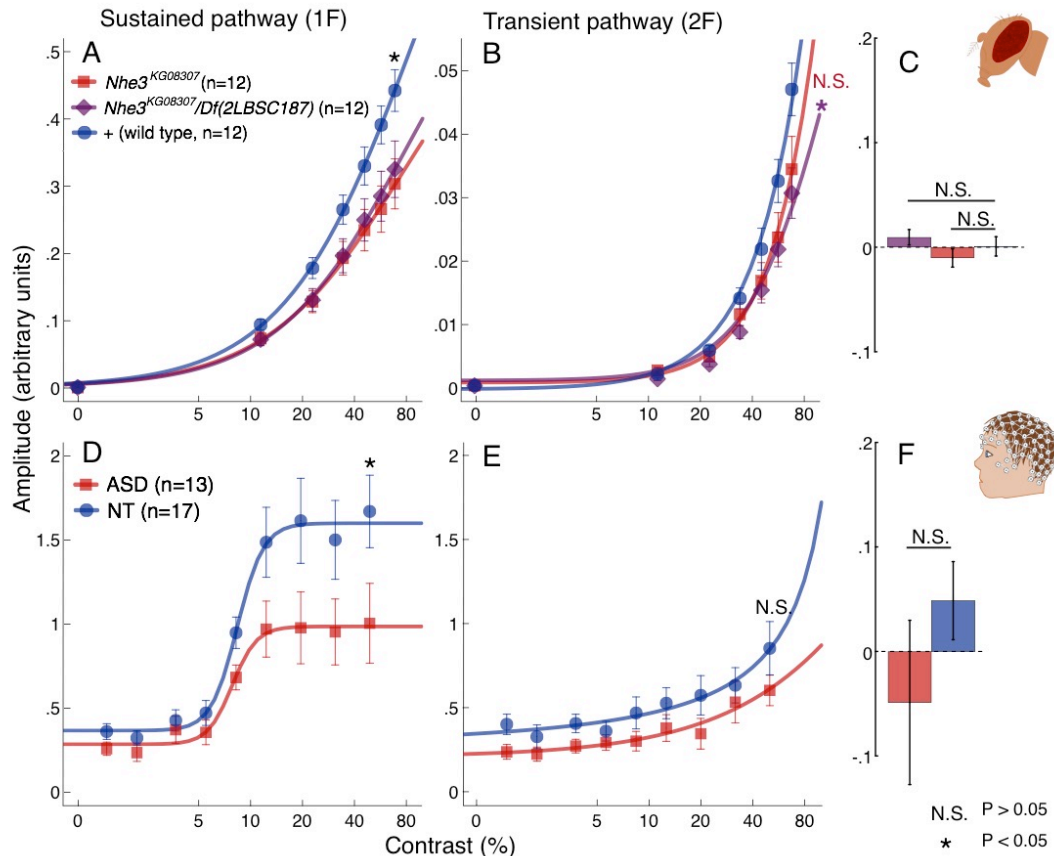
Figure 6.3. Young ASD-mimic flies and children with ASD have visual deficits in the sustained pathway. Young fruit flies showed reduced responses at the 1st harmonic ($F_{2,33}$ = 3.73, P = 0.035; panel A) with P/P and P/Df flies showing a significant difference from control flies (respectively, P = 0.016 and P = 0.040). There was also a significant effect of genotype at the 2nd harmonic ($F_{2,33}$ = 3.39, P = 0.046, panel B). P/Df flies showed a significant difference from control flies (P = 0.018), however, P/P showed a non-significant difference from controls (P = 0.064). The flies had normal frequency ratios (panel C). Children with ASD also showed reduced 1st harmonic (t_{28} = 2.065, P = 0.048; panel D) but not 2nd harmonic responses (t_{28} = 1.26, P = 0.22; panel E) and had frequency ratios similar to that of control children (t_{28} = 1.21, P = 0.24; panel F). Curved lines are hyperbolic function fits to the data. Frequency ratios are baselined in respect to the mean over groups of each comparison for display purposes.

6.4.2 High autistic trait population show similar ssVEPs to Nhe3 flies

To assess the relevance of the *Nhe3* model to the human ASD phenotype we used a comparable and equally sensitive steady-state EEG paradigm in human participants. One hundred neurotypical participants with putative autistic traits measured using the Autism Spectrum Quotient (AQ) questionnaire (Baron-Cohen et al., 2001) were tested with the ssVEP paradigm. Visual responses were recorded from an occipital electrode (Oz, located at the back of the head over the

visual cortex) to grating stimuli flickered at 7Hz. Seven contrast conditions (each repeated eight times) were presented in a randomized order. First and second harmonic ssVEP responses were again derived via Fourier analysis. The evoked response data were averaged separately over participants split by their median AQ score: high (n = 53, AQ mean = 11.53, SD = 3.68) and low (n = 47, AQ mean = 5.32, SD = 1.81) AQ (high AQ implying many autistic traits). The first harmonic response was similar in both groups whereas the second harmonic was notably reduced in the high AQ group (Figure 6.2D, 6.2E). A two-way ANOVA showed the interaction between group and frequency to be significant ($F_{1,98} = 6.17$, P = 0.015). The high AQ group also had a significantly higher frequency ratio than the low AQ group ($t_{98} = 2.86$, P < 0.01, Figure 6.2F). Moreover, a regression analysis showed that AQ scores correlated with the frequency ratio, with high AQ scores being predictive of higher ratios (R = 0.26 $F_{1,98} = 6.87$, P = 0.01; see Figure 6.4). This result shows a relationship between the amplitude of the second harmonic response and the severity of the subclinical ASD phenotype, however, this effect cannot be directly generalized to clinical autism as the AQ is not diagnostic of full-blown ASD.
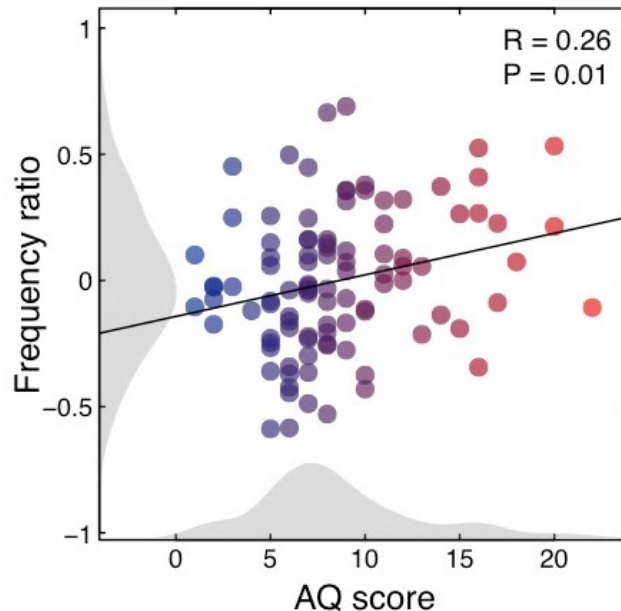
Figure 6.4. Positive relationship between the number of autistic traits and first/second harmonic ratio. Scatterplot showing a significant positive relationship between AQ scores and frequency ratios in the 100 neurotypical adult dataset indicating a gradual increase of impairment with the number of reported autistic traits. The black line indicates the regression line of best fit. Shaded grey areas show histograms of AQ scores and frequency ratios. Blue-red color transition indicates number of AQ traits with subjects split by median into low and high AQ groups as presented in Figure 6.2.

6.4.3 Autistic individuals show the same pattern of responses as Nhe3 flies

We assess this difference between harmonics in clinical ASD by testing 12 typical-IQ autistic adults (diagnosis confirmed with the Autism Diagnostic Observation Schedule, Second Edition (ADOS-2), Lord et al., 2000) and 12 age- and gender-matched controls using the same human ssVEP paradigm. The pattern of data again mimicked that of the previous adult data sets: there was a significant interaction between group and frequency ($F_{1,22} = 5.85$, P = 0.02; Figures 6.2G, 6.2h). The ratio between harmonics was again significantly larger in the ASD group than in the control group ($t_{22} = 2.13$, P = 0.04; Figure 6.2I).

6.4.4 Young Nhe3 fly responses predict autistic children's responses

Considering the striking similarity between the adult human data sets and the adult fruit fly model, it is reasonable to ask if similarities also exist between younger humans and young Drosophila ASD models. Specifically, our fly model predicts that the visual system of autistic children should show reduced responses in both the first and second harmonics. To examine this, we recorded from 13 autistic children (5 – 13 years old) and 17 neurotypical age- and gender-ratio-matched controls using an ssVEP contrast-sweep paradigm. Artifact rejection was employed to control for movement and blinking in both groups. The stimulus in each sweep trial increased continuously in contrast from 0% to 50% in logarithmic steps. Data were binned into 9 contrast levels before being Fourier transformed to compute response amplitudes.

As predicted by the fly data, the ASD group showed impaired processing in the sustained response ($t_{28} = 2.07$, P = 0.04; Figure 6.3D, 6.3E). A two-way ANOVA also revealed a significant group effect over both frequencies ($F_{1,28} = 4.23$, P = 0.049). Unlike adults, children exhibited no difference in frequency ratios between the groups (t = 1.41, P = 0.17; Figure 6.3F). Children showed impaired processing in the sustained pathway as predicted by the fruit fly model. However, the smaller effect of amplitude reduction observed in the fruit fly second harmonic responses was present, but not statistically reliable in the children ($t_{28} = 1.26$, P = 0.219). This may be due to the more variable nature of human EEG data.

6.5 Discussion

We found a selective deficit in second order responses in autistic adults, individuals with high levels of autistic traits and *Nhe3* fruit flies suggesting that this impairment is specific to the autistic phenotype. Autistic children and young *Nhe3* flies showed a more global deficit in visual processing at early stages of life. The *Nhe3* fruit fly model of autism was highly predictive of these ASD visual response deficits both in children and in adults, suggesting a fundamental and pervasive change in visual impairment during development. High AQ individuals showed consistent visual responses to participants with diagnosed ASD suggesting robust visual response properties between samples. This was unsurprising as previous research has found that AQ scores in the general population are highly correlated (R = 0.77) with sensory processing difficulties, as measured by the Glasgow Sensory Questionnaire (Robertson & Simmons, 2013), indicating that high AQ individuals exhibit milder forms of sensory difficulties.

The intact first harmonic response in adult flies and humans indicates normal functioning of mechanisms which give rise to the sustained response. Conversely, the reduced second harmonic response suggests a deficit in the transient dynamics of the visual system. In fly, the first harmonic has been associated with sustained photoreceptor polarization and the second harmonic with second-order lamina cells (Afsari et al., 2014b). In human, an association has been made between simple cell and sustained responses to pattern onset and complex cells and transient responses at both stimulus onset and offset (Mckeefry, Russell, Murray, & Kulikowski, 1996). Although simple cells exhibit some transient response properties as well (Mckeefry et al., 1996; Mclelland, Baker, Ahmed, & Bair, 2010), the intact first harmonic suggests that the impairment is specific to human complex cells that only generate even-order response components. This early, cell-type-specific deficit may explain previous findings of atypical neural dynamics of spatial frequency processing in ASD in the face of normal sensitivity thresholds (Jemel, Mimeault, Saint-Amour, Hosein, & Mottron, 2010; Pei, Baldassi, & Norcia, 2014).

The differential impairment of sustained and transient modules observed in our *Nhe3* model mimics the pathway abnormality in autistic adults. *Nhe3* affects the

exchange of sodium and hydrogen ions in cell membranes directly affecting neural signaling (Kondapalli et al., 2013; Schwede et al., 2013). Differential expression of *Nhe3* and other genes in ASD, which has been observed in other parts of the brain (Kondapalli et al., 2013; Voineagu et al., 2013) may extend to differential expression in color and motion modules in the *Drosophila* visual system. As *Nhe3* (*SLC9A9* in humans) is only a single gene in a multifaceted genetic etiology of autism, it is likely that the expression of several genes in human autism affects simple and complex cell dynamics, producing similar effects on the neural population level. Furthermore, such abnormality in gene expression in other parts of autistic brains, as well as environmental influences and gene-environment interactions, may give rise to a wide range of cognitive and social impairments in childhood and adulthood.

Our data indicate little or no over-responsivity in the visual responses predicted by the E/I theory, consistent with some previous studies (Dickinson et al., 2016; Said et al., 2013). However, it is possible that E/I imbalance in autism, stemming from GABA-ergic mechanism deficits, affects different neuron types or processing pathways in distinct ways and to different extents. Regardless, cell-type level processing abnormalities may explain previous inconsistencies in sensory deficits in ASD in which pathways were not differentiated (Simmons et al., 2009). Furthermore, the current results can provide an amended explanation to the magnocellular (M pathway) dysfunction hypothesis. As it is difficult to isolate the M pathway by changing stimulus properties (Skottun & Skoyles, 2007), the paradigms previously used to investigate magnocellular dysfunction in ASD may have been selectively activating complex cells rather than the M pathway in particular (Greenaway et al., 2013; Sutherland & Crewther, 2010).

Developmentally, the observed change in the nature of the abnormality in both species with increasing age is in accordance with previous findings showing reduction or complete rescue of neuroanatomical abnormalities present in early ASD childhood over the course of maturation (Courchesne, Redcay, & Kennedy, 2004). Previous longitudinal research has also shown that symptom severity in individuals diagnosed with ASD in childhood decreases over time (Mcgovern & Sigman, 2005; Seltzer et al., 2003). McGovern & Sigman (2005) found that 48 adolescents, who were diagnosed with ASD as children, showed marked

improvement in social interaction, repetitive/stereotyped behaviors and other symptoms, with two no longer meeting criteria for ASD under ADI-R criteria, and four under ADOS criteria. This might be explained by a change in neural processing during development, which would likely affect both behavioral and sensory outcomes.

One possible mechanism that would explain the present results is that the neural signaling abnormalities (such as ion balance in the case of Nhe3), change over time. In flies, reduced Nhe3 expression may reduce the rate at which sodium ions and protons are exchanged across the cell membrane. At least in Mosquito, this exchanger is found in the gut, and Malpighian tubules (the fly equivalent of the kidney) (Pullikuth, Aimanova, Kang'ethe, Sanders, & Gill, 2006). Failure to properly regulate ionic balance in young adult flies might affect the sodium concentration, or proton levels in the body and brain, and affect the speed and intensity of action potentials. Later in life, the normal balance may be restored. A similar reduction in efficacy of *SLC9A9,* linked to ASD may also be present and explain the homology. In this respect, we note that another transporter, the potassium/chloride exchanger, has been linked to epilepsy in young people: with age the kcc/KCC2 eventually achieves a normal ionic balance and proper inhibitory GABA signaling (Ben-Ari, 2014).

The *Nhe3* model may serve for further research into the development of ASD in young brains as well as early biomarkers and treatments. Consistency between the fly and human datasets at both ages indicates a breakdown of a fundamental sensory mechanism comprising two components that have been conserved over 500 million years of evolution. The conservation of the phenotype and mechanisms from fly to human opens up the option to utilize the unrivaled genetic tractability of the fly to dissect the molecular mechanisms underpinning the disorder.

6.6 Methods

6.6.1 Drosophila stocks

Two *Drosophila melanogaster* genotypes were used as ASD models. The *Nhe3* loss-of-function P-element insertion (*Nhe3*^{KG08307} homozygotes) mutation was homozygous *P{SUPor-P}Nhe3*^{KG08307} (Bloomington Drosophila Stock Center (BDSC) 14715). The deficiency was Df(2L)BSC187 (BDSC 9672). To avoid second site mutations in the P-element stock, we used the hemizygote *Nhe3*^{KG08307} */Df(2L)BSC187* as a second experimental genotype.

For our control cross we mated the lab stock of *Canton-S (CS)* flies with those with isogenic chromosomes 2C and 3J (Sharma et al., 2005). All tested flies had dark red eyes. All genotypes were raised in glass bottles on yeast-cornmeal-agar-sucrose medium (10g agar, 39g cornmeal, 37g yeast, 93.75g sucrose per litre). They were kept at 25°C on a 12 hour light-dark cycle. Male flies were collected on CO_2 the day after eclosion and placed on Carpenter (1950) (Carpenter, 1950) medium in the same environmental conditions for either 3 days or 14 days. Flies were tested approximately between the 4th and 9th hour of the daylight cycle.

6.6.2 Drosophila electroretinography

Steady-state visual evoked potentials (SSVEPs) were obtained from the fruit flies (Afsari et al., 2014b; West et al., 2015). Flies were recorded in pairs in a dark room. They were placed in small pipette tips and secured in place with nail varnish. One glass saline-filled electrode was placed inside the proboscis of the fly and another on the surface of the eye. A blue (467nm wavelength) LED light (Prizmatix FC5-LED) with a Gaussian spectral profile (FWHM 34nm) was placed in front of the flies together with a diffuser screen and used for temporal contrast stimulation. Flies were dark adapted for at least two minutes and then tested for signal quality with six light flashes. Steady-state stimulation lasted 12 min and comprised seven contrast levels (0 – 69% in linear steps) each with five repetitions. The frequency of the light flicker was 12Hz. Each trial (contrast level

repetition) was 11 s. The order of the contrast conditions was randomized. The stimulation and the recording from the fly was controlled by in-house MATLAB (Mathworks) scripts (scripts can be found in https://github.com/wadelab/flyCode).

6.6.3 Adult EEG

One-hundred neurotypical adult (32 males, mean age 21.87, range 18 − 49, no reported diagnosis of ASD, reportedly normal or corrected to normal vision) subjects took part in the autism spectrum quotient (AQ) measurement study. The AQ is an instrument used for quantifying autistic traits in the neurotypical population and has been shown to have high face validity and reliability in these populations (Baron-Cohen et al., 2001). The AQ consists of 50 Likert scale items and the scores in this study were calculated according to Baron-Cohen et al. (Baron-Cohen et al., 2001). Each participant completed the AQ questionnaire on a computer in the laboratory.

For the autistic adult ssVEP study, 12 typical-IQ autistic participants and 12 gender- and age- matched controls (11 males, mean age 23.53, range 18 − 39, reportedly normal or corrected to normal vision) were recruited. Autistic participants were recruited through advertisements in an autism charity (Aspire), and in the University of York Disability Services. Control participants were recruited by word of mouth and through the Department of Psychology at the University of York participant database. ASD diagnosis was confirmed with the Autism Diagnostic Observation Schedule, second edition (ADOS-2). Although IQ was not explicitly measured in this study, all adults had normal speech and a high level of independence (the majority were university students). The absence of ASD diagnosis in the neurotypical participants was also confirmed with ADOS-2 (none of the control participants met criteria for ASD). All participants in the study gave informed consent and were debriefed on the purposed of the study after the experiment. The experiments were approved by the Department of Psychology Ethics Committee at the University of York.

Steady-state VEPs were recorded using the ANT Neuro system with a 64-channel Waveguard cap. EEG data were acquired at 1kHz and were recorded using

ASALab, with stimuli presented using MATLAB. The timing of the recording and the stimulation was synchronized using 8-bit low-latency digital triggers. All sessions were performed in a darkened room, testing lasted 45-60min with approximately 20min set up time.

Stimuli were presented on a ViewPixx display (VPixx Technologies Inc., Quebec, Canada) with a mean luminance of 51cd/m^2 and a refresh rate of 120Hz. Stimuli were 0.5 cycle/deg sine-wave gratings enveloped by a raised cosine envelope. Gratings subtended 3 degrees of visual angle and were tiled in a 17x9 grid. The participants fixated on a circle in the middle of the screen and performed a fixation task (two-interval-forced-choice contrast discrimination) to maintain attention. All participants were able to perform the task at above chance levels. There were seven contrast conditions for the flickering gratings (0%, and 2 - 64% in logarithmic steps, where $C_\% = 100(L_{max}-L_{min})/(L_{max}+L_{min})$, L is luminance) and eight repetitions. Stimuli flickered on/off sinusoidally at 7Hz. Trials were presented in random order in four testing blocks with short breaks in between. Each trial was 11 seconds long and contained gratings of a random spatial orientation to avoid orientation adaptation effects. These trials were intermixed with orthogonal masking trials that are not presented as part of this study. Data were taken from the occipital electrode Oz.

6.6.4 Child EEG

Thirteen children with a diagnosis of ASD and 20 neurotypical controls matched on gender ratio (10 and 12 males respectively) and average age (mean age 9.31 and 8.94 respectively, range 5 – 13) completed the study. Three of the neurotypical children were tested but excluded due to having autistic siblings (17 participants were included).

Steady state EEG data were acquired with a 128-channel HydroCell Geodesic Sensor Net (Electrical Geodesics Inc.). Data were digitized at 432Hz and band-pass filtered from 0.3Hz to 50Hz and were recorded using NetStation 4.3 Software. Highly noisy data were excluded by removing repetitions with amplitudes that were four standard deviations away from the group mean (for

each contrast level and harmonic individually). There were 10 repetitions in total, however, two autistic and one neurotypical child only completed 8 repetitions.

Increasing contrast sweep ssVEPs were used. Stimuli for this experiment were presented on an HP1320 CRT monitor with 800x600 pixel resolution, 72Hz refresh rate and mean luminance of $50cd/m^2$. Stimuli were random binary noise patterns of two luminance levels that increased in contrast in 9 logarithmic steps (0% – 50%) of 1 second each. Each trial contained a prelude at the initial value of the sweep and a postlude at the final sweep value, lasting 12 seconds in total. Stimuli flickered at 5.12Hz. Data from the middle 9 seconds during the sweep were binned according to contrast steps. Methodological differences between the adult and child datasets were due to different conventions being used by the two laboratories in which data were collected.

6.6.5 Data analysis

A Fast Fourier transform (in MATLAB) was used to retrieve steady-state response amplitudes at the stimulation frequency (12Hz for fruit flies, 7Hz for adult participants and 5.12Hz for children) and at the second harmonic (24Hz, 14Hz and 10.24Hz respectively). Fourier transforms were applied to 10 s of each trial (first 1s discarded; total trial length was 11s) for the fruit fly and the adult participant data sets and to 1 second binned data for the children's data set. Contrast response functions were obtained by coherently averaging the amplitudes over repetitions for each contrast level within a participant. Group/genotype scalar means over response amplitude (discarding phase angle) were then calculated for each contrast across participants/flies.

Two-way (harmonic x group) ANOVAs were performed on amplitudes at the highest contrast level amplitudes to investigate the interactions and group effects in all human data sets where only two groups were compared. To identify at which harmonic the autistic children showed a decreased response, two independent samples t-tests were also conducted. One-way ANOVAs with simple planned contrasts were conducted to assess the genotype differences in fruit fly

first and second harmonic responses separately as that aided the interpretability of the results between the three genotypes.

To investigate the dissociation between first and second harmonic responses a scaled ratio $\frac{1F-2F}{1F+2F}$ (where 1F is the first and 2F is the second harmonic) was calculated for each participant/fly and each contrast condition. To increase the power of statistical analyses and to decrease the type I error rate, the ratios were then averaged over the contrast conditions that had first harmonic amplitudes significantly above the baseline response (0% contrast condition). For fruit flies this was six conditions (11.5 – 69%), for adult participants this was four conditions (8 – 64%) and for children this was five conditions (8.5 – 50%). This procedure resulted in a single frequency-ratio index for each participant/fly. One-way ANOVAs with simple planned contrasts (comparing mutant genotypes with the control genotype) were conducted on the fly frequency ratios for each age separately. Independent t-tests were used to compare frequency ratios in all human data sets between groups. Additionally, a linear regression was conducted on the adult AQ measurement data set to assess the predictive power of AQ scores on the ratios between frequencies. All statistical tests were two-tailed.

Chapter 7

General discussion

7.1 Summary of findings

This thesis addressed several aspects of two properties of the visual system: neural noise and suppression (gain control). The first study presented in the thesis (*Chapter 2*) investigated the source of neural noise during sensory processing. It was found that the percept rather than the stimulus was encoded in early visual cortex, meaning that the perceptually-relevant neural noise is located early in the visual stream. The experiments in *Chapter 3* compared three psychophysical paradigms for measuring noise and found that contrast discrimination thresholds and double-pass consistency were more suited for estimating internal noise than the equivalent noise paradigm. The chapter also demonstrated the suitability of both paradigms, in particular double-pass, for fast, easy and reliable measurement of noise.

In pursuit of a way to experimentally manipulate the levels of neural noise and sensory signal suppression, *Chapter 4* investigated the neural mechanisms behind

transcranial magnetic stimulation. It was found that online TMS protocols have the potential to selectively change suppression and neural noise levels in the visual system but offline protocols had little or no effect on sensory signal processing.

Chapter 5 related neural noise levels to autism spectrum traits by psychophysically measuring noise when processing contrast, facial expressions and number summation. A global neural noise term was found to underlie individual variability in all three tasks. This noise was correlated with autistic traits, indicating that the sub-clinical ASC phenotype is related to higher levels of neural noise. *Chapter 6* further investigated visual processing in clinical ASC, neurotypical individuals and in a *Drosophila* model of autism. The results were indicative of abnormal visual processing, likely due to gain control deficits in ASC individuals, participants with high numbers of autistic traits and in the *Nhe3* model fruit flies. The findings also indicate that this abnormality in processing changes over the course of development.

The remainder of this chapter will discuss the wider implications of the findings and common themes throughout the empirical chapters. It will also address the possible directions for future research.

7.2 Psychophysical measurement of neural noise and suppression

7.2.1 Comparing three noise measurement methods

Chapter 3 addressed the issue of measuring neural noise psychophysically with three different paradigms. Using high numbers of trials and contrast conditions in seven subjects, the equivalent noise (EN) paradigm (Pelli, 1985) was compared to estimating neural noise from contrast discrimination data fitted with the normalisation model. It was found that the normalisation model was better at predicting double-pass consistency data than the EN paradigm with the linear amplifier model (LAM). The difference between both model predictions was marginal: Akaike's Information Criterion was 20.17 for the normalisation model with two free parameters and 21.61 for LAM. This suggests that although contrast

discrimination noise measures are more accurate than EN, EN (when used with LAM) is still a good estimate of internal noise, provided that zero-dimensional noise is used in stimuli instead of white noise. In some cases LAM can be used for simplicity when predicting double-pass data, such as when only a small selection of double-pass conditions can be tested. For example, in *Chapter 4* LAM was used to model double-pass data as it provided better differentiation between the efficiency and noise parameters than the normalisation model in which the role of some of the parameters is less clear.

Double-pass consistency was highly correlated with normalisation model estimates of noise as well as with the thresholds of TvC curves (dipper functions). Considering that double-pass is a well established and (relatively) model free method of measuring noise, it is reasonable to ask whether there are situations when contrast discrimination is the preferred method. Indeed, double-pass consistency can be measured in only several minutes and can be implemented in challenging conditions (e.g. *Chapter 4*). Furthermore, it can be applied to any stimulus dimension that is measured on a continuum, e.g. facial expressions, number sums (*Chapter 5*), auditory tones (Green, 1964; Jones et al., 2013) and lexical difficulty (Diependaele et al., 2012). However, normalisation model estimates of noise can be applied to existing contrast discrimination data. For example, the contrast discrimination experiment comparing ASC and neurotypical individuals in Greenaway, Davis, & Plaisted-Grant (2013) could be reanalyzed to test whether the differences in thresholds are due to neural noise.

7.2.2 Differentiating neural noise and suppression

Another advantage of the normalisation model fits is that neural noise and gain control can be measured as parameters. In study 1 of *Chapter 3* all seven subjects had well-fitted models with RMS errors below 2.23, suggesting accurate estimates of the free parameters. Furthermore, the normalisation model can be used with three or four free parameters, with the p and q exponents being also allowed to vary. As the ratio of p and q govern the saturation of contrast response functions, it can be used to assess neural suppression at high contrast levels. In fact, both the Z parameter and the p/q ratio have been shown to correlate, suggesting that they

represent properties of the same suppressive mechanism in neural processing (Vilidaite et al., 2015).

In *Chapter 3*, double-pass consistency was highly correlated with the normalisation noise parameter (R = 0.68) but not the gain control parameter (R = 0.14). This indicates that double-pass consistency is a good measure of neural noise and is not influenced by gain control, unlike the noise parameter in EN, when used with white noise masking (Pelli, 1985). Although it may be tempting to use double-pass accuracy as a measure of stimulus-related signal strength (the opposite of suppression), this must be done with caution. Consider a situation where the accuracy is at ceiling in both passes: the consistency between the passes will also be at ceiling. Therefore, accuracy and consistency must be related. This was found to be true in *Chapter 5* where accuracy and consistency were correlated in all three tasks (R > 0.41). To get around this problem, model simulations were used to take into account both accuracy and consistency when estimating neural noise. This was taken a step further in *Chapter 4* in order to simulate TMS-induced changes in neural noise, signal suppression or both. As can be seen in Figure 4.1, each case produced distinct patterns of double-pass consistency and accuracy.

7.3 Origin of neural noise in sensory processing

Previous psychophysical studies investigating neural noise levels in sensory systems have either averaged the neural noise estimates over observers (Jones et al., 2013; McAnany, Alexander, Genead, & Fishman, 2013; Pardhan, 2004) or used very small samples (Burgess & Colborne, 1988; Legge et al., 1987; Skoczenski & Norcia, 1998). However, it is important to consider variability in neural noise levels between individuals as well as between areas of the brain in order to better understand sensory processing. The findings of *Chapter 3* indicate that a large proportion of variance in contrast discrimination is due to individual differences in levels of neural noise.

Furthermore, high correlations in neural noise were observed between three different tasks in *Chapter 5*. This study was designed to measure neural noise

using double-pass in three different tasks that require different levels of sensory-cognitive processing. The first task, contrast discrimination, can be regarded as a purely sensory, low level visual process; the second, facial expression intensity discrimination, is likely to engage higher sensory areas of the visual system (e.g. fusiform face area; Kanwisher, Mcdermott, & Chun, 1997) as well as temporal areas (Winston, Henson, & Dolan, 2004); the third, number summation, can be assumed to involve higher cognitive processing that can be traced to parietal regions (Arsalidou & Taylor, 2011). A single factor ('global internal noise') was found to underlie 76.81% of the variance across the double-pass consistency scores in the three tasks. This can be explained in two ways.

First, each observer's brain has a natural level of neural noise, which is correlated between different parts of the brain and different neural systems. This view is partly supported by the suggestion that neural computations across the brain are canonical (Carandini & Heeger, 2012; Rosenberg, Patterson, & Angelaki, 2015) and so the neural noise term may also be common across the brain. Furthermore, Fox, Snyder, Zacks, & Raichle (2006) showed that fluctuations in spontaneous neural activity covary across the two hemispheres, indicating that neural noise can be correlated across large distances in the brain.

The second explanation is that the neural noise observed psychophysically in all three tasks stems from neural fluctuations in the decision making mechanism of the brain, most likely located in prefrontal cortical areas (Heekeren, Marrett, Bandettini, & Ungerleider, 2004). However, the findings of *Chapter 2* suggest that this is most likely not the case. It was found that the behavioural decision of the observer during contrast discrimination could be decoded from occipital regions, but not the stimulus being presented. Furthermore, the decision could be decoded very early after stimulus onset and coincided with the timing of visual signals reaching V1 (Wibral, Bledowski, Kohler, Singer, & Muckli, 2009). This suggests that neural noise affects the representation of the stimulus very early in the visual processing stream and the resulting 'noisy' percept influences the subsequent perceptual decision. If early sensory noise, rather than late decision making noise influences contrast perception, this may also apply to other perceptual and cognitive processes. These findings shed light on the results of *Chapter 5* and indicate that neural noise levels may be correlated across the

sensory and cognitive regions rather than stemming from a single decision making mechanism. However, it should be noted that *Chapter 2* did not investigate the source of neural noise during face and number processing, thus caution must be used when generalizing these findings beyond contrast perception. Furthermore, although neural noise seems to affect sensory signals early in the visual system, the current studies cannot determine whether this noise originates from the occipital cortex or is inherited from sub-cortical structures.

If the origin of neural noise is the visual cortex, it would be expected that the stimulus representation would be intact to some extent, and could be decoded at above chance levels from occipital responses. In the EEG experiment of *Chapter 2* this was not the case for either of the low target contrast conditions (2% or 4%). However, this may be due to a lower signal-to-noise ratio of EEG compared to MEG. It is possible that some above-chance stimulus decoding could have been achieved if these conditions were repeated in the MEG experiment. Unfortunately, due to MEG experiment time constraints and participant fatigue, these conditions could not be included. However, if that were the case, it would suggest that cortical neural connections are the dominant source of neural noise in sensory processing.

The effects of induced cortical neural noise on task performance are demonstrated by the results of *Chapter 4*, where TMS induced noise affected performance in double-pass. In this study, noise could not have originated from sub-cortical areas as TMS cannot penetrate the cortex under normal conditions (Deng, Lisandby, & Peterchev, 2013; Stokes et al., 2013). However, this does not rule out the existence of naturally occurring sub-cortical neural noise.

In summary, the origin of sensory processing noise is likely to be early sensory regions and the inter-observer differences in neural noise levels are likely correlated between brain regions.

7.4 Modulating neural noise and suppression

In *Chapter 4* it was found that certain types of TMS independently increase neural noise levels or suppress sensory signals during contrast discrimination. In particular, spTMS produced decreases in double-pass accuracy and consistency, as predicted by a decrease in the sensitivity parameter in LAM simulations. This was unsurprising as previous studies also found suppressive effects of spTMS (Harris et al., 2008; Ruzzoli et al., 2010) and TMS has long been assumed to induce "virtual lesions" in the cortex (Pascual-Leone et al., 2000; Walsh & Cowey, 1998). Of more interest was the fact that rTMS had no suppressive effect but rather elevated neural noise levels. This was the first direct comparison of these two protocols using consistent conditions and the same behavioural task. Previous investigations into the neural effects of TMS assumed that rTMS and spTMS would affect neural processing in the same manner and attributed mixed findings to differences in conditions and tasks (Ruzzoli et al., 2011; Schwarzkopf et al., 2011). However, it is clear from *Chapter 4* that the most likely explanation of these discrepancies is to do with the stimulation protocols themselves. These differences may also account for some of the 'replicability crisis' in TMS research as inappropriate protocols would produce different effects in experiment replications (Héroux et al., 2015). These findings are particularly important in informing TMS protocol choices in future research.

It is unclear why three magnetic pulses would act differently on neural processing than a single pulse. One explanation is that during the window of temporal integration a single TMS pulse depolarizes neurons in the gain pool, producing a suppressive effect on the detecting channel (Silvanto & Muggleton, 2008; Silvanto et al., 2007). Yet when three pulses are applied during this temporal integration window each pulse produces a similar depolarisation, which cascades through synaptic connections. Combinations of these cascading signals may act as neural noise in the sensory system. This is similar to the origin of endogenous multiplicative noise, which stems from random combinations of stimulus-related neural signals (Carandini, 2004).

Online TMS only had an effect on sensory processing in the group of participants that could reliably perceive phosphenes during screening. This is unsurprising as

anatomical differences in skull thickness and cortical folding are likely to have substantial effects on magnetic field strength and depth (Herbsman et al., 2009; Janssen et al., 2013). Magnetic field attenuation also explains why offline cTBS and iTBS did not have any behavioural effects on either group of participants, as it was applied at below neural activation threshold levels. This was deliberate as TBS was originally intended to be used below this threshold intensity (Huang et al., 2005) and has continued to be used that way both in basic science (Allen et al., 2014; Di Lazzaro et al., 2008; Rahnev et al., 2013) and in clinical applications (Hanlon et al., 2017; Li et al., 2014). It may be that TBS has no particular effect on sensory signal transduction but rather induces more subtle and long-term changes in neural signalling and connectivity (Hanlon et al., 2017; Li et al., 2014). In either case, it does not seem to be suitable for research into sensory processing.

7.5 Neural mechanisms in ASC

This thesis presents several major findings on sensory processing in individuals with ASC and neurotypicals with high numbers of ASC traits. Firstly, levels of global neural noise in the brain were found to be correlated with the number of autistic traits in neurotypical participants (*Chapter 5*). Secondly, an impairment of early visual processing was observed in both adults with ASC and neurotypical adults with high numbers of autistic traits. Thirdly, this impairment was found to be different in children with ASC, suggesting a change in neural signalling occurs over the course of development. Lastly, this impairment was also found in a fruit fly model of ASC, suggesting a possible genetic link.

7.5.1 Noise in ASC

Several previous studies have suggested high neural noise levels in ASC visual systems (Dinstein et al., 2012; Milne, 2011; Simmons et al., 2009; Weinger et al., 2014). *Chapter 5* extends these findings to sub-clinical populations with high numbers of autistic traits, as measured by AQ. Previous research has found that AQ scores in the general population were highly correlated (R = 0.77) with

sensory processing difficulties (Robertson & Simmons, 2013). The current findings suggest that one of the neural correlates of both sensory difficulties and autistic traits might be the level of neural noise in sensory systems. Considering that neural noise was highly correlated between three different tasks in *Chapter 5* (contrast, facial expression and number sum discrimination); and that perceptually-relevant neural noise lies within early sensory cortex (*Chapter 2*), it is likely that high neural noise affects neural structures beyond the occipital cortex. The increased 'noisiness' of the brain may contribute to sensory and cognitive processing leading to more complex social and behavioural symptoms.

7.5.2 Suppression in ASC

The experiments of *Chapter 6* indicate a robust transient visual response impairment is linked to the autistic phenotype in humans, and to the *Nhe3* gene mutation in fruit flies. The reduced 2nd harmonic and increased 1st harmonic ssVEP responses in ASC and high AQ individuals suggest a differential impairment in two neural cell populations. In humans, the 1st harmonic response has been related to sustained simple cell responses that respond to the onset of a stimulus. Conversely, the 2nd harmonic response has been related to transient On/Off responses of complex cells (Mckeefry et al., 1996). This suggests that in ASC, neural signalling in complex cells is reduced but simple cells show a possible hyper-responsivity. However, in *Nhe3* mutant fruit flies only the transient (2nd harmonic) response reduction is apparent.

The reduction in transient responses in adults and fruit flies was contrast dependent: there was little or no difference between the ASC and neurotypical groups at low contrast levels but a marked impairment at high contrast. This suggests that the response reduction is due to a gain control mechanism of complex cells. These results are compatible with the view that gain control observed in V1 is primarily the product of pre-cortical depression (Carandini, Heeger, & Senn, 2002; Priebe & Ferster, 2006). In particular, this theory explains how transient visual responses posses non-linear properties that can be traced to the lateral geniculate nucleus (Carandini, Heeger, & Senn, 2002). This particular

gain control mechanism seems to be impaired in ASC individuals and neurotypicals with high numbers of autistic traits.

Although the original purpose of the experiments in *Chapter 6* was to investigate the E/I balance in ASC, evidence for a straightforward E/I impairment was not found. Previous accounts of this theory have suggested an overall hyper-reactivity to sensory stimulation in ASC (Markram & Markram, 2010; Rubenstein, 2010; Rubenstein & Merzenich, 2003), which would predict increased responses in both 1st and 2nd harmonics. The findings of *Chapter 6* do not support this increase in E/I balance. However, the results are compatible with differential levels of E/I in different parts of the visual system, suggesting increased suppression in complex cells (reduced E/I) but decreased suppression in simple cells (increased E/I). This may explain why ASC individuals show inconsistent deficits and enhancements in processing stimuli of different levels of complexity. For example, orientation discrimination tuning curves in clinical ASC suggest increased rather than decreased inhibition (Dickinson, Bruyns-Haylett, Smith, Myles, & Milne, 2016). Furthermore, differences between the processing of luminance and contrast modulated stimuli (Bertone et al., 2003, 2005; Simmons et al., 2009) may also be to do with differential properties of simple and complex cells.

An important finding is that the visual response impairment in children with ASC lay in the sustained response and not the transient response. The main difference between ASC and neurotypical children was the reduction in the 1st harmonic response in ASC. The 2nd harmonic responses were comparable between groups. The difference between ASC children and adults suggests that a change in the neural dynamics of the visual system occurs during development. It also means that the development of the visual system in ASC is different from neurotypical development. It may be that the initial impairment lies in simple cell signalling but over time this deficit affects complex cells further down the visual processing stream. At the same time, simple cells increase their sensitivity to compensate for reduced responses resulting in increased sustained responses in adulthood. As these results were replicated in young *Nhe3* model flies, this developmental compensation seems to be universal to vertebrate and invertebrate animals. Although it is unusual to see such similarities between insects and humans, it should be noted that the pathways and computations in the fruit fly's visual

system closely resembles that of humans (Afsari et al., 2014; Behnia & Desplan, 2015; Borst & Euler, 2011; Clark et al., 2014; Olsen et al., 2011).

7.5.3 Genetic influences

It is unclear whether the impairments in gain control in ASC found in *Chapter 6* are due to GABA-ergic neural connections. Although the *Nhe3* gene mutation was partly chosen because it does not directly affect the GABA-ergic system, such an effect is difficult to rule out. It may be that the sodium/hydrogen ion exchange was disproportionately affected in inhibitory GABA-ergic neural connections thus producing gain control abnormalities. On the other hand, one study into human *Nhe9* found that this gene modulated the pH of excitatory glutaminergic cells. This is also a probable explanation for the gain control-like deficits seen in *Chapter 6* as previous studies suggest that sensory suppression is also regulated by excitatory synapses (Katzner et al., 2011).

In fruit flies the sustained response is produced by photoreceptors whilst the transient response originates in the lamina (Afsari et al., 2014), which is a structure a few synapses later in the visual stream. The lamina combines visual signals from the photoreceptors in order to produce transient responses, similarly to complex cells in humans. Considering that the neural deficit caused by *Nhe3* was localized to the lamina in older fruit flies, it is highly likely that other parts of the brain show various levels of *Nhe3* expression (Voineagu et al., 2013). This is supported by previous studies that have found differences in *Nhe6* and *Nhe9* gene expression and location in post-mortem ASC brains compared to controls (Schwede et al., 2013).

Widespread variability in ion concentrations in the brain could cause a host of neural signalling deficits leading to behavioural and sensory symptoms, such as those seen in ASC. The change in the neural dynamics of ASC individuals over the course of development is likely to also be genetically driven. In the *Nhe3* mutant fruit flies the lack or excess of inhibitory signalling can be explained by abnormal concentrations of sodium and hydrogen ions. During development this balance may be restored in certain cell populations. An analogy of this has

previously been found in the potassium/chloride exchanger gene (*kcc*), which regains normal functioning over time in epilepsy patients (Ben-Ari, 2014).

However, it is extremely unlikely that all our participants with ASC and neurotypicals with high AQ had *Nhe3* mutations. In fact, single genes can only account for a small number of clinical ASC cases (Ciernia & Lasalle, 2016; Morrow et al., 2008). More commonly, a complex and diverse selection of gene mutations and gene-environment interactions produce the ASC phenotype and the broader autism phenotype (Ciernia & Lasalle, 2016; Folstein, Rosen-Sheidley, & Street, 2001; Miles, 2011). This collection of gene mutations and gene-environment interactions are likely to be what causes sub-clinical and clinical ASC-like traits in the participants of *Chapter 6*. This is supported by previous studies suggesting that non-ASC relatives of individuals with clinical ASC exhibit milder forms of autistic symptoms (Eisenberg, 1957; Folstein & Rutter, 1977). Furthermore, gamma-band phase locking, indicative of increased neural noise has been found both in ASC individuals and their parents (Rojas et al., 2008). It follows from this that the sensory ASC deficits found in *Chapter 5* and *Chapter 6* might also have genetic origins.

7.6 Future directions

7.6.1 Measuring noise

This thesis presented major advances in quick and accurate measurement of neural noise, in particular the double-pass methodology paired with zero-dimensional stimulus noise. This method could be used to re-investigate research questions in which neural noise levels may implicated. Of particular interest would be early and late stages of life in normal development, as increased neural noise has been suggested to account for poorer sensory processing in childhood and infanthood (Brown, 1994; Skoczenski & Norcia, 1998) as well as in old age (Pardhan, Gilchrist, Elliot, & Beh, 1996). Similarly, neurological disorders in which neural noise levels may be influencing sensory processing, such as dyslexia (Sperling, Lu, Manis, & Seidenberg, 2005), could also be investigated. Improved

measurement methodology would help distinguish between neural noise and other sensory processing differences.

The type of neural noise detected psychophysically and when measured with neuroimaging technology differs (additive versus multiplicative noise; Carandini, 2004). It is therefore important to find a way to link these two ways of measurement and investigate how these types of noise influence neural processing. A possible solution would be an EEG double-pass paradigm in which the consistency of neural responses is taken as a measure of neural noise. The ssVEP method is particularly well suited for this, as two stimuli (with contrast values drawn from Gaussian distributions) can be presented simultaneously at different frequencies (e.g. 5Hz and 7Hz). This frequency tagging would stand in for the two intervals in a normal psychophysical double-pass paradigm. The amplitude of neural responses at both frequencies would be measured and compared to extract a binary 'decision' (which stimulus elicited the higher amplitude). Then the same trial could be repeated (pass two) to test whether the same stimulus would elicit the higher response. From this a double-pass consistency score could be calculated over many trials. Such a paradigm would be useful as behavioural double-pass responses could also be collected at the same time and therefore psychophysical and electrophysiological comparison of neural noise in sensory processing could be achieved.

7.6.2 Further research in TMS

Directions of future research in TMS, stemming from this thesis are two-fold. First, rTMS and spTMS could be used to differentiate between neural noise and suppression at different stages of sensory processing. For example to test whether rTMS to fronto-temporal executive areas would affect perceptual decision making. This could shed light on whether neural noise in the decision making stage of perceptual processing has an effect on behavioural responses. A stimulation study has previously been done with intracranial electrical stimulation in monkey visual cortex (Salzman, Britten, & Newsome, 1990), but TMS provides the opportunity to do stimulation research in humans. Furthermore, the links between neural noise and signal suppression can be established in other

stimuli using the methodology from *Chapter 4*. For example, TMS could be used to see how induction of neural noise or suppression of signals in V5/MT would affect detection thresholds on motion coherence tasks that are commonly used to measure internal noise (Manning et al., 2015; Strong, Silson, Gouws, Morland, & Mckeefry, 2017).

Secondly, the successful application of the double-pass paradigm to measure the neural mechanisms of TMS opens doors to investigate other TMS protocols as well as electrical stimulation methods in a similar way. Offline 1Hz repetitive TMS (Lozeron et al., 2017) was a widely used stimulation protocol before the introduction of TBS. The neural effects of this protocol could prove to be more suitable for researching task-related neural processing than TBS, which was shown to not influence sensory signals in *Chapter 4*. In a similar manner, paired-pulse TMS as well as transcranial direct-current stimulation protocols could be investigated.

7.6.3 Further research in ASC

The experiments in *Chapter 5* and *Chapter 6* link autistic traits in the neurotypical population to elevated levels of sensory neural noise and a selective impairment in transient visual responses. As this line of research aims to further the understanding of sensory symptoms in ASC, it would be particularly useful to investigate whether these impairments relate to the strength and numerosity of sensory traits in neurotypical and ASC individuals. Specifically, the Glasgow Sensory Questionnaire (Robertson & Simmons, 2013) could be used to measure sensory difficulties and relate them to ssVEP responses and double-pass consistency scores.

The *Nhe3* fruit fly model of sensory processing in ASC is also a promising avenue for future research. To test the suitability of this model beyond the sensory domain, fruit fly social behaviour paradigms could be employed. Such paradigms on fruit fly interaction, mating calls and male-male aggressiveness have previously been used to validate other ASC models (Hahn et al., 2013).

Furthermore, *Nhe3* fruit fly visual responses could be used as a starting point for developing an easy early diagnosis paradigm for children with ASC. Previously, machine learning has been used successfully to classify Parkinson's model fruit flies from wild type flies (Himmelberg, West, Elliott, & Wade, 2017). A similar approach could be used first on ASC model flies and then on visual responses of children with ASC.

7.7 Conclusions

This thesis demonstrated that the effects of neural noise and suppression on sensory processing are best measured using contrast discrimination curves with a fitted non-linear model or with a double-pass paradigm. The double-pass paradigm was shown to have wide applicability to measuring neural noise (and suppression) in a wide range of stimuli and under various challenging conditions. By applying this method to transcranial magnetic stimulation, it was found that online single pulse and repetitive stimulation protocols have differential effects on neural noise and suppression. This has wide-reaching implications for future TMS methodology and additionally adds to the arsenal of techniques that can be used to further investigate the neural mechanisms of sensory processing.

Furthermore, neural noise and suppression were found to both be implicated in autism spectrum conditions, neurotypical individuals with high autistic traits and a fruit fly model of autism. Although autistic traits were related to an increase in brain-wide sensory neural noise, the suppression mechanism deficit in ASC was found to be more specific. Gain control-like impairment was found to exist in sustained visual responses of children with ASC. However, this impairment was found to change over the course of development, suggesting a differential trajectory of sensory system development in ASC individuals. Taken together, a genetic cause could explain neural signalling deficits that appear both as neural noise and suppression impairments.

Appendix A

Supplementary data for Chapter 2
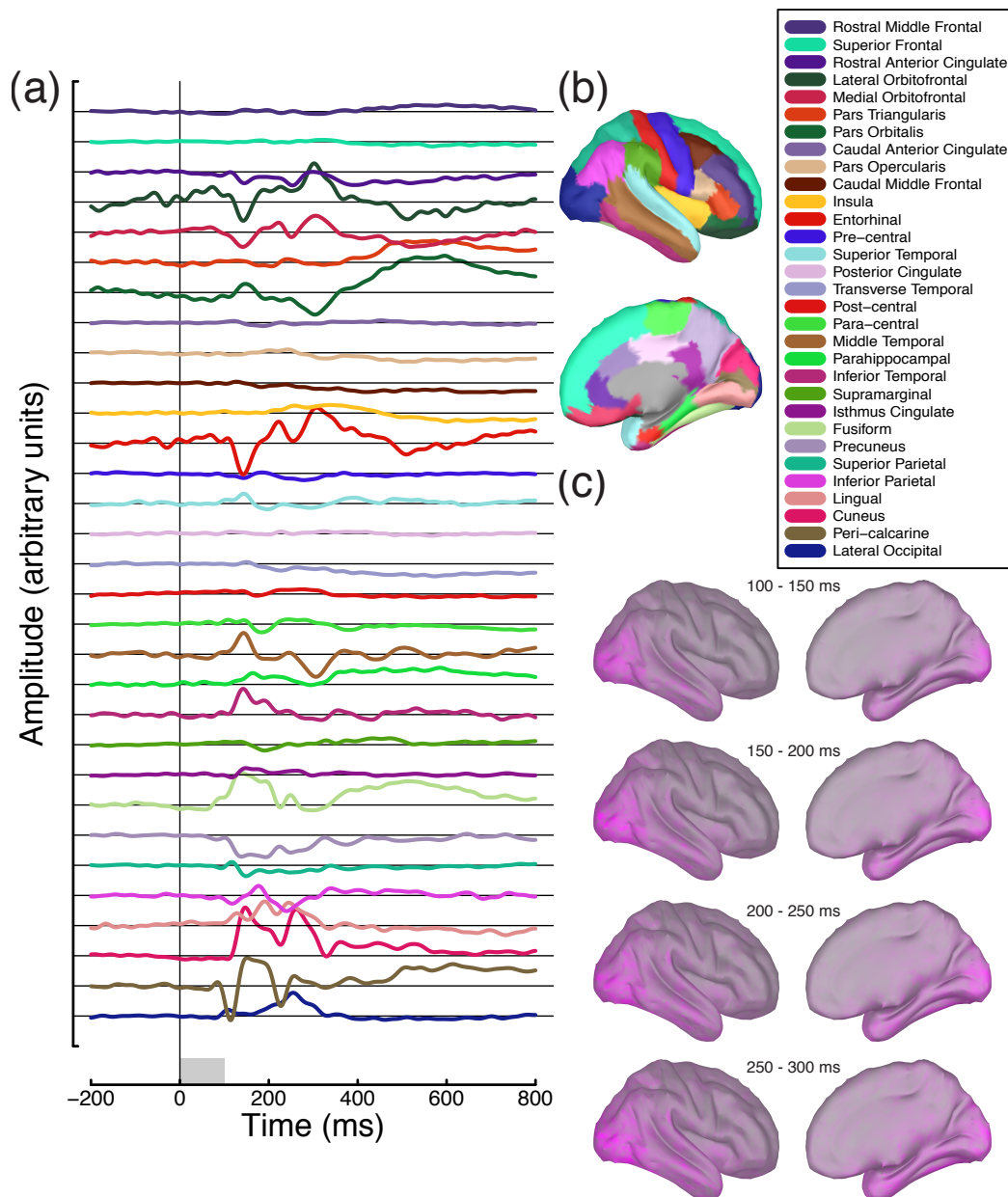
Figure A.1: Maximal evoked responses in different anatomical regions. Each trace in panel A plots the timecourse of the vertex in the named region (see legend in panel B) with the largest absolute deflection from baseline. Panel C shows absolute activity averaged across four time windows, demonstrating that the majority of activity occurs in occipito-temporal regions.

.
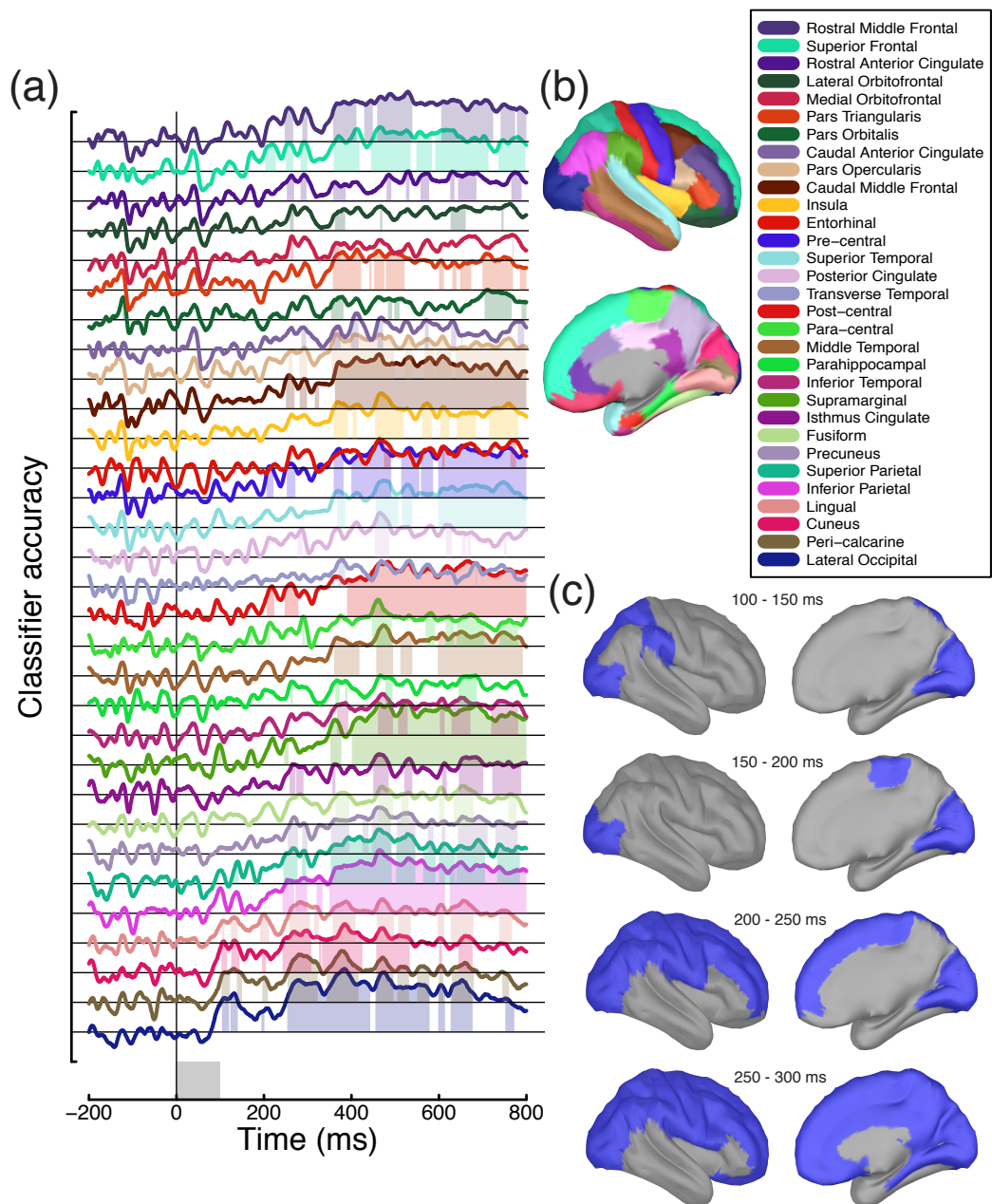
Figure A.2. Atlas-based classification of decisions in the 16% target condition.
Plotting conventions mirror those of Figure 2.4.

Table A.1: Numbers of vertices on the cortical mesh. Individual regions were taken from a mesh consisting of around 3000 vertices, and pooled across hemispheres. The 'whole brain' mesh (final row) was subsampled to around 500 vertices. Precise numbers of vertices varied across individual participants owing to individual differences in brain size and morphology. Entries in the 'Colour' column correspond to the colours used in Figures 2.4, A.1 & A.2.

Region	Colour	Mean size	Minimum size	Maximum size
Rostral Middle Frontal		157	145	173
Superior Frontal		342	317	384
Rostral Anterior Cingulate		31	27	37
Lateral Orbitofrontal		100	83	113
Medial Orbitofrontal		53	45	62
Pars Triangularis		63	56	69
Pars Orbitalis		31	27	35
Caudal Anterior Cingulate		29	25	34
Pars Opercularis		53	43	61
Caudal Middle Frontal		75	59	91
Insula		60	53	69
Entorhinal		16	9	25
Pre-central		140	124	155
Superior Temporal		166	150	183
Posterior Cingulate		38	32	45
Transverse Temporal		9	6	11
Post-central		142	130	156
Para-central		48	41	61
Middle Temporal		134	123	152
Parahippocampal		21	17	25
Inferior Temporal		118	96	149
Supramarginal		123	102	155
Isthmus Cingulate		28	23	34
Fusiform		81	73	87
Precuneous		119	93	140
Superior Parietal		148	136	168
Inferior Parietal		149	131	157
Lingual		101	69	125
Cuneus		67	58	74
Peri-calcarine		38	24	45
Lateral Occipital		162	139	181
Whole brain		503	503	504

References

Adams, W. J., Gray, K. L. H., Garner, M., & Graf, E. W. (2010). High-level face adaptation without awareness. *Psychological Science*, *21*(2), 205–210. http://doi.org/10.1177/0956797609359508

Afsari, F., Christensen, K. V., Smith, G. P., Hentzer, M., Nippe, O. M., Elliott, C. J. H., & Wade, A. R. (2014). Abnormal visual gain control in a Parkinson's disease model. *Human Molecular Genetics*, *23*(17), 4465–4478. http://doi.org/10.1093/hmg/ddu159

Allard, R., & Faubert, J. (2013). Zero-dimensional noise is not suitable for characterizing processing properties of detection mechanisms. *Journal of Vision*, *13(10)*(25), 1–3. http://doi.org/10.1167/13.10.25.doi

Allen, C. P. G., Dunkley, B. T., Muthukumaraswamy, S. D., Edden, R., Evans, C. J., Sumner, P., … Chambers, C. D. (2014). Enhanced awareness followed reversible inhibition of human visual cortex: A combined TMS, MRS and MEG study. *PLoS ONE*, *9*(6). http://doi.org/10.1371/journal.pone.0100350

American Psychiatric Association. (2013). *Diagnostic and statistical manual of mental disorders* (5th ed.). Arlington, VA: American Psychiatric Publishing.

Arsalidou, M., & Taylor, M. J. (2011). Is 2 + 2 = 4 ? Meta-analyses of brain areas needed for numbers and calculations. *NeuroImage*, *54*(3), 2382–2393. http://doi.org/10.1016/j.neuroimage.2010.10.009

Ashwin, E., Ashwin, C., Rhydderch, D., Howells, J., & Baron-cohen, S. (2008). Eagle-Eyed Visual Acuity : An Experimental Investigation of Enhanced Perception in Autism. *BPS*, *65*(1), 17–21. http://doi.org/10.1016/j.biopsych.2008.06.012

Avidan, G., Harel, M., Hendler, T., Ben-Bashat, D., Zohary, E., & Malach, R.

(2002). Contrast sensitivity in human visual areas and its relationship to object recognition. *Journal of Neurophysiology*, *87*(6), 3102–3116.

Bach, M., & Dakin, S. (2009). Regarding "Eagle-Eyed Visual Acuity: An Experimental Investigation of Enhanced Perception in Autism." *Biol Psychiatry*, *66*, e19–e20. http://doi.org/10.1016/j.biopsych.2009.02.035

Baker, D. H. (2013). What Is the Primary Cause of Individual Differences in Contrast Sensitivity? *PLoS ONE*, *8*(7). http://doi.org/10.1371/journal.pone.0069536

Baker, D. H., & Cass, J. (2013). A dissociation of performance and awareness during binocular rivalry. *Psychological Science*, *24*(12), 2563–2568.

Baker, D. H., & Meese, T. S. (2012). Zero-dimensional noise: The best mask you never saw. *Journal of Vision*, *12:10*(20), 1–12. http://doi.org/10.1167/12.10.20.Introduction

Baker, D. H., & Meese, T. S. (2013). Regarding the benefit of zero-dimensional noise. *Journal of Vision*, *13:10*(26), 1–6. http://doi.org/10.1167/13.10.26.doi

Baker, D. H., & Vilidaite, G. (2014). Broadband noise masks suppress neural responses to narrowband stimuli. *Frontiers in Psychology*, *5*, 1–9. http://doi.org/10.3389/fpsyg.2014.00763

Baker, D. H., & Wade, A. R. (2017). Evidence for an Optimal Algorithm Underlying Signal Combination in Human Visual Cortex. *Cerebral Cortex*, *27*, 254–264. http://doi.org/10.1093/cercor/bhw395

Bakker, N., Shahab, S., Giacobbe, P., Blumberger, D. M., Daskalakis, Z. J., Kennedy, S. H., & Downar, J. (2015). Brain Stimulation rTMS of the Dorsomedial Prefrontal Cortex for Major Depression: Safety, Tolerability, Effectiveness, and Outcome Predictors for 10 Hz Versus Intermittent Theta-burst Stimulation. *Brain Stimulation*, *8*, 208–215. http://doi.org/10.1016/j.brs.2014.11.002

Baldwin, A. S., Baker, D. H., & Hess, R. F. (2016). What Do Contrast Threshold Equivalent Noise Studies Actually Measure? Noise vs. Nonlinearity in

Different Masking Paradigms. *PLoS ONE*, *11*(3), 1–25. http://doi.org/10.1371/journal.pone.0150942

Barlow, H. B. (1956). Retinal noise and absolute threshold. *Journal of the Optical Society of America*, *46*(8), 634–639.

Barlow, H. B. (1962). A method of determining the over-all quantum efficiency of visual discriminations. *The Journal of Physiology*, *160*, 155–168.

Barlow, H. B., Hawken, M., Parker, A. J., & Kaushal, T. P. (1987). Human contrast discrimination and the threshold of cortical neurons. *Journal of the Optical Society of America A*, *4*(12), 2366. http://doi.org/10.1364/JOSAA.4.002366

Barlow, H., & Tripathy, S. P. (1997). Correspondence noise and signal pooling in the detection of coherent visual motion. *The Journal of Neuroscience*, *17*(20), 7954–66. Retrieved from http://www.ncbi.nlm.nih.gov/pubmed/9315913

Baron-Cohen, S., Wheelwright, S., Skinner, R., Martin, J., & Clubley, E. (2001). The Autism Spectrum Quotient : Evidence from Asperger syndrome/high functioning autism, males and females, scientists and mathematicians. *Journal of Autism and Developmental Disorders*, *31*, 5–17. http://doi.org/10.1023/A:1005653411471

Beauchamp, M. S., Nath, A. R., & Pasalar, S. (2010). fMRI-Guided Transcranial Magnetic Stimulation Reveals That the Superior Temporal Sulcus Is a Cortical Locus of the McGurk Effect. *J Neurosci*, *30*(7), 2414–2417. http://doi.org/10.1523/JNEUROSCI.4865-09.2010

Behnia, R., & Desplan, C. (2015). Visual circuits in flies: beginning to see the whole picture. *Current Opinion in Neurobiology*, *34*, 125–132. http://doi.org/10.1016/j.conb.2015.03.010

Ben-Ari, Y. (2014). The GABA excitatory/inhibitory developmental sequence: a personal journey. *Neuroscience*, *279*, 187–219. http://doi.org/10.1016/j.neuroscience.2014.08.001

Ben-Sasson, A., Hen, L., Fluss, R., Cermak, S. A., Engel-Yeger, B., & Gal, E. (2009). A Meta-Analysis of Sensory Modulation Symptoms in Individuals with Autism Spectrum Disorders. *J Autism Dev Disord*, *39*, 1–11. http://doi.org/10.1007/s10803-008-0593-3

Benali, A., Trippe, J., Weiler, E., Mix, A., Petrasch-Parwez, E., Girzalsky, W., … Funke, K. (2011). Theta-burst transcranial magnetic stimulation alters cortical inhibition. *J Neurosci*, *31*(4), 1193–1203. http://doi.org/10.1523/JNEUROSCI.1379-10.2011

Bennetto, L., Kuschner, E. S., & Hyman, S. L. (2007). Olfaction and Taste Processing in Autism. *Biol Psychiatry*, *62*(9), 1015–1021.

Bernier, P., Burle, B., & Vidal, F. (2009). Direct Evidence for Cortical Suppression of Somatosensory Afferents during Visuomotor Adaptation. *Cerebral Cortex*, *19*, 2106–2113. http://doi.org/10.1093/cercor/bhn233

Bertone, A., Mottron, L., Jelenic, P., & Faubert, J. (2003). Motion Perception in Autism: A "Complex" Issue. *Journal of Cognitive Neuroscience*, *15*(2), 218–225.

Bertone, A., Mottron, L., Jelenic, P., & Faubert, J. (2005). Enhanced and diminished visuo-spatial information processing in autism depends on stimulus complexity. *Brain*, *128*, 2430–2441. http://doi.org/10.1093/brain/awh561

Bolte, S., Schlitt, S., Gapp, V., Hainz, D., Schirman, S., Poustka, F., … Walter, H. (2012). A Close Eye on the Eagle-Eyed Visual Acuity Hypothesis of Autism. *J Autism Dev Disord*, *42*, 726–733. http://doi.org/10.1007/s10803-011-1300-3

Boroojerdi, B., Meister, I. G., Foltys, H., Sparing, R., Cohen, L. G., & To, R. (2002). Visual and motor cortex excitability : a transcranial magnetic stimulation study, *113*, 1501–1504.

Borst, A., & Euler, T. (2011). Review Seeing Things in Motion : Models ,. *Neuron*, *71*(6), 974–994. http://doi.org/10.1016/j.neuron.2011.08.031

Boynton, G. M., Demb, J. B., Glover, G. H., & Heeger, D. J. (1999). Neuronal basis of contrast discrimination. *Vision Research*, *39*(2), 257–269. http://doi.org/10.1016/S0042-6989(98)00113-8

Britten, K. H., Newsome, W. T., Shadlen, M. N., Celebrini, S., & Movshon, J. A. (1996). A relationship between behavioral choice and the visual responses of neurons in macaque MT. *Visual Neuroscience*, *13*(1), 87–100. http://doi.org/10.1017/S095252380000715X

Britten, K. H., Shadlen, M. N., Newsome, W. T., & Movshon, J. A. (1992). The analysis of visual motion: a comparison of neuronal and psychophysical performance. *The Journal of Neuroscience: The Official Journal of the Society for Neuroscience*, *12*(12), 4745–4765.

Brouwer, G. J., & Heeger, D. J. (2011). Cross-orientation suppression in human visual cortex, 2108–2119. http://doi.org/10.1152/jn.00540.2011.

Brown, A. M. (1994). Intrinsic contrast noise and infant visual contrast discrimination. *Vision Research*, *34*(15), 1947–1964. http://doi.org/10.1016/0042-6989(94)90025-6

Burd, L., & Gascon, G. G. (1988). Rett syndrome: review and discussion of current diagnostic criteria. *J Child Neurol*, *3*, 263–8.

Burgess, A. E., & Colborne, B. (1988). Visual signal detection. IV. Observer inconsistency. *Journal of the Optical Society of America*, *5*(4), 617–627. http://doi.org/10.1364/JOSAA.5.000617

Buss, E., Hall, J. W., & Grose, J. H. (2009). Psychometric functions for pure tone intensity discrimination: slope differences in school-aged children and adults. *The Journal of the Acoustical Society of America*, *125*(2), 1050–1058. http://doi.org/10.1121/1.3050273

Busse, L., Wade, A. R., & Carandini, M. (2009). Representation of Concurrent Stimuli by Population Activity in Visual Cortex. *Neuron*, *64*(6), 931–942. http://doi.org/10.1016/j.neuron.2009.11.004

Butler, J. S., Molholm, S., Andrade, G. N., & Foxe, J. J. (2016). An Examination

of the Neural Unreliability Thesis of Autism, 1–16. http://doi.org/10.1093/cercor/bhw375

Cabrera, C. A., Lu, Z.-L., & Dosher, B. A. (2015). Separating decision and encoding noise in signal detection tasks. *Psychological Review*, *122*(3), 429–460. http://doi.org/10.1037/a0039348

Cai, P., Chen, N., & Zhou, T. (2014). Global versus local : double dissociation between MT + and V3A in motion processing revealed using continuous theta burst transcranial magnetic stimulation, 4035–4041. http://doi.org/10.1007/s00221-014-4084-9

Campbell, B. F. W., & Kulikowski, J. J. (1966). Orientational selectivity of the human visual system. *J Physiol*, *187*(2), 437–445.

Campbell, F. W., & Kulikowski, J. J. (1972). The visual evoked potential as a function of contrast of a grating pattern. *The Journal of Physiology*, *222*(2), 345–356. http://doi.org/10.1113/jphysiol.1972.sp009801

Carandini, M. (2004). Amplification of trial-to-trial response variability by neurons in visual cortex. *PLoS Biology*, *2*(9). http://doi.org/10.1371/journal.pbio.0020264

Carandini, M., & Heeger, D. (2012). Normalization as a canonical neural computation. *Nature Reviews Neuroscience*, (November), 1–12. http://doi.org/10.1038/nrn3136

Carandini, M., & Heeger, D. J. (1994). Normalization as a canonical neural computation. *Nature Reviews Neuroscience*, *13*, 51–62. http://doi.org/10.1038/nrn3136

Carandini, M., Heeger, D. J., & Senn, W. (2002). A Synaptic Explanation of Suppression in Visual Cortex, *22*(22), 10053–10065.

Cárdenas-Morales, L., Nowak, D. A., Kammer, T., Wolf, R. C., & Schönfeldt-Lecuona, C. (2010). Mechanisms and applications of theta-burst rTMS on the human motor cortex. *Brain Topography*, *22*(4), 294–306. http://doi.org/10.1007/s10548-009-0084-7

Carpenter, J. M. (1950). A new semisynthetic food medium for Drosophila. *Dros. Inf. Serv.*, *24*, 96–97.

Cascio, C., McGlone, F., Folger, S., Tannan, V., Baranek, G., Pelphrey, K. A., & Essick, G. (2008). Tactile Perception in Adults with Autism: a Multidimensional Psychophysical Study. *J Autism Dev Disord*, *38*(1), 127–137.

Chen, Y., Geisler, W. S., & Seidemann, E. (2006). Optimal decoding of correlated neural population responses in the primate visual cortex. *Nature Neuroscience*, *9*(11), 1412–1420. http://doi.org/10.1038/nn1792

Chung, S. W., Hill, A. T., Rogasch, N. C., Hoy, K. E., & Fitzgerald, P. B. (2016). Use of theta-burst stimulation in changing excitability of motor cortex: A systematic review and meta-analysis. *Neuroscience and Biobehavioral Reviews*, *63*, 43–64. http://doi.org/10.1016/j.neubiorev.2016.01.008

Cichy, R. M., Pantazis, D., & Oliva, A. (2014). Resolving human object recognition in space and time. *Nature Neuroscience*, *17*(3), 455–462. http://doi.org/10.1038/nn.3635

Ciernia, A. V., & Lasalle, J. (2016). The landscape of DNA methylation amid a perfect storm of autism aetiologies. *Nat Rev Neurosci*, *17*, 411–423. http://doi.org/10.1038/nrn.2016.41

Clark, D. A., Fitzgerald, J. E., Ales, J. M., Gohl, D. M., Silies, M. A., Norcia, A. M., & Clandinin, T. R. (2014). Flies and humans share a motion estimation strategy that exploits natural scene statistics. *Nature Publishing Group*, *17*(2), 296–303. http://doi.org/10.1038/nn.3600

Clarke, A., Devereux, B. J., Randall, B., & Tyler, L. K. (2015). Predicting the Time Course of Individual Objects with MEG. *Cerebral Cortex*, *25*(10), 3602–3612. http://doi.org/10.1093/cercor/bhu203

Clifford, C. W. G., Webster, M. A., Stanley, G. B., Stocker, A. A., Kohn, A., Sharpee, T. O., & Schwartz, O. (2007). Visual adaptation: Neural, psychological and computational aspects, *47*, 3125–3131. http://doi.org/10.1016/j.visres.2007.08.023

Coghlan, S., Horder, J., Inkster, B., Mendez, M. A., Murphy, D. G., & Nutt, D. J. (2012). GABA system dysfunction in autism and related disorders: From synapse to symptoms. *Neuroscience and Biobehavioral Reviews*, *36*(9), 2044–2055. http://doi.org/10.1016/j.neubiorev.2012.07.005

Cohn, T. E. (1976). Detectability of a luminance increment : Effect of superimposed random luminance fluctuation *. *Journal of Optical Society of America*, *66*(12), 1426–1428.

Courchesne, E., Redcay, E., & Kennedy, D. P. (2004). The autistic brain: birth through adulthood. *Current Opinion in Neurology*, *17*, 489–496. http://doi.org/10.1097/01.wco.0000137542.14610.b4

Dakin, S. C., Bex, P. J., Cass, J. R., & Watt, R. J. (2009). Dissociable effects of attention and crowding on orientation averaging. *Journal of Vision*, *9(11)*(28), 1–16. http://doi.org/10.1167/9.11.28

Davis, G., & Plaisted-Grant, K. (2014). Low endogenous neural noise in autism. *Autism : The International Journal of Research and Practice*, *19*(3), 351–62. http://doi.org/10.1177/1362361314552198

Deng, Z.-D., Lisandby, S. H., & Peterchev, A. V. (2013). Electric field depth–focality tradeoff in transcranial magnetic stimulation: simulation comparison of 50 coil designs. *Brain Stimulation*, *6*(1), 1–13. http://doi.org/10.1016/j.brs.2012.02.005.Electric

Di Lazzaro, V., Pilato, F., Dileone, M., Profice, P., Oliviero, A., Mazzone, P., … Rothwell, J. C. (2008). The physiological basis of the effects of intermittent theta burst stimulation of the human motor cortex. *Journal of Physiology-London*, *586*(16), 3871–3879. http://doi.org/DOI 10.1113/jphysiol.2008.152736

Di Lazzaro, V., Pilato, F., Saturno, E., Oliviero, A., Dileone, M., Mazzone, P., … Rothwell, J. C. (2005). Theta-burst repetitive transcranial magnetic stimulation suppresses specific excitatory circuits in the human motor cortex. *The Journal of Physiology*, *565*(3), 945–50. http://doi.org/10.1113/jphysiol.2005.087288

Dickinson, A., Bruyns-Haylett, M., Smith, R., Myles, J., & Milne, E. (2016). Superior orientation discrimination and increased peak gamma frequency in autism spectrum conditions. *Journal of Abnormal Psychology*, *125*(3), 412–422.

Dickinson, A., Jones, M., & Milne, E. (2014). Individual differences in visual search: Relationship to autistic traits, discrimination thresholds, and speed of processing. *Perception*, *40*(6), 739–742. http://doi.org/10.1068/p6953

Dickinson, A., Jones, M., & Milne, E. (2016). Measuring neural excitation and inhibition in autism: Different approaches, different findings and different interpretations. *Brain Research*, *1648*, 277–289. http://doi.org/10.1016/j.brainres.2016.07.011

Diependaele, K., Brysbaert, M., & Neri, P. (2012). How noisy is lexical decision? *Frontiers in Psychology*, *3*, 1–9. http://doi.org/10.3389/fpsyg.2012.00348

Dinstein, I., Heeger, D. J., & Behrmann, M. (2015). Neural variability: Friend or foe? *Trends in Cognitive Sciences*, *9*(6), 322–328. http://doi.org/10.1016/j.tics.2015.04.005

Dinstein, I., Heeger, D. J., Lorenzi, L., Minshew, N., Malach, R., & Behrmann, M. (2012). Unreliable evoked responses in autism. *Neuron*, *75*(6), 981–991. http://doi.org/10.1038/nature13314.A

Dinstein, I., Thomas, C., Humphreys, K., Minshew, N., Behrmann, M., & Heeger, D. J. (2010). Normal movement-selectivity in autism. *Neuron*, *66*(3), 461–469. http://doi.org/10.1016/j.neuron.2010.03.034.Normal

Eisenberg, L. (1957). The fathers of autistic children. *American Journal of Orthopsychiatry*, *27*(4), 715–724.

Ekman, P., & Friesen, W. V. (1971). Constants across cultures in the face and emotion. *Journal of Personality and Social Psychology*, *17*(2), 124–129.

Ey, E., Leblond, C. S., & Bourgeron, T. (2011). Behavioral profiles of mouse models for Autism Spectrum Disorders. *Autism Research*, *4*, 5–16.

Faisal, A. A., Selen, L. P. J., & Wolpert, D. M. (2008). Noise in the nervous

system. *Nature Reviews Neuroscience*, *9*, 292–303.
http://doi.org/10.1038/nrn2258

Finney, D. J. (1971). *Probit Analysis* (3rd ed.). London: Cambridge University
Press.

Fischbach, K.-F., & Dittrich, A. P. M. (1989). The optic lobe of Drosophila
melanogaster . I. A Golgi analysis of wild-type structure. *Cell Tissue
Research*, *258*, 441–475.

Foley, J. M., & Chen, C. (1999). Pattern detection in the presence of maskers that
differ in spatial phase and temporal offset : threshold measurements and a
model, *39*, 3855–3872.

Folstein, S. E., Rosen-sheidley, B., & Street, W. (2001). Genetics of autism:
complex aetiology for a heterogenous disorder. *Nature Reviews Genetics*, *2*,
943–955.

Folstein, S., & Rutter, M. (1977). Infantile autism: a genetic study of 21 twin
pairs. *Journal of Child Psychology {&} Psychiatry {&} Allied Disciplines*,
18. http://doi.org/10.1111/j.1469-7610.1977.tb00443.x

Fontanini, A., & Katz, D. B. (2011). Behavioral Modulation of Gustatory Cortical
Activity. *Annual Reviews Neuroscience*, *34*, 89–103.
http://doi.org/10.1111/j.1749-6632.2009.03922.x.Behavioral

Fox, M. D., Snyder, A. Z., Zacks, J. M., & Raichle, M. E. (2006). Coherent
spontaneous activity accounts for trial-to-trial variability in human evoked
brain responses, *9*(1), 2005–2007. http://doi.org/10.1038/nn1616

Freeman, T. C. B., Durand, S., Kiper, D. C., & Carandini, M. (2002). Suppression
without inhibition in visual cortex. *Neuron*, *35*(4), 759–771.
http://doi.org/10.1016/S0896-6273(02)00819-X

Gaetz, W., Bloy, L., Wang, D. J., Port, R. G., Blaskey, L., Levy, S. E., & Roberts,
T. P. L. (2014). GABA estimation in the brains of children on the autism
spectrum: Measurement precision and regional cortical variation.
NeuroImage, *86*, 1–9. http://doi.org/10.1016/j.neuroimage.2013.05.068

Gao, R., & Penzes, P. (2015). Common mechanisms of excitatory and inhibitory imbalance in schizophrenia and autism spectrum disorders. *Current Molecular Medicine*, *15*(2), 146–67. http://doi.org/10.1016/j.jaac.2013.12.025

Gentner, R., Wankerl, K., Reinsberger, C., Zeller, D., & Classen, J. (2008). Depression of human corticospinal excitability induced by magnetic theta-burst stimulation: evidence of rapid polarity-reversing metaplasticity. *Cereb Cortex*, *18*, 2046–2053. http://doi.org/10.1093/cercor/bhm239

Georgeson, M. A., & Meese, T. S. (2006). Fixed or variable noise in contrast discrimination? The jury's still out.. *Vision Research*, *46*(25), 4294–4303. http://doi.org/10.1016/j.visres.2005.08.024

Goodbourn, P. T., Bosten, J. M., Hogg, R. E., Bargary, G., Lawrance-Owen, A. J., & Mollon, J. D. (2012). Do different "magnocellular tasks" probe the same neural substrate? *Proc. R. Soc. B*, *279*, 4263–4271. http://doi.org/10.1098/rspb.2012.1430

Graham, N. V. (2011). Beyond multiple pattern analyzers modeled as linear filters (as classical V1 simple cells): useful additions of the last 25 years. *Vision Research*, *51*(13), 1397–1430. http://doi.org/10.1016/j.visres.2011.02.007

Green, D. M. (1964). Consistency of auditory detection judgments. *Psychological Review*, *71*(5), 392–407. http://doi.org/10.1037/h0044520

Green, D. M., & Swets, J. A. (1974). *Signal detection theory and psychophysics (A reprint, with corrections of the original 1966 ed.)*. Huntington, NY: Robert E. Krieger Publishing Co.

Green, S. A., Rudie, J. D., Colich, N. L., Wood, J. J., Shirinyan, D., Hernandez, L., … Bookheimer, S. Y. (2013). Overreactive Brain Responses to Sensory Stimuli in Youth With Autism Spectrum Disorders. *Journal of the American Academy of Child & Adolescent Psychiatry*, *52*(11), 1158–1172. http://doi.org/10.1016/j.jaac.2013.08.004

Greenaway, R., Davis, G., & Plaisted-Grant, K. (2013). Marked selective impairment in autism on an index of magnocellular function.

Neuropsychologia, *51*(4), 592–600.
http://doi.org/10.1016/j.neuropsychologia.2013.01.005

Grosbras, Á., & Hab, Q. C. (2003). Transcranial magnetic stimulation of the human frontal eye ® eld facilitates visual awareness, *18*, 3121–3126. http://doi.org/10.1046/j.1460-9568.2003.03055.x

Haesen, B., Boets, B., & Wagemans, J. (2011). A review of behavioural and electrophysiological studies on auditory processing and speech perception in autism spectrum disorders. *Research in Autism Spectrum Disorders*, *5*, 701–714. http://doi.org/10.1016/j.rasd.2010.11.006

Hahn, N., Geurten, B., Gurvich, A., Piepenbrock, D., Kastner, A., Zanini, D., … Heinrich, R. (2013). Monogenic heritable autism gene neuroligin impacts Drosophila social behaviour. *Behavioural Brain Research*, *252*, 450–457. http://doi.org/10.1016/j.bbr.2013.06.020

Haigh, S. M., Heeger, D. J., Dinstein, I., Minshew, N., & Hall, W. (2016). Cortical variability in the sensory-evoked response in autism, *45*(5), 1176–1190. http://doi.org/10.1007/s10803-014-2276-6.Cortical

Hamada, M., Murase, N., Hasan, A., Balaratnam, M., & Rothwell, J. C. (2013). The role of interneuron networks in driving human motor cortical plasticity. *Cereb Cortex*, *23*, 1593–1605. http://doi.org/10.1093/cercor/bhs147

Hanlon, C. A., Dowdle, L. T., Correia, B., Mithoefer, O., Kearney-ramos, T., Lench, D., … George, M. S. (2017). Left frontal pole theta burst stimulation decreases orbitofrontal and insula activity in cocaine users and alcohol users, *178*(March), 310–317. http://doi.org/10.1016/j.drugalcdep.2017.03.039

Harada, M., Taki, M. M., & Naa, M. Á. (2011). Non-Invasive Evaluation of the GABAergic / Glutamatergic System in Autistic Patients Observed by MEGA-Editing Proton MR Spectroscopy Using a Clinical 3 Tesla Instrument. *J Autism Dev Disord*, *41*, 447–454. http://doi.org/10.1007/s10803-010-1065-0

Harms, M. B., Martin, A., & Wallace, G. L. (2010). Facial Emotion Recognition in Autism Spectrum Disorders : A Review of Behavioral and Neuroimaging

Studies. *Neuropsychological Review, 20*, 290–322.
http://doi.org/10.1007/s11065-010-9138-6

Harris, J. A., Clifford, C. W. G., & Miniussi, C. (2008). The functional effect of
transcranial magnetic stimulation: signal suppression or neural noise
generation? *Journal of Cognitive Neuroscience, 20*(4), 734–740.
http://doi.org/10.1162/jocn.2008.20048

Hasan, B. A. S., Joosten, E., & Neri, P. (2012). Estimation of internal noise using
double passes : Does it matter how the second pass is delivered ? *Vision
Research, 69*, 1–9. http://doi.org/10.1016/j.visres.2012.06.014

Heeger, D. (1992). Normalization of cell responses in cat striate cortex. *Visual
Neuroscience*. http://doi.org/10.1017/S0952523800009640

Heeger, D. J. (2009). Inter-ocular contrast normalization in human visual cortex
Farshad Moradi, *9*, 1–22. http://doi.org/10.1167/9.3.13.Introduction

Heekeren, H. R., Marrett, S., Bandettini, P. A., & Ungerleider, L. G. (2004). A
general mechanism for perceptual decision-making in the human brain,
276(2001), 859–862.

Herbsman, T., Forster, L., Molnar, C., Dougherty, R., Christie, D., Ramsey, D., …
Carolina, S. (2009). Motor Threshold in Transcranial Magnetic Stimulation:
The Impact of White Matter Fiber Orientation and Skull-to-Cortex Distance.
Human Brain Mapping, 30(7), 2044–2055.
http://doi.org/10.1002/hbm.20649.Motor

Héroux, M. E., Taylor, J. L., & Gandevia, S. C. (2015). The use and abuse of
transcranial magnetic stimulation to modulate corticospinal excitability in
humans. *PLoS ONE, 10*(12), 1–10.
http://doi.org/10.1371/journal.pone.0144151

Hesselmann, G., Kell, C. A., Eger, E., & Kleinschmidt, A. (2008). Spontaneous
local variations in ongoing neural activity bias perceptual decisions.
*Proceedings of the National Academy of Sciences of the United States of
America, 105*(31), 10984–10989. http://doi.org/10.1073/pnas.0712043105

Hillyard, S. A., Squires, K. C., Bauer, J. W., & Lindsay, P. H. (1971). Evoked Potential Correlates of Auditory Signal Detection. *Science*, *172*(3990), 1357–1360.

Himmelberg, M., West, R. J. H., Elliott, C. J. H., & Wade, A. R. (2017). Abnormal visual gain control and excitotoxicity in early-onset Parkinson's disease Drosophila models. *Journal of Neurophysiology*.

Horder, J., Wilson, C. E., Mendez, M. A., & Murphy, D. G. (2014). Autistic Traits and Abnormal Sensory Experiences in Adults, 1461–1469. http://doi.org/10.1007/s10803-013-2012-7

Huang, Y. Z., Edwards, M. J., Rounis, E., Bhatia, K. P., & Rothwell, J. C. (2005). Theta burst stimulation of the human motor cortex. *Neuron*, *45*(2), 201–206. http://doi.org/10.1016/j.neuron.2004.12.033

Hubel, D. H., & Wiesel, T. N. (1962). Receptive fields, binocular interaction and functional architecture in the cat's visual cortex. *J Physiol*, *160*(1), 106–154.

Hubel, D. H., & Wiesel, T. N. (1968). Receptive fields and functional architecture of monkey striate cortex. *J. Psysiol.*, *195*, 215–243.

Hughes, C., Russell, J., & Robbins, T. W. (1994). Evidence for executive dysfunction in autism. *Neuropsychologia*, *32*(4), 477–492.

Iuculano, T., Rosenberg-Lee, M., Supekar, K., Lynch, C. J., Khouzam, A., Phillips, J., … Menon, V. (2014). Brain organization underlying superior mathematical abilities in children with autism. *Biological Psychiatry*, *75*(3), 223–230. http://doi.org/10.1016/j.biopsych.2013.06.018.Brain

Janssen, A. M., Rampersad, S. M., Lucka, F., Lanfer, B., Lew, S., Aydin, U., … Oostendorp, T. F. (2013). The influence of sulcus width on simulated electric fields induced by transcranial magnetic stimulation. *Phys Med Biol*, *58*(14), 4881–4896. http://doi.org/10.1088/0031-9155/58/14/4881.The

Jemel, B., Mimeault, D., Saint-Amour, D., Hosein, A., & Mottron, L. (2010). VEP contrast sensitivity responses reveal reduced functional segregation of mid and high filters of visual channels in Autism. *Journal of Vision*, *10*(6),

13–13. http://doi.org/10.1167/10.6.13

Jolij, J., Meurs, M., & Haitel, E. (2011). Why do we see what's not there? *Communicative & Integrative Biology*, *4*(6), 764–767.

Jones, D. G., Anderson, N. D., & Murphy, K. M. (2003). Orientation discrimination in visual noise using global and local stimuli. *Vision Research*, *43*, 1223–1233. http://doi.org/10.1016/S0042-6989(03)00095-6

Jones, P. R., Moore, D. R., Amitay, S., & Shub, D. E. (2013). Reduction of internal noise in auditory perceptual learning. *The Journal of the Acoustical Society of America*, *133*(2), 970–81. http://doi.org/10.1121/1.4773864

Jones, R. S. P., Quigney, C., & Huws, J. C. (2003). First-hand accounts of sensory perceptual experiences in autism: a qualitative analysis. *Journal of Intellectual & Developmental Disability*, *28*(2), 112–121. http://doi.org/10.1080/1366825031000147058

Kanwisher, N., Mcdermott, J., & Chun, M. M. (1997). The Fusiform Face Area : A Module in Human Extrastriate Cortex Specialized for Face Perception, *17*(11), 4302–4311.

Katzner, S., Busse, L., & Carandini, M. (2011). GABAA inhibition controls response gain in visual cortex. *J Neurosci*, *31*(16), 5931–5941. http://doi.org/10.1016/j.surg.2006.10.010.Use

Keine, C., & Ru, R. (2016). Inhibition in the auditory brainstem enhances signal representation and regulates gain in complex acoustic environments. *eLife*, *5*, 1–33. http://doi.org/10.7554/eLife.19295

Kenworthy, L., Black, D. O., Harrison, B., della Rosa, A., & Wallace, G. L. (2009). Are Executive Control Functions Related to Autism Symptoms in High-Functioning Children? *Child Neuropsychology*, *15*, 425–440. http://doi.org/10.1080/09297040802646983

Kingdom, F. A. A. (2016). Fixed versus variable internal noise in contrast transduction: The significance of Whittle's data. *Vision Research*, *128*, 1–5. http://doi.org/10.1016/j.visres.2016.09.004

Klein, A., Ghosh, S. S., Bao, F. S., Giard, J., Häme, Y., Stavsky, E., … Keshavan, A. (2017). Mindboggling morphometry of human brains. *PLOS Computational Biology*, *13*(2), e1005350. http://doi.org/10.1371/journal.pcbi.1005350

Klein, S. A., Kontsevich, L. L., Chen, C. C., Tyler, C. W., Maattanen, L. M., Koenderink, J. J., … Newsome, W. T. (2015). Neural variability: Friend or foe? *Vision Research*, *19*(6), 322–328. http://doi.org/10.1016/j.tics.2015.04.005

Klein, S. A., & Levi, D. M. (2009). Stochastic model for detection of signals in noise. *Journal of Optical Society of America*, *26*(11), 110–126.

Koh, C. H., Milne, E., & Dobkins, K. R. (2010). Spatial Contrast sensitivity in adolescents with autism spectrum disorders. *J Autism Dev Disord*, *40*(8), 978–987.

Koivisto, M., Harjuniemi, I., Railo, H., & Salminen-vaparanta, N. (2017). Transcranial magnetic stimulation of early visual cortex suppresses conscious representations in a dichotomous manner without gradually decreasing their precision. *NeuroImage*, *158*, 308–318. http://doi.org/10.1016/j.neuroimage.2017.07.011

Koivisto, M., Railo, H., & Salminen-vaparanta, N. (2011). Transcranial magnetic stimulation of early visual cortex interferes with subjective visual awareness and objective forced-choice performance. *Consciousness and Cognition*, *20*(2), 288–298. http://doi.org/10.1016/j.concog.2010.09.001

Kondapalli, K. C., Hack, A., Schushan, M., Landau, M., Ben-Tal, N., & Rao, R. (2013). Functional evaluation of autism associated mutations in NHE9. *Nature Communications*, *4*(2510), 1–12. http://doi.org/10.1038/ncomms3510

Kontsevich, L. L., Chen, C.-C., & Tyler, C. W. (2002). Separating the effects of response nonlinearity and internal noise psychophysically. *Vision Research*, *42*(14), 1771–1784.

Kouh, M., & Poggio, T. (2008). Communicated by Bartlett Mel A Canonical Neural Circuit for Cortical Nonlinear Operations, *1451*, 1427–1451.

LeBlanc, J. J., DeGregorio, G., Centofante, E., Vogel-Farley, V. K., Barnes, K., Kaufmann, W. E., … Nelson, C. A. (2015). Processing Deficits in Rett Syndrome. *Annals of Neurology*, *78*, 775–786. http://doi.org/10.1002/ana.24513

Legge, G. E., & Foley, J. M. (1980). Contrast masking in human vision. *Journal of the Optical Society of America*, *70*(12), 1458–1471. http://doi.org/10.1364/JOSA.70.001458

Legge, G. E., Kersten, D., & Burgess, A. E. (1987). Contrast discrimination in noise. *Journal of the Optical Society of America*, *4*(2), 391–404. http://doi.org/10.1364/JOSAA.4.000391

Levi, D. M., Klein, S. A., & Chen, I. (2007). The response of the amblyopic visual system to noise. *Vision Research*, *47*(19), 2531–2542. http://doi.org/10.1016/j.visres.2007.06.014

Li, B., Thompson, J. K., Duong, T., Peterson, M. R., & Freeman, R. D. (2006). Origins of Cross-Orientation Suppression in the Visual Cortex. *J Neurophysiol*, *96*, 1755–1764. http://doi.org/10.1152/jn.00425.2006.

Li, C.-T., Chen, M.-H., Juan, C.-H., Huang, H.-H., Chen, L.-F., Hsieh, J.-C., … Su, T.-P. (2014). Efficacy of prefrontal theta-burst stimulation in refractory depression : a randomized sham-controlled study. *Brain*, *137*, 2088–2098. http://doi.org/10.1093/brain/awu109

López-Alonso, V., Cheeran, B., Río-Rodríguez, D., & Fernández-del-Olmo, M. (2014). Inter-individual Variability in Response to Non-invasive Brain Stimulation Paradigms. *Brain Stimulation*, *7*, 372–380. http://doi.org/10.1016/j.brs.2014.02.004

Lord, C., Risi, S., Lambrecht, L., Cook, E. H., Leventhal, B. L., DiLavore, P. C., … Rutter, M. (2000). The autism diagnostic observation schedule-generic: a standard measure of social and communication deficits associated with the spectrum of autism. *J Autism Dev Disord*, *30*, 205–223. http://doi.org/10.1023/A:1005592401947

Lorenzo, F. Di, Martorana, A., Ponzo, V., Bonnì, S., D'Angelo, E., Caltagirone,

C., & Koch, G. (2013). Cerebellar theta burst stimulation modulates short latency afferent inhibition in Alzheimer's disease patients. *Frontiers in Aging Neuroscience*, *5*, 1–8. http://doi.org/10.3389/fnagi.2013.00002

Lozeron, P., Poujois, A., Meppiel, E., Masmoudi, S., Magnan, T. P., Vicaut, E., … Kubis, N. (2017). Inhibitory rTMS applied on somatosensory cortex in Wilson's disease patients with hand dystonia. *J Neural Transm*, *124*(10), 1161–1170. http://doi.org/10.1007/s00702-017-1756-1

Lu, Z.-L., & Dosher, B. A. (2008). Characterizing observers using external noise and observer models: Assessing internal representations with external noise. *Psychological Review*, *115*(1), 44–82. http://doi.org/10.1037/0033-295X.115.1.44

Macmillan, N. A., & Creelman, C. D. (2005). *Detection theory: A users guide* (2nd ed.). New York: Cambridge University Press.

Majaj, N. J., Carandini, M., & Movshon, J. A. (2007). Motion Integration by Neurons in Macaque MT Is Local , Not Global, *27*(2), 366–370. http://doi.org/10.1523/JNEUROSCI.3183-06.2007

Manning, C., & Baker, D. H. (2015). Response to Davis and Plaisted-Grant: Psychophysical data do not support the low-noise account of autism. *Austism*, *19*(3), 365–6. http://doi.org/10.1002/elan.

Manning, C., Charman, T., & Pellicano, E. (2013). Processing Slow and Fast Motion in Children With Autism Spectrum Conditions. *Autism Research*, *6*, 531–541. http://doi.org/10.1002/aur.1309

Manning, C., Tibber, M. S., Charman, T., Dakin, S. C., & Pellicano, E. (2015). Enhanced Integration of Motion Information in Children With Autism. *Journal of Neuroscience*, *35*(18), 6979–6986. http://doi.org/10.1523/JNEUROSCI.4645-14.2015

Maris, E., & Oostenveld, R. (2007). Nonparametric statistical testing of EEG- and MEG-data. *Journal of Neuroscience Methods*, *164*(1), 177–190. http://doi.org/10.1016/j.jneumeth.2007.03.024

Markram, K., & Markram, H. (2010). The Intense World Theory – a unifying theory of the neurobiology of autism, *4*(December), 1–29. http://doi.org/10.3389/fnhum.2010.00224

Martin, P. G., Gandevia, S. C., & Taylor, J. L. (2006). Theta burst stimulation does not reliably depress all regions of the human motor cortex. *Clinical Neurophysiology*, *117*, 2684–2690. http://doi.org/10.1016/j.clinph.2006.08.008

McAnany, J., Alexander, K. R., Genead, M. A., & Fishman, G. A. (2013). Equivalent intrinsic noise, sampling efficiency, and contrast sensitivity in patients with retinitis pigmentosa. *Investigative Ophthalmology and Visual Science*, *54*(6), 3857–3862. http://doi.org/10.1167/iovs.13-11789

Mcgovern, C. W., & Sigman, M. (2005). Continuity and change from early childhood to adolescence in autism. *J Child Psychol Psychiatry*, *46*(4), 401–408. http://doi.org/10.1111/j.1469-7610.2004.00361.x

Mckeefry, D. J., Gouws, A., Burton, M. P., & Morland, A. B. (2009). The Noninvasive Dissection of the Human Visual Cortex: Using fMRI and TMS to Study the Organization of the Visual Brain, 489–506.

Mckeefry, D. J., Russell, M. H. A., Murray, I. J., & Kulikowski, J. J. (1996). Amplitude and phase variations of harmonic components in human achromatic and chromatic visual evoked potentials. *Visual Neuroscience*, *13*, 639–653.

Mclelland, D., Baker, P. M., Ahmed, B., & Bair, W. (2010). Neuronal Responses during and after the Presentation of Static Visual Stimuli in Macaque Primary Visual Cortex. *The Journal of Neuroscience*, *30*(38), 12619–12631. http://doi.org/10.1523/JNEUROSCI.0815-10.2010

Meese, T. S., & Harris, M. G. (2001). Broad direction bandwidths for complex motion mechanisms. *Vision Research*, *41*, 1901–1914.

Michelson, C. A., Pillow, J. W., & Seidemann, E. (2017). Majority of choice-related variability in perceptual decisions is present in early sensory cortex. *Preprint*.

Miles, J. H. (2011). Genetics in Medicine Autism spectrum disorders — A genetics review. *Genetics in Medicine*, *13*(4), 278–294. http://doi.org/10.1097/GIM.0b013e3181ff67ba

Milne, E. (2011). Increased intra-participant variability in children with autistic spectrum disorders: Evidence from single-trial analysis of evoked EEG. *Frontiers in Psychology*, *2*, 1–12. http://doi.org/10.3389/fpsyg.2011.00051

Milne, E., Swettenham, J., Hansen, P., Campbell, R., Jefferies, H., & Plaisted, K. (2002). Visual motion coherence thresholds in people with autism. *Journal of Child Psychology and Psychiatry*, *43*(2), 255–263. http://doi.org/10.1111/1469-7610.00018

Milne, E., Swettenham, J., Hansen, P., Campbell, R., Jeffries, H., & Plaisted, K. (2002). High motion coherence thresholds in children with autism. *J Child Psychol Psychiatry*, *43*(2), 255–263.

Moliadze, V., Fritzsche, G., & Antal, A. (2014). Comparing the Efficacy of Excitatory Transcranial Stimulation Methods Measuring Motor Evoked Potentials. *Neural Plasticity*, 1–6.

Moliadze, V., Zhao, Y., Eysel, U., & Funke, K. (2003). Effect of transcranial magnetic stimulation on single-unit activity in the cat primary visual cortex. *The Journal of Physiology*, *553*(Pt 2), 665–679. http://doi.org/10.1113/jphysiol.2003.050153

Moloney, A., Sattelle, D. B., Lomas, D. A., & Crowther, D. C. (2009). Alzheimer's disease: insights from Drosophila melanogaster models. *Trends in Biochemical Sciences*, *35*(4), 228–235. http://doi.org/10.1016/j.tibs.2009.11.004

Mori, T., Mori, K., Fujii, E., Toda, Y., & Miyazaki, M. (2012). Evaluation of the GABAergic nervous system in autistic brain : I-iomazenil SPECT study. *Brain and Development*, *34*(8), 648–654. http://doi.org/10.1016/j.braindev.2011.10.007

Morrone, M. C., Burr, D. C., & Maffei, L. (1982). Functional Implications of Cross-Orientation Inhibition of Cortical Visual Cells . I. Neurophysiological

Evidence. *Proc R Soc Lond B Biol Sci*. http://doi.org/10.1098/rspb.1982.0078

Morrow, E. M., Yoo, S., Flavell, S. W., Kim, T., Lin, Y., Hill, R. S., … Walsh, C. A. (2008). Identifying Autism Loci and Genes by Tracing Recent Shared Ancestry. *Science*, *321*(5886), 218–223. http://doi.org/10.1126/science.1157657.Identifying

Moser, D. J., Jorge, R. E., Manes, F., Paradiso, S., Benjamin, M. L., & Robinson, R. G. (2002). Improved executive functioning following repetitive transcranial. *Neurology*, *58*(2), 1288–1290.

Mostert, P., Kok, P., & Lange, F. P. De. (2015). Dissociating sensory from decision processes in human perceptual decision making. *Scientific Reports*, *5*(18253), 1–13. http://doi.org/10.1038/srep18253

Mueller, S. T., & Weidemann, C. T. (2008). Decision noise: An explanation for observed violations of signal detection theory. *Psychonomic Bulletin & Review*, *15*(3), 465–494. http://doi.org/10.3758/PBR.15.3.465

Nachmias, J., & Sansbury, R. V. (1974). Grating contrast: discrimination may be better than detection. *Vision Research*, *14*, 1039–1042. http://doi.org/10.1111/j.1528-1167.2007.01060_5.x

Naka, K. I., & Rushton, W. A. H. (1966). S-potentials from colour units in the retina of fish (Cyprinidae). *Journal of Physiology*, *185*, 536–555.

Nelson, S. B., & Valakh, V. (2015). Excitatory / Inhibitory Balance and Circuit Homeostasis in Autism Spectrum Disorders. *Neuron*, *87*(4), 684–698. http://doi.org/10.1016/j.neuron.2015.07.033

Nguyen, B. N., McKendrick, A. M., & Vingrys, A. J. (2015). Abnormal inhibition-excitation imbalance in migraine. *Cephalalgia*, *0*(0), 1–10. http://doi.org/10.1177/0333102415576725

Nienborg, H., Cohen, M. R., & Cumming, B. G. (2012). Decision-related activity in sensory neurons: correlations among neurons and with behavior. *Annual Review of Neuroscience*, *35*, 463–483. http://doi.org/10.1146/annurev-neuro-062111

Nyffeler, T., Cazzoli, D., Hess, C. W., & Muri, R. M. (2009). One Session of Repeated Parietal Theta Burst Stimulation Trains Induces Long-Lasting Improvement of Visual Neglect. *Stroke*, *40*(8), 2791–2797. http://doi.org/10.1161/STROKEAHA.109.552323

Olsen, S. R., Bhandawat, V., & Wilson, R. I. (2011). Divisive normalization in olfactory population codes. *Neuron*, *66*(2), 287–299. http://doi.org/10.1016/j.neuron.2010.04.009.Divisive

Oostenveld, R., Fries, P., Maris, E., & Schoffelen, J.-M. (2011). FieldTrip: Open Source Software for Advanced Analysis of MEG, EEG, and Invasive Electrophysiological Data. *Computational Intelligence and Neuroscience*, *2011*, 1–9. http://doi.org/10.1155/2011/156869

Osaki, H., Naito, T., Sadakane, O., Okamoto, M., & Sato, H. (2011). Surround suppression by high spatial frequency stimuli in the cat primary visual cortex, (March 2010), 1–10. http://doi.org/10.1111/j.1460-9568.2010.07572.x

Palmer, C. R., Cheng, S. Y., & Seidemann, E. (2005). Linking Neuronal and Psychophysical Performance in a Visual Detection Task. *Society for Neuroscience Abstracts*, *27*(30), 8122–8137. http://doi.org/10.1523/JNEUROSCI.1940-07.2007

Pardhan, S. (2004). Contrast sensitivity loss with aging: sampling efficiency and equivalent noise at different spatial frequencies. *Journal of the Optical Society of America*, *21*(2), 169–175. http://doi.org/10.1364/JOSAA.21.000169

Pardhan, S., Gilchrist, J., Elliot, D. B. F., & Beh, G. K. (1996). A Comparison of Sampling Efficiency and Internal Noise Level in Young and Old Subjects, *36*(11), 1641–1648.

Pascual-Leone, a, Walsh, V., & Rothwell, J. (2000). Transcranial magnetic stimulation in cognitive neuroscience – virtual lesion, chronometry, and functional connectivity. *Current Opinion in Neurobiology*, *10*(2), 232–7. http://doi.org/10.1016/S0959-4388(00)00081-7

Pei, F., Baldassi, S., & Norcia, A. M. (2014). Electrophysiological measures of low-level vision reveal spatial processing deficits and hemispheric asymmetry in autism spectrum disorder. *Journal of Vision*, *14*(11), 1–12. http://doi.org/10.1167/14.11.3

Peirce, J. W. (2007). PsychoPy—Psychophysics software in Python. *Journal of Neuroscience Methods*, *162*(1–2), 8–13. http://doi.org/10.1016/j.jneumeth.2006.11.017

Pelli, D. G. (1985). Uncertainty explains many aspects of visual contrast detection and discrimination. *Journal of the Optical Society of America. A, Optics and Image Science*, *2*(9), 1508–1532. http://doi.org/10.1364/JOSAA.2.001508

Pellicano, E., Gibson, L., Maybery, M., Durkin, K., & Badcock, D. R. (2005). Abnormal global processing along the dorsal visual pathway in autism : a possible mechanism for weak visuospatial coherence? *Neuropsychologia*, *43*, 1044–1053. http://doi.org/10.1016/j.neuropsychologia.2004.10.003

Peterzell, D. H., & Teller, D. Y. (1996). Individual Differences in Contrast Sensitivity Functions : The Lowest Spatial Frequency Channels. *Vision Res*, *36*(19), 3077–3085.

Peterzell, D. H., Werner, J. S., & Kaplan, P. S. (1995). Individual Differences in Contrast Sensitivity Functions : Longitudinal Study of 4- , 6- and 8-Month-old Human Infants, *6989*(7), 961–979.

Petrov, Y., Carandini, M., & Mckee, S. (2005). Two Distinct Mechanisms of Suppression in Human Vision, *25*(38), 8704–8707. http://doi.org/10.1523/JNEUROSCI.2871-05.2005

Petrov, Y., & Mckee, S. P. (2006). The effect of spatial configuration on surround suppression of contrast sensitivity. *Journal of Vision*, *6*, 224–238.

Pitcher, D., Duchaine, B., & Walsh, V. (2014). Report Combined TMS and fMRI Reveal Dissociable Cortical Pathways for Dynamic and Static Face Perception. *Current Biology*, *24*(17), 2066–2070. http://doi.org/10.1016/j.cub.2014.07.060

Plaisted, K., Swettenham, J., & Rees, L. (1999). Children with autism show local precedence in a divided attention task and global precedence in a selective attention task. *Journal of Child Psychology and Psychiatry, and Allied Disciplines*, *40*(5), 733–42. http://doi.org/10.1111/1469-7610.00489

Porciatti, V., Bonanni, P., Fiorentini, A., & Guerrini, R. (2000). Lack of cortical contrast gain control in human photosensitive epilepsy. *Nature Neuroscience*, *3*(3), 259–263. http://doi.org/10.1038/72972

Priebe, N. J., & Ferster, D. (2006). Mechanisms underlying cross-orientation suppression in cat visual cortex. *Nature Neuroscience*, *9*(4), 552–561. http://doi.org/10.1038/nn1660

Pullikuth, A. K., Aimanova, K., Kang'ethe, W., Sanders, H. R., & Gill, S. S. (2006). Molecular characterization of sodium / proton exchanger 3 (NHE3) from the yellow fever vector , Aedes aegypti. *The Journal of Experimental Biology*, *209*, 3529–3544. http://doi.org/10.1242/jeb.02419

Ragert, P., Franzkowiak, S., Schwenkreis, P., Tegenthoff, M., & Dinse, H. R. (2008). Improvement of tactile perception and enhancement of cortical excitability through intermittent theta burst rTMS over human primary somatosensory cortex. *Exp Brain Res*, *184*, 1–11. http://doi.org/10.1007/s00221-007-1073-2

Rahnev, D. A., Maniscalco, B., Luber, B., Lau, H., & Lisanby, S. H. (2012). Direct injection of noise to the visual cortex decreases accuracy but increases decision confidence, 1556–1563. http://doi.org/10.1152/jn.00985.2011

Rahnev, D., Kok, P., Munneke, M., Bahdo, L., de Lange, F. P., & Lau, H. (2013). Continuous theta burst transcranial magnetic stimulation reduces resting state connectivity between visual areas. *Journal of Neurophysiology*, *110*(8), 1811–21. http://doi.org/10.1152/jn.00209.2013

Rai, N., Premji, A., Tommerdahl, M., & Nelson, A. J. (2012). Clinical Neurophysiology Continuous theta-burst rTMS over primary somatosensory cortex modulates tactile perception on the hand. *Clinical Neurophysiology*, *123*, 1226–1233. http://doi.org/10.1016/j.clinph.2011.09.026

Reiter, L. T., Potocki, L., Chien, S., Gribskov, M., & Bier, E. (2001). A Systematic Analysis of Human Disease-Associated Gene Sequences In. *Genome Research*, 1114–1125. http://doi.org/10.1101/gr.169101.sophila

Ress, D., & Heeger, D. J. (2003). Neuronal correlates of perception in early visual cortex. *Nature Neuroscience*, *6*(4), 414–420. http://doi.org/10.1038/nn1024

Reynolds, J. H., & Heeger, D. J. (2009). The Normalization Model of Attention. *Neuron*, *61*(2), 168–185. http://doi.org/10.1016/j.neuron.2009.01.002.The

Robertson, A. E., & Simmons, D. R. (2013). The Relationship between Sensory Sensitivity and Autistic Traits in the General Population. *J Autism Dev Disord*, *43*, 775–784. http://doi.org/10.1007/s10803-012-1608-7

Roelfsema, P. R., & Spekreijse, H. (2001). The representation of erroneously perceived stimuli in the primary visual cortex. *Neuron*, *31*(5), 853–863. http://doi.org/10.1016/S0896-6273(01)00408-1

Rojas, D. C., Benkers, T. L., Rogers, S. J., Teale, P. D., Reite, M. L., & Hagerman, R. J. (2001). Auditory evoked magnetic fields in adults with fragile X syndrome. *Neuroreport*, *12*. http://doi.org/10.1097/00001756-200108080-00056

Rojas, D. C., Maharajh, K., Teale, P., & Rogers, S. J. (2008). Reduced neural synchronization of gamma-band MEG oscillations in first-degree relatives of children with autism. *BMC Psychiatry*, *8*(1), 1–9. http://doi.org/10.1186/1471-244X-8-66

Rolls, E. T., & Baylis, G. C. (1986). Size and contrast have only small effects on the responses to faces of neurons in the cortex of the superior temporal sulcus of the monkey. *Experimental Brain Research*, *65*(1), 38–48.

Rosenberg, A., Patterson, J. S., & Angelaki, D. E. (2015). A computational perspective on autism. *PNAS*, *112*(30), 9158–9165. http://doi.org/10.1073/pnas.1510583112

Rossi, S., Hallett, M., Rossini, P. M., Pascual-Leone, A., Avanzini, G., Bestmann, S., … Ziemann, U. (2009). Safety, ethical considerations, and application

guidelines for the use of transcranial magnetic stimulation in clinical practice and research. *Clinical Neurophysiology*, *120*(12), 2008–2039. http://doi.org/10.1016/j.clinph.2009.08.016

Rounis, E., Maniscalco, B., Rothwell, J. C., Richard, E., Lau, H., Rounis, E., … Lau, H. (2010). Theta-burst transcranial magnetic stimulation to the prefrontal cortex impairs metacognitive visual awareness Theta-burst transcranial magnetic stimulation to the prefrontal cortex impairs metacognitive visual awareness, *8928*(October 2017). http://doi.org/10.1080/17588921003632529

Rubenstein, J. L. R. (2010). Three hypotheses for developmental defects that may underlie some forms of autism spectrum disorder. *Current Opinion in Neurology*, *23*, 118–123. http://doi.org/10.1097/WCO.0b013e328336eb13

Rubenstein, J. L. R., & Merzenich, M. M. (2003). Model of autism: increased ratio of excitation/inhibition in key neural systems. *Genes, Brain, and Behavior*, *2*(5), 255–267. http://doi.org/10.1046/j.1601-183X.2003.00037.x

Rutter, M. (2000). Genetic Studies of Autism : From the 1970s into the Millennium, *28*(1), 3–14.

Ruzzoli, M., Abrahamyan, A., Clifford, C. W. G., Marzi, C. A., Miniussi, C., & Harris, J. A. (2011). The effect of TMS on visual motion sensitivity: an increase in neural noise or a decrease in signal strength? *Journal of Neurophysiology*, *106*, 138–143. http://doi.org/10.1152/jn.00746.2010

Ruzzoli, M., Marzi, C. A., & Miniussi, C. (2010). The neural mechanisms of the effects of transcranial magnetic stimulation on perception. *Journal of Neurophysiology*, *103*(6), 2982–9. http://doi.org/10.1152/jn.01096.2009

Said, C. P., Egan, R. D., Minshew, N. J., Behrmann, M., & Heeger, D. J. (2013). Normal binocular rivalry in autism : Implications for the excitation / inhibition imbalance hypothesis. *Vision Research*, *77*, 59–66. http://doi.org/10.1016/j.visres.2012.11.002

Salzman, C. D., Britten, K. H., & Newsome, W. T. (1990). Cortical microstimulation influences perceptual judgements of motion direction.

Nature, *374*, 174–177. http://doi.org/10.1016/0021-9797(80)90501-9

Schiller, P. H., Finlay, B. L., & Volman, S. F. (1976). Short-term response variability of monkey striate neurons. *Brain Research*, *105*, 347–349.

Schneeweis, D. M., & Schnapf, J. L. (1999). The Photovoltage of Macaque Cone Photoreceptors : Adaptation , Noise , and Kinetics. *The Journal of Neuroscience*, *19*(4), 1203–1216.

Schölvinck, M. L., Friston, K. J., & Rees, G. (2012). The influence of spontaneous activity on stimulus processing in primary visual cortex. *NeuroImage*, *59*, 2700–2708. http://doi.org/10.1016/j.neuroimage.2011.10.066

Schwarzkopf, D. S., Silvanto, J., & Rees, G. (2011). Stochastic resonance effects reveal the neural mechanisms of transcranial magnetic stimulation. *J Neurosci*, *31*(9), 3143–3147. http://doi.org/10.1523/JNEUROSCI.4863-10.2011

Schwede, M., Garbett, K., Mirnics, K., Geschwind, D. H., & Morrow, E. M. (2013). Genes for endosomal NHE6 and NHE9 are misregulated in autism brains. *Molecular Psychiatry*, *19*(3), 1–3. http://doi.org/10.1038/mp.2013.28

Seltzer, M. M., Krauss, M. W., Shattuck, P. T., Orsmond, G., Swe, A., & Lord, C. (2003). The Symptoms of Autism Spectrum Disorders in Adolescence and Adulthood. *J Autism Dev Disord*, *33*(6), 565–581.

Shao, Y., Cuccaro, M. L., Hauser, E. R., Raiford, K. L., Menold, M. M., Wolpert, C. M., … Pericak-Vance, M. A. (2003). Fine Mapping of Autistic Disorder to Chromosome 15q11-q13 by Use of Phenotypic Subtypes. *Am. J. Hum. Genet.*, *72*, 539–548.

Shapley, R. M., & Victor, J. D. (1981). How The Contrast Gain Control Modifies The Frequency of Cat Retinal Ganglion Cells. *J Physiol*, *318*, 161–179.

Sharma, P., Asztalos, Z., Ayyub, C., de Bruyne, M., Dornan, A. J., Gomez-Hernandez, A., … O'Kane, C. J. (2005). Isogenic autosomes to be applied in optimal screening for novel mutants with viable phenotypes in Drosophila

melanogaster. *Journal of Neurogenetics*, *19*(2), 57–85. http://doi.org/10.1080/01677060591007155

Silson, E. H., Mckeefry, D. J., Rodgers, J., Gouws, A. D., Hymers, M., & Morland, A. B. (2013). Specialized and independent processing of orientation and shape in visual field maps LO1 and LO2. *Nature Neuroscience*, *16*, 1–4. http://doi.org/10.1038/nn.3327

Silvanto, J., & Muggleton, N. G. (2008). New light through old windows: Moving beyond the "virtual lesion" approach to transcranial magnetic stimulation. *NeuroImage*, *39*, 549–552. http://doi.org/10.1016/j.neuroimage.2007.09.008

Silvanto, J., Muggleton, N. G., Cowey, A., & Walsh, V. (2007). Neural adaptation reveals state-dependent effects of transcranial magnetic stimulation. *European Journal of Neuroscience*, *25*, 1874–1881. http://doi.org/10.1111/j.1460-9568.2007.05440.x

Simmons, D., & Milne, E. (2014). Response to Davis and Plaisted-Grant: Low or high endogenous neural noise in autism spectrum disorder? *Autism*, *19*, 363–364. http://doi.org/10.1177/1362361314557683

Simmons, D. R., Robertson, A. E., McKay, L. S., Toal, E., McAleer, P., & Pollick, F. E. (2009). Vision in autism spectrum disorders. *Vision Research*, *49*(22), 2705–2739. http://doi.org/10.1016/j.visres.2009.08.005

Skoczenski, A. M., & Norcia, A. M. (1998). Neural noise limitations on infant visual sensitivity. *Nature*, *391*, 697–700. http://doi.org/10.1038/35630

Skottun, B. C. (2000). The magnocellular deficit theory of dyslexia : the evidence from contrast sensitivity, *40*, 111–127.

Skottun, B. C., & Skoyles, J. R. (2007). Some remarks on the use of visually evoked potentials to measure magnocellular activity. *Clinical Neurophysiology*, *118*, 1903–1905. http://doi.org/10.1016/j.clinph.2007.06.007

Smith, M. A., Bair, W., & Movshon, J. A. (2006). Dynamics of Suppression in Macaque Primary Visual Cortex, *26*(18), 4826–4834.

http://doi.org/10.1523/JNEUROSCI.5542-06.2006

Smith, R. A., & Swift, D. J. (1985). Spatial-frequency masking and Birdsall's theorem. *Journal of the Optical Society of America. A, Optics and Image Science*, *2*(9), 1593–1599.

Smith, R. A., & Swift, D. J. (1985). Spatial-frequency masking and Birdsall ' s theorem, *2*(9), 1593–1599.

Sperling, A. J., Lu, Z., Manis, F. R., & Seidenberg, M. S. (2005). Deficits in perceptual noise exclusion in developmental dyslexia, *8*(7), 862–863. http://doi.org/10.1038/nn1474

Squires, N. K., Squires, K. C., & Hillyard, S. A. (1975). Two varieties of long-latency positive waves evoked by unpredictable auditory stimuli in man. *Electroencephalography and Clinical Neurophysiology*, *38*(4), 387–401.

Stapells, D. R., Linden, D., Suffield, J. B., Hamel, G., & Picton, T. W. (1984). Human Auditory Steady State Potentials. *Ear and Hearing*, *5*(2), 105–113.

Stewart, L., Walsh, V. R., & Hwell, J. C. (2001). Motor and phosphene thresholds: a TMS correlation study, *39*, 415–419. Retrieved from http://eprints.ucl.ac.uk/4286/

Stokes, M. G., Barker, A. T., Dervinis, M., Verbruggen, F., Maizey, L., & Adams, R. C. (2013). Biophysical determinants of transcranial magnetic stimulation : effects of excitability and depth of targeted area. *Journal of Neurophysiology*, *109*(2), 437–444. http://doi.org/10.1152/jn.00510.2012

Strong, S. L., Silson, E. H., Gouws, A. D., Morland, A. B., & Mckeefry, D. J. (2017). A Direct Demonstration of Functional Differences between Subdivisions of Human V5 / MT +. *Cerebral Cortex*, *27*, 1–10. http://doi.org/10.1093/cercor/bhw362

Sundaram, S. K., Kumar, A., Makki, M. I., Behen, M. E., Chugani, H. T., & Chugani, C. (2008). Diffusion Tensor Imaging of Frontal Lobe in Autism Spectrum Disorder. *Cerebral Cortex*, *18*, 2659–2665. http://doi.org/10.1093/cercor/bhn031

Sutherland, A., & Crewther, D. P. (2010). Magnocellular visual evoked potential delay with high autism spectrum quotient yields a neural mechanism for altered perception. *Brain*, *133*, 2089–2097. http://doi.org/10.1093/brain/awq122

Sweeny, T. D., Grabowecky, M., Kim, Y. J., & Suzuki, S. (2011). Internal curvature signal and noise in low- and high-level vision. *Journal of Neurophysiology*, *105*(3), 1236–1257. http://doi.org/10.1152/jn.00061.2010

Tadel, F., Baillet, S., Mosher, J. C., Pantazis, D., & Leahy, R. M. (2011). Brainstorm: A User-Friendly Application for MEG/EEG Analysis. *Computational Intelligence and Neuroscience*, *2011*, 1–13. http://doi.org/10.1155/2011/879716

Talelli, P., Greenwood, R. J., & Rothwell, J. C. (2007). Exploring Theta Burst Stimulation as an intervention to improve motor recovery in chronic stroke q. *Clinical Neurophysiology*, *118*, 333–342. http://doi.org/10.1016/j.clinph.2006.10.014

Tolhurst, D. J., Movshon, J. A., & Dean, A. F. (1983a). The statistical reliability of signals in single neurons in cat and monkey visual cortex. *Vision Research*, *23*(8), 775–785. http://doi.org/10.1016/0042-6989(83)90200-6

Tolhurst, D. J., Movshon, J. A., & Dean, A. F. (1983b). The statistical reliability of signals in single neurons in cat and monkey visual cortex. *Vision Research*, *23*(8), 775–785.

Tsai, J. J., Norcia, A. M., Ales, J. M., & Wade, A. R. (2011). Contrast Gain Control Abnormalities in Idiopathic Generalized Epilepsy. *Annals of Neurology*, *70*(4), 574–82. http://doi.org/10.1002/ana.22462

Tsai, J. J., Wade, A. R., & Norcia, A. M. (2012). Dynamics of normalization underlying masking in human visual cortex. *The Journal of Neuroscience : The Official Journal of the Society for Neuroscience*, *32*(8), 2783–9. http://doi.org/10.1523/JNEUROSCI.4485-11.2012

Turrigiano, G. (2011). Too Many Cooks? Intrinsic and Synaptic Homeostatic Mechanisms in Cortical Circuit Refinement. *Annu Rev Neurosci, 34*, 89–103.

http://doi.org/10.1146/annurev-neuro-060909-153238

Van Alphen, B., & Van Swinderen, B. (2013). Drosophila strategies to study psychiatric disorders. *Brain Research Bulletin*, *92*, 1–11. http://doi.org/10.1016/j.brainresbull.2011.09.007

van Loon, A. M., Knapen, T., Scholte, H. S., St John-Saaltink, E., Donner, T. H., & Lamme, V. A. F. (2013). Report GABA Shapes the Dynamics of Bistable Perception. *Current Biology*, *23*, 823–827. http://doi.org/10.1016/j.cub.2013.03.067

Vernet, M., Bashir, S., Yoo, W., Oberman, L., Mizrahi, I., Ifert-miller, F., … Pascual-leone, A. (2014). Reproducibility of the effects of theta burst stimulation on motor cortical plasticity in healthy participants. *Clinical Neurophysiology*, *125*, 320–326. http://doi.org/10.1016/j.clinph.2013.07.004

Vilidaite, G., & Baker, D. H. (2016). Individual differences in internal noise are consistent across two measurement techniques. *Vision Research*, 1–23. http://doi.org/10.1016/j.visres.2016.10.008

Vilidaite, G., Gutmanis, N., Harris, S., Kitching, R. E., Melton, H. A., Norman, R., … Baker, D. H. (2015). Estimating inter-observer variability in GABA-ergic suppression. *Perception*, *44*, 157–158.

Vilidaite, G., Yu, M., & Baker, D. H. (2016). Highly correlated internal noise across three perceptual and cognitive modalities. *Journal of Vision*.

Vilidaite, G., Yu, M., & Baker, D. H. (2017). Internal noise estimates correlate with autistic traits. *Autism Research*, *10*, 1384–1391. http://doi.org/10.1002/aur.1781

Voineagu, I., Wang, X., Johnston, P., Lowe, J. K., Tian, Y., Mill, J., … Daniel, H. (2013). Transcriptomic Analysis of Autistic Brain Reveals Convergent Molecular Pathology. *Nature.*, *474*(7351), 380–384. http://doi.org/10.1038/nature10110.Transcriptomic

Walsh, V., & Cowey, A. (1998). Magnetic stimulation studies of visual cognition. *Trends in Cognitive Sciences*, *2*(3), 103–110. http://doi.org/10.1016/S1364-

6613(98)01134-6

Wassermann, E. M. (1998). Risk and safety of repetitive transcranial magnetic stimulation. *Electroencephalography and Clinical Neurophysiology*, *108*(1), 1–16. http://doi.org/10.1016/S0168-5597(97)00096-8

Weinger, P. M., Zemon, V., Soorya, L., & Gordon, J. (2014). Low-contrast response deficits and increased neural noise in children with autism spectrum disorder. *Neuropsychologia*, *63*, 10–18. http://doi.org/10.1016/j.neuropsychologia.2014.07.031

West, R. J. H., Furmston, R., Williams, C. A. C., & Elliott, C. J. H. (2015). Neurophysiology of Drosophila Models of Parkinson ' s Disease. *Parkinson's Disease*, *2015*, 1–11. Retrieved from http://dx.doi.org/10.1155/2015/381281

Wibral, M., Bledowski, C., Kohler, A., Singer, W., & Muckli, L. (2009). The Timing of Feedback to Early Visual Cortex in the Perception of Long-Range Apparent Motion, (July). http://doi.org/10.1093/cercor/bhn192

Wilkinson, F., Karanovic, O., & Wilson, H. R. (2008). Binocular rivalry in migraine, (21). http://doi.org/10.1111/j.1468-2982.2008.01696.x

Winston, J. S., Henson, R. N. A., & Dolan, R. J. (2004). fMRI-Adaptation Reveals Dissociable Neural Representations of Identity and Expression in Face Perception, *1*, 1830–1839.

Zhu, P., Frank, T., & Friedrich, R. W. (2013). Equalization of odor representations by a network of electrically coupled inhibitory interneurons. *Nature Publishing Group*, *16*(11), 1678–1686. http://doi.org/10.1038/nn.3528